

UNCLASSIFIED

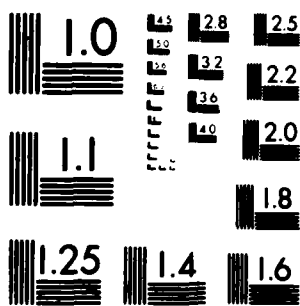
USCG-D-52-81

F/G 17/7  
DIFFERENCE GRID --ETC(U)  
DOT-CR-A1-77-1785  
NL

1-2  
AG  
AG 2007  
■

[illegible]

08074



MICROCOPY RESOLUTION TEST CHART  
NATIONAL BUREAU OF STANDARDS 1963-A

Report No. CG-D-52-81

**LEVEL II**

*12*

# QUANTIFICATION OF ST. MARYS RIVER LORAN-C TIME DIFFERENCE GRID INSTABILITY

THE ANALYTIC SCIENCES CORPORATION

ONE JACOB WAY

READING, MASSACHUSETTS 01867



AUGUST 1980

FINAL REPORT

Document is available to the public through the  
National Technical Information Service,  
Springfield, Virginia 22151

VOLUME 1

TEMPORAL INSTABILITY

Prepared for

**U.S. DEPARTMENT OF TRANSPORTATION**

**United States Coast Guard**

Office of Research and Development

Washington, D.C. 20500

**DTIC**  
**ELECTE**  
**S** DEC 2 1981 **D**  
**D**

AD A108074

6-1  
ENC-FILE COPY

81 12 02 027

### **NOTICE**

**This document is disseminated under the sponsorship of the Department of Transportation in the interest of information exchange. The United States Government assumes no liability for its contents or use thereof.**

**The contents of this report do not necessarily reflect the official view or policy of the Coast Guard; and they do not constitute a standard, specification, or regulation.**

**This report, or portions thereof may not be used for advertising or sales promotion purposes. Citation of trade names and manufacturers does not constitute endorsement or approval of such products.**

# METRIC CONVERSION FACTORS

## Approximate Conversions to Metric Measures

Symbol	When You Know	Multiply by	To Find	Symbol
<b>LENGTH</b>				
in	inches	2.5	centimeters	cm
ft	feet	30	centimeters	cm
y	yards	0.9	meters	m
m	miles	1.6	kilometers	km
<b>AREA</b>				
sq in	square inches	6.5	square centimeters	cm <sup>2</sup>
sq ft	square feet	0.09	square meters	m <sup>2</sup>
sq yd	square yards	0.8	square meters	m <sup>2</sup>
sq mi	square miles	2.6	square kilometers	km <sup>2</sup>
ac	acres	0.4	hectares	ha
<b>MASS (weight)</b>				
oz	ounces	28	grams	g
lb	pounds	0.45	kilograms	kg
sh	short tons (2000 lb)	0.9	tonnes	t
<b>VOLUME</b>				
teaspoon	teaspoons	5	milliliters	ml
tablespoon	tablespoons	15	milliliters	ml
fluid ounce	fluid ounces	30	milliliters	ml
cup	cups	0.24	liters	l
quart	quarts	0.95	liters	l
gallon	gallons	3.8	liters	l
cu in	cubic inches	0.03	cubic centimeters	cm <sup>3</sup>
cu ft	cubic feet	0.03	cubic meters	m <sup>3</sup>
cu yd	cubic yards	0.76	cubic meters	m <sup>3</sup>
<b>TEMPERATURE (exact)</b>				
°F	Fahrenheit temperature	5/9 (after subtracting 32)	Celsius temperature	°C

\* 1 in = 2.54 exactly. For other exact conversions and more detailed tables, see NBS Misc. Publ. 286, Units of Weight and Measure, Price \$2.25, SO Catalog No. C13 10 286.

## Approximate Conversions from Metric Measures

When You Know	Multiply by	To Find	Symbol
<b>LENGTH</b>			
millimeters	0.04	inches	in
centimeters	0.4	inches	in
meters	3.3	feet	ft
kilometers	1.1	miles	mi
millimeters	0.9	miles	mi
<b>AREA</b>			
square centimeters	0.36	square inches	sq in
square meters	1.2	square yards	sq yd
square kilometers	0.4	square miles	sq mi
hectares (10,000 m <sup>2</sup> )	2.5	acres	ac
<b>MASS (weight)</b>			
grams	0.005	ounces	oz
kilograms	2.2	pounds	lb
tonnes (1000 kg)	1.1	short tons	sh
<b>VOLUME</b>			
milliliters	0.03	fluid ounces	fl oz
liters	2.1	pints	pt
liters	1.06	quarts	qt
liters	0.26	gallons	gal
cubic centimeters	36	cubic feet	cu ft
cubic meters	1.3	cubic yards	cu yd

## TEMPERATURE (exact)

°C	Celsius temperature	9/5 (then add 32)	Fahrenheit temperature	°F
----	---------------------	-------------------	------------------------	----



Technical Report Documentation Page

1. Report No. CG-D-52-81	2. Government Accession No. AD-A108 074	3. Recipient's Catalog No.	
4. Title and Subtitle QUANTIFICATION OF ST. MARYS RIVER LORAN-C TIME DIFFERENCE GRID INSTABILITY.		5. Report Date August 1980	
		6. Performing Organization Code	
7. Author(s)		8. Performing Organization Report No.	
9. Performing Organization Name and Address The Analytic Sciences Corporation One Jacob Way Reading, Massachusetts 01867		10. Work Unit No. (TRAIS)	
		11. Contract or Grant No. DOT-CG-81-77-1785	
12. Sponsoring Agency Name and Address Department of Transportation United States Coast Guard Research and Development Center Groton, CT 06340		13. Type of Report and Period Covered Final Report May 1979 to May 1980.	
		14. Sponsoring Agency Code	
15. Supplementary Notes			
<p>16. Abstract</p> <p>Time Difference (TD) data collected in the St. Marys River Loran-C chain coverage area between May 1979 and May 1980 are analyzed to quantify previously-reported temporal TD grid instability. The data included TD samples, nominally recorded every 15 min. at three fixed site monitors and the System Area Monitor (SAM), Local Phase Adjustment (LPA) data, and meteorological data from the National Weather Service Station at Sault Sainte Marie, Michigan. Assorted non-parametric data analyses, including spectral and correlation analyses, are conducted to separate diurnal and seasonal components of grid instability and identify relationships among the various TDs. The relative magnitude of the seasonal TD variations and the correlation of pairs of TDs are not consistent with expected weather-related variations in signal propagation time, thereby suggesting that the grid instability may be partially transmitter and/or receiver-related. The Loran-C data are also employed to evaluate the U.S. Coast Guard low-density (five 15-min. samples, twice daily) data analysis approach. The low-density approach is found to be adequate for monitoring seasonal TD variations, but inadequate for monitoring diurnal variations. An increase in the sampling rate is recommended for low-density Loran-C data collection in harbors.</p>			
17. Key Words LORAN-C, Time difference Seasonal Variations Grid Instability Diurnal Variations		18. Distribution Statement Document is available to the U.S. public through the National Information Service, Springfield, VA 22161	
19. Security Classif. (of this report) Unclassified	20. Security Classif. (of this page) Unclassified	21. No. of Pages 110	22. Price

4.4-60

## TABLE OF CONTENTS

	<u>Page No.</u>
1. INTRODUCTION	1-1
1.1 Background	1-1
1.2 Objectives	1-3
1.3 Report Overview	1-5
2. DESCRIPTION OF DATA BASE AND EDITING PROCEDURE	2-1
2.1 Introduction	2-1
2.2 Editing Procedure	2-1
2.2.1 Editing Mark 1: Loran-C Transmitter	2-1
2.2.2 Editing Mark 2: Signal-Quality Check	2-3
2.2.3 Editing Mark 3: Tolerance Check	2-3
2.2.4 Editing Mark 4: Manual Editing	2-3
2.2.5 Editing Mark 5: Differential- Correction Indicator	2-4
2.2.6 Editing Mark 6: Outlier Editing	2-5
2.3 TD Data Inventory	2-5
2.4 TOA Data Base	2-15
2.5 LPA Data Inventory	2-15
2.6 Data-Base Tapes Delivered to U.S. Coast Guard	2-17
3. QUANTIFICATION OF ST. MARYS RIVER LORAN-C TD GRID INSTABILITY	3-1
3.1 Introduction	3-1
3.2 TD Time Series Plots and Related Statistics	3-1
3.2.1 Seasonal Variations	3-1
3.2.2 Monthly Variations	3-8
3.2.3 Diurnal Variations	3-17
3.3 Correlation and Spectral Analyses	3-24
3.3.1 Autocorrelation Functions and Power Spectral Densities	3-24
3.3.2 Correlation of TD Pairs	3-31
3.3.3 Correlation of TDs with Temperature and Refractive Index	3-34
3.4 LPA Statistics	3-38
3.5 Comparison of Theoretical and Observed TD Variations	3-41

Accession For	
NTIS GRA&I	<input checked="" type="checkbox"/>
DTIC TAB	<input type="checkbox"/>
Unannounced	<input type="checkbox"/>
Justification	
By	
Distribution/	
Availability Codes	
Dist	Avail and/or Special
A	

S DTIC ELECTE D

DEC 2 1981

D

TABLE OF CONTENTS (Continued)

	<u>Page No.</u>
4. EVALUATION OF LOW-DENSITY DATA ANALYSIS APPROACH	4-1
4.1 Introduction	4-1
4.2 Comparison of Edited Low-Density and High-Density Data	4-1
4.2.1 Seasonal Variations	4-2
4.2.2 Monthly Variations	4-4
4.2.3 Diurnal Variations	4-6
4.3 Effect of Outliers on Low-Density Data	4-9
4.4 Assessment of Low-Density Data Analysis Techniques	4-10
5. CONCLUSIONS AND RECOMMENDATIONS	5-1
5.1 Quantification of St. Marys River Loran-C TD Grid Instability	5-1
5.2 Evaluation of Low-Density Data Analysis Approach	5-4
APPENDIX A FORMATS FOR LORAN-C DATA SUPPLIED TO TASC	A-1
APPENDIX B FORMATS FOR LORAN-C DATA DELIVERED TO U.S. COAST GUARD	B-1
APPENDIX C PARTIAL LISTING OF LORAN-C DATA BASE	C-1
REFERENCES	R-1



## LIST OF FIGURES

<u>Figure No.</u>		<u>Page No.</u>
1.1-1	Locations of River Waypoints, Data Collection Sites, and Transmitters in Reconfigured St. Marys River Loran-C Mini-Chain	1-3
1.2-1	Objectives of St. Marys River Temporal Loran-C Data Analyses	1-4
2.3-1	TD Data Inventory for DeTour/LC-204/1	2-8
2.3-2	TD Data Inventory for DeTour/LC-204/2	2-9
2.3-3	TD Data Inventory for Dunbar/BRN-5/1	2-10
2.3-4	TD Data Inventory for Dunbar/LC-204/2	2-11
2.3-5	TD Data Inventory for Iroquois/LC-204/1	2-12
2.3-6	TD Data Inventory for Iroquois/LC-204/2	2-13
2.3-7	TD Data Inventory for SAM/Austron/1	2-14
2.5-1	LPA Data Inventory	2-16
3.2-1	TDX Seasonal Time Series	3-3
3.2-2	TDY Seasonal Time Series	3-4
3.2-3	TDZ Seasonal Time Series	3-5
3.2-4	SAM Seasonal Time Series	3-6
3.2-5	TDX Monthly Time Series for July	3-9
3.2-6	TDY Monthly Time Series for July	3-10
3.2-7	TDZ Monthly Time Series for July	3-11
3.2-8	SAM Monthly Time Series for July	3-12
3.2-9	TDX Monthly Time Series for January	3-13
3.2-10	TDY Monthly Time Series for January	3-14

LIST OF FIGURES (Continued)

<u>Figure No.</u>		<u>Page No.</u>
3.2-11	TDZ Monthly Time Series for January	3-15
3.2-12	SAM Monthly Time Series for January	3-16
3.2-13	TDX Diurnal Cycles and Histograms for July	3-18
3.2-14	TDY Diurnal Cycles and Histograms for July	3-19
3.2-15	TDZ Diurnal Cycles and Histograms for July	3-20
3.2-16	TDX Diurnal Cycles and Histograms for January	3-21
3.2-17	TDY Diurnal Cycles and Histograms for January	3-22
3.2-18	TDZ Diurnal Cycles and Histograms for January	3-23
3.3-1	Autocorrelation Functions and Power Spectral Densities for TDX	3-27
3.3-2	Autocorrelation Functions and Power Spectral Densities for TDY	3-28
3.3-3	Autocorrelation Functions and Power Spectral Densities for TDZ	3-29
3.3-4	Effect of High-Pass Filtering on the ACF (TDY for Dunbar/LC-204/2)	3-30
3.3-5	Cross-Correlation Function and Coherency Spectrum for TDX vs TDY Data (Dunbar/BRN-5/1)	3-35
3.3-6	Temperature Seasonal Time Series	3-36
3.3-7	Refractivity Seasonal Time Series	3-36
3.3-8	Cross-Correlation Function and Coherency Spectrum for TDY (Iroquois/LC-204/2) vs Temperature Data	3-38
3.4-1	Daily Sum of LPAs	3-39
3.4-2	Cumulative Sum of LPAs	3-40
3.5-1	TDX Temporal Variation Sensitivity	3-42
3.5-2	TDY Temporal Variation Sensitivity	3-43

LIST OF FIGURES (Continued)

<u>Figure No.</u>		<u>Page No.</u>
3.5-3	TDZ Temporal Variation Sensitivity	3-44
3.5-4	Comparison of Seasonal TD Time Series	3-46
4.2-1	Accuracy of Edited Low-Density Seasonal Time Series (TDY for Iroquois/LC-204/2)	4-3
4.2-2	Accuracy of Edited Low-Density Monthly Time Series (TDX for Iroquois/LC-204/1)	4-5
4.2-3	Accuracy of Edited Low-Density Diurnal Cycle (TDZ for Iroquois/LC-204/2)	4-7
4.3-1	Effect of Outliers on Low-Density Monthly Time Series (TDY for DeTour/LC-204/1)	4-11
5.1-1	TDY Seasonal Time Series for Iroquis/LC-204/2	5-3
5.1-2	TDY Diurnal Cycle for DeTour/LC-204/2	5-3
5.1-3	TDZ Power Spectral Density for Dunbar/LC-204/2	5-3

### LIST OF TABLES

<u>Table No.</u>		<u>Page No.</u>
2.2-1	Interpretation of Editing Mark Values	2-2
2.3-1	Summary of Editing Operations	2-6
2.6-1	Summary of Data-Base Tapes Delivered to U.S. Coast Guard	2-17
3.2-1	Seasonal TD Statistics	3-7
3.3-1	Correlation Coefficients for DeTour	3-32
3.3-2	Correlation Coefficients for Dunbar	3-32
3.3-3	Correlation Coefficients for Iroquois	3-32
3.3-4	Correlation Coefficients for TDX	3-33
3.3-5	Correlation Coefficients for TDY	3-33
3.3-6	Correlation Coefficients for TDZ	3-33
3.3-7	Correlation of TDs with Temperature and Refractivity	3-37

1.

## INTRODUCTION

### 1.1 BACKGROUND

The U.S. Coast Guard conducted a comprehensive data collection effort from May 1979 to May 1980 to quantify an apparent temporal instability in the St. Marys River Loran-C Time Difference (TD) grid. Detailed analyses of the resulting Loran-C data base are documented in this report.

TASC's involvement with the St. Marys River Loran-C mini-chain began with the calibration of a spatial TD grid prediction model based on data collected during September and October 1977 (Refs. 1 and 2). A limited amount of data collected monthly between November 1977 and March 1978 exhibited temporal TD variations as large as 0.4  $\mu$ sec peak-to-peak at some data collection sites. Because the utility of the TD grid prediction model and the mini-chain depends on the assumption of a stable grid, it was important that the validity of the observed temporal variations be confirmed. In particular, collection of additional data under more carefully controlled conditions (e.g., well-sheltered receivers and ideal grounding) was judged to be necessary. The need for confirmation was further highlighted by a theoretical sensitivity analysis, which revealed that the observed TD variations could not be explained by expected seasonal variations in signal propagation conditions (Ref. 3). In order to resolve the discrepancy between the theory and observations, it was recommended that the U.S. Coast Guard initiate the yearlong data collection effort outlined in Ref. 4. Loran-C Data-Base Management Software was subsequently designed and implemented at TASC, to support the editing and analysis of the collected data (Ref. 5).

The data consist of TD samples and associated signal-quality indicators, recorded nominally every 15 min at three fixed sites: DeTour Village, Dunbar Experimental Forest, and Pt. Iroquois\* (see Fig. 1.1-1). Two Internav LC-204 Loran-C receivers are located at both the DeTour and Iroquois sites, and one Internav LC-204 and one Magnavox AN/BRN-5 receiver are located at the Dunbar site.† The BRN-5 receiver is interfaced with a cesium frequency standard to also provide measurements of Time-of-Arrival (TOA). The following additional data are collected to support the analyses: System Area Monitor (SAM) TDs from the Austron-5000 receiver used for chain control, Local Phase Adjustments (LPAs) from the Calculator Assisted Loran Controller (CALOC) system, and meteorological data from the National Weather Service Station at Sault Sainte Marie, Michigan.

In addition to the 15-min TD data, which are termed high-density data, the U.S. Coast Guard collects low-density data for in-house analyses. The low-density data are recorded with a microprocessor-based system which is independent of the Texas Instruments Silent 700 cassette tape recorder used to obtain the high-density data. The low-density data consist of five 15-min samples recorded twice daily, which are then averaged and transmitted over a telephone data link in a weekly message. A similar low-density data-recording system is under development by the U.S. Coast Guard for use in harbor and harbor entrance Loran-C navigation experiments.

---

\*Referred to as DeTour, Dunbar, and Iroquois in this report.

†Referred to as LC-204 and BRN-5 in this report.

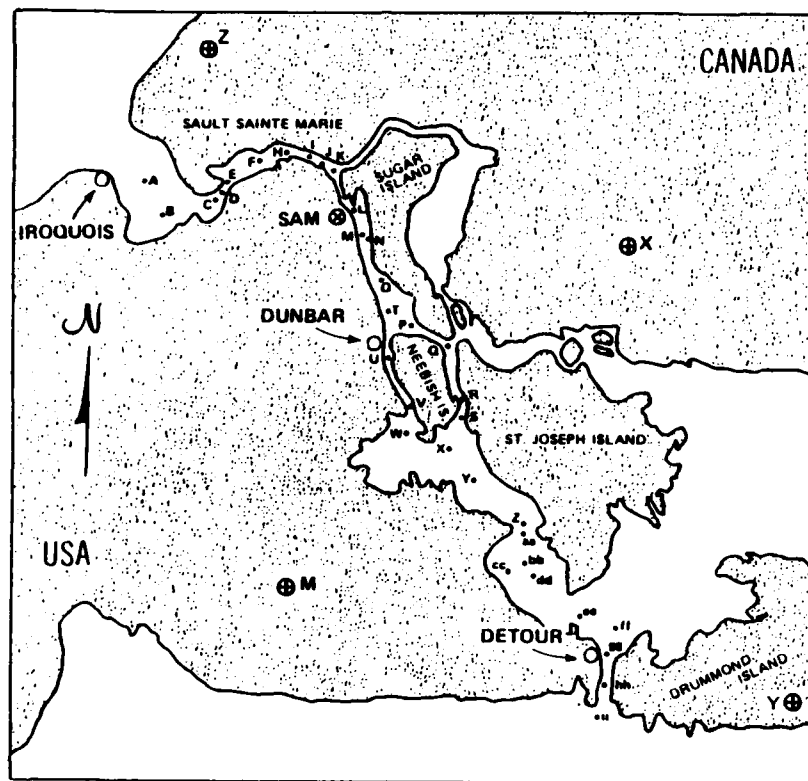


Figure 1.1-1 Locations of River Waypoints, Data Collection Sites, and Transmitters in Reconfigured St. Marys River Loran-C Mini-Chain

## 1.2 OBJECTIVES

The objectives of the study documented herein, as indicated in Fig. 1.2-1, are to:

- Conduct high-density data analyses to quantify TD grid instability in the St. Marys River Loran-C mini-chain

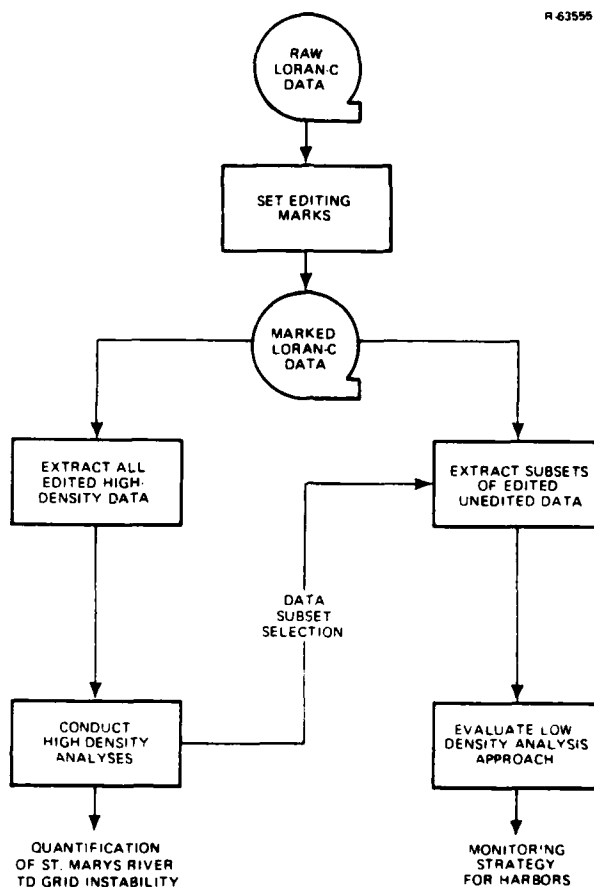


Figure 1.2-1 Objectives and Technical Approach for St. Marys River Temporal Loran-C Data Analyses

- Evaluate the low-density data analysis approach to establish an efficient Loran-C monitoring strategy for harbors.

To meet these objectives, the raw Loran-C data are first organized and edited, using the TASC Loran-C Data-Base Management Software. Editing marks are set by the software to indicate the quality of each TD sample, thus making it straight-



forward to extract "good" and/or "bad" data without affecting the master data base. Specifically, a criterion for editing is selected for the high-density analyses, and all corresponding data are extracted and analyzed (see Fig. 1.2-1). Availability of the high-density analysis results then permits the low-density evaluation to be limited to a subset of all possible site/receiver/TD combinations. Both edited and unedited TD data are extracted for the selected combinations to determine the effect of outliers on the low-density approach.

It should be kept in mind that the primary objective of the high-density data analyses is to quantify TD grid instability. Although the determination and modeling of cause/effect relationships is beyond the scope of the current effort, the analyses are selected and presented in a manner which facilitates possible future studies by the U.S. Coast Guard. A comparison is made between the data analysis results herein and the theoretical sensitivity analysis results from Ref. 3, to provide a basis for future research.

### 1.3 REPORT OVERVIEW

A description of the Loran-C data base and editing procedure is provided in Chapter 2. The high-density data analysis results are given in Chapter 3 and the low-density data analysis approach is evaluated in Chapter 4. The study conclusions are contained in Chapter 5, together with a recommended sampling/editing/analysis strategy for harbor Loran-C monitor data.

The TASC Loran-C data base is being delivered to the U.S. Coast Guard on three magnetic tapes which supplement this report. The tape layouts are described in Section 2.6 and the record formats are given in the appendices.

## 2. DESCRIPTION OF DATA BASE AND EDITING PROCEDURE

### 2.1 INTRODUCTION

Data from the St. Marys River temporal TD instability experiment are provided to TASC on 11 half-inch magnetic tapes with the record format listed in Appendix A. The tapes contain a total of 137 site files, 286 SAM files, and 11 weather files, which are sorted and ordered by the Loran-C Data-Base Management Software. The record formats are changed to those presented in Appendices B and C, which include six editing mark characters for every TD and TOA sample.

### 2.2 EDITING PROCEDURE

The editing marks indicate the quality of the data, each mark corresponding to a different editing operation as indicated in Table 2.2-1. The manner in which the editing marks are determined is detailed in Ref. 5 and summarized below.

#### 2.2.1 Editing Mark 1: Loran-C Transmitter

Editing Mark 1 indicates which Loran-C transmitter is associated with the TOA, or which secondary transmitter is associated with the TD. In the cases of the LC-204 and BRN-5 receivers, the transmitter is determined by examining the first two digits of the TD. If the digits do not match one of the three possibilities -- "11" for TDX, "22" for TDY, or "33" for TDZ -- Editing Marks 1 to 6 are set to "?".

TABLE 2.2-1  
INTERPRETATION OF EDITING MARK VALUES

EDITING MARK	OPERATION	VALUES*	INTERPRETATION
1	Loran-C Transmitter	M X Y Z	TOAM TOAX or TDX TOAY or TDY TOAZ or TDZ
2	Signal Quality Check	0 1 2 3	Good Data Quality Control Unit Switch on B Insufficient Signal Both Characteristics 1 and 2 Apply
3	Tolerance Check	0 1 2	Data Differs from Seasonal Mean by $\leq 0.5 \mu\text{sec}$ $0.5 \mu\text{sec} < \text{Difference} \leq 1.0 \mu\text{sec}$ $\text{Difference} > 1.0 \mu\text{sec}$
4	Manual Editing	0 6	No Manual Editing Duplicate Data
5	Differential Correction Computation	0 A B C 1 2 3	<u>Differential Correction Computed</u> No Interpolation Required Interpolation Interval $\leq 6$ hr $6 \text{ hr} < \text{Interval} \leq 24$ hr Interval $> 24$ hr <u>Differential Correction Not Computed</u> Uncertain LPA Times Bad SAM TD Data Based on Editing Marks 1 to 4 and 6 No LPA and/or SAM TD Data Available
6	Outlier Editing	0 1,2,3,4 5,6 S U	Data Is Not an Outlier Data Differs from Daily Trend Line by $> 0.05, 0.10, 0.15, 0.20 \mu\text{sec}$ (Second Iteration) Data Differs from Trend Line by $> 0.15, 0.20 \mu\text{sec}$ (First Iteration) Less Than 20 Samples per Day Available to Compute Trend Line Bad Data Based on Editing Marks 1 to 4

\* Editing marks are set to 0 if no problem and to ? if not computable

#### 2.2.2 Editing Mark 2: Signal-Quality Check

Editing Mark 2 summarizes various Loran-C signal-quality indicators which appear in each data record. The indicators which are checked are SWITCH and SUFFSIG for the LC-204, SUFFSIG for the BRN-5, and MODE for the Austron-5000 receiver (see Appendix A). Editing Mark 2 is the only editing mark which is not based on the TD/TOA data itself.

#### 2.2.3 Editing Mark 3: Tolerance Check

Editing Mark 3 indicates whether or not the TD lies between expected lower and upper bounds, which are selected based on U.S. Coast Guard low-density data available at the beginning of the study. Specifically, the TD is compared to the mean of the low-density data for the period May 1979 to February 1980 (Ref. 5).<sup>\*</sup> Three tolerance bands (see Table 2.2-1) are distinguished to permit the editing of gross outliers, while retaining the capability to accommodate TD variations during the March 1980 to May 1980 time period. Editing Mark 3 serves primarily to identify TDs which are affected by receiver cycle jumps and transmitter and control malfunctions.

#### 2.2.4 Editing Mark 4: Manual Editing

Editing Mark 4 is employed to manually flag suspect data which are not flagged automatically by other editing marks. The large volume of data makes it impractical to employ the Test Director's Log for manual editing. Consequently, the only use made of Editing Mark 4 is to identify duplicate data which arise either in the transferral of tape cassette data to half-inch magnetic tape by the U.S. Coast Guard, or in the

---

<sup>\*</sup>The mean of the high-density TD data for the entire year differs from this value by less than 0.05  $\mu$ sec.

processing of the half-inch magnetic tapes by TASC. The absence of further manual editing does not detract from the data quality in view of the comprehensive automatic editing employed.

#### 2.2.5 Editing Mark 5: Differential-Correction Indicator

Differential corrections are computed and included in the site data records to show the difference between measured SAM TDs and the Controlling Standard TD (the reference used for chain control). Differential corrections can be added to the measured site TDs in post-time to simulate perfect chain control. When site and SAM TDs are not measured at the same times, the SAM TDs are estimated by linear interpolation (Ref. 5). Care is taken to include the effects of LPAs and receiver averaging times (~50 sec) in the interpolated TDs. An offset of 850 sec in the LC-204 recording times relative to the actual sampling times is also accounted for in this procedure.

Editing Mark 5 indicates the length of the interpolation interval used in the differential-correction computation (see Table 2.2-1). Intervals greater than a quarter of the diurnal cycle (6 hr) are judged to be excessive, because the linear approximation no longer holds. Table 2.2-1 indicates circumstances under which no differential correction can be computed. Noteworthy in this regard is the period from 22 January 1980 to 31 March 1980, for which LPAs were provided to TASC in hand-written form with time to the nearest minute, rather than on the CALOC system printout with time to the nearest second. Editing Mark 5 is set to "3" in this case because the accuracy of the LPA data has not been verified by TASC.

### 2.2.6 Editing Mark 6: Outlier Editing

Editing Mark 6 is employed to flag data which are inconsistent with the short-term behavior of the TD time series, but are not flagged by other editing marks. These outlying data represent isolated "events" caused by low signal-to-noise ratio, transmitter/receiver/control malfunctions, or anomalous propagation conditions. Although the outliers must be edited to permit an orderly analysis of typical TD variations, they are marked in the data base for use in possible future cause/effect studies.

Outliers are detected automatically by comparing each TD sample to a trend line fit to all data in a daily time window (Ref. 5). Samples which differ from the trend line by greater than 0.15  $\mu$ sec are marked "5" or "6" as indicated in Table 2.2-1, and a new trend line is computed from the remaining samples. The samples are then compared to the refined trend line and marked "0" to "4" to indicate which 0.05- $\mu$ sec error-bin they fall into (see Table 2.2-1). This procedure produces a histogram of TD errors relative to the trend line.

### 2.3 TD DATA INVENTORY

The operations involved in editing the TD data base for high-density analyses are summarized in Table 2.3-1. The editing mark values which define the data base are noted below:

- Editing Mark 1 = "X", "Y", or "Z": two TD time series are extracted for each site receiver and three for the SAM receiver
- Editing Mark 2 = "0": 87.7 to 98.4 percent of the data are associated with good signal quality

TABLE 2.3-1  
SUMMARY OF EDITING OPERATIONS

SITE	RECEIVER TYPE/ NUMBER	TIME DIFFERENCE	TOTAL NUMBER OF SAMPLES	PERCENT OF DATA RETAINED AFTER EACH EDITING OPERATION			NUMBER OF RETAINED SAMPLES	STANDARD DEVIATION (μsec)
				SIGNAL- QUALITY CHECK	PERFORMANCE CHECK	OUTLIER EDITING		
DeLour	LC-206/1	X	17,576	90.6	93.0	97.5	16,617	0.015
		Y	19,186	92.7	69.4	92.7	11,603	0.026
DeLour	LC-206/2	Y	20,632	93.1	98.6	96.3	17,910	0.020
		Z	19,067	91.0	97.1	95.6	16,095	0.020
Dunbar	BRN-5/1	X	21,772	98.2	98.3	95.3	20,037	0.023
		Y	21,863	98.6	98.5	89.2	18,873	0.031
Dunbar	LC-206/2	Y	20,219	91.9	98.6	96.0	17,593	0.019
		Z	16,983	92.1	98.6	95.3	16,460	0.020
Froquarts	LC-206/1	X	28,650	88.2	99.2	97.8	26,527	0.017
		Z	28,685	88.0	99.2	96.6	23,959	0.020
Froquarts	LC-206/2	Y	29,366	90.3	98.3	96.2	25,052	0.020
		Z	29,662	87.7	98.8	97.6	25,061	0.018
SAH	Austcon/1	X	37,686	97.6	97.6	98.1	36,995	0.016
		Y	37,686	95.6	97.9	97.6	36,135	0.019
		Z	37,363	97.2	98.0	96.9	36,463	0.018

Standard deviation of the differences between the retained 3d data and trend lines fit to daily data segments.

- Editing Mark 3 = "0": 93.0 to 99.2 percent of the data are within 1.0  $\mu$ sec of the seasonal mean, except for TDY for DeTour/ LC-204/1\* which exhibits numerous cycle jumps
- Editing Mark 4 = "0": duplicate data are ignored in the "Total Number of Samples" column in Table 2.3-1
- Editing Mark 5 = any value: differential corrections are not applied because of their small magnitude relative to site TD variations (see Section 3.2) and because they are not available for the entire year
- Editing Mark 6 = "0": 89.2 to 98.1 percent of the data are within 0.05  $\mu$ sec of the daily trend lines used for outlier detection.

The number of samples retained after all editing operations ranges from 10,000 to 35,000 for the 15 TD time series (see Table 2.3-1).

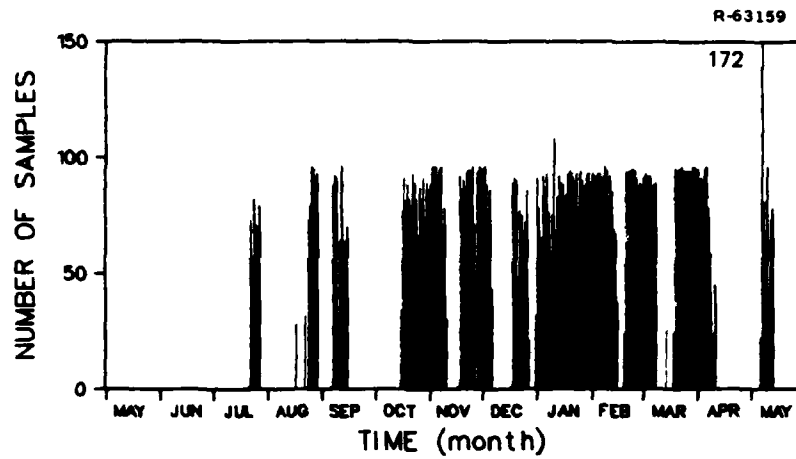
The quality of the edited data base is judged to be excellent. Not only do all edited data lie within a  $\pm 0.05$   $\mu$ sec band centered on the daily trend line, but the standard deviations of the TD/trend line differences are between 0.015  $\mu$ sec and 0.031  $\mu$ sec (see Table 2.3-1). The short-term fluctuations are caused by atmospheric noise and the diurnal TD cycle, and are consistent with those measured in the laboratory (Ref. 7).

An inventory of the edited TD data is presented in Figs. 2.3-1 to 2.3-7, where the bars indicate the number of samples per day (nominally, 96). The large gaps which appear

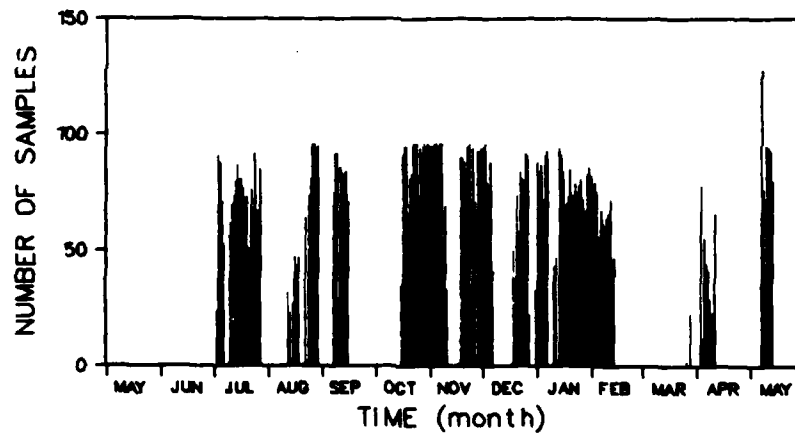
---

\*Each receiver is uniquely identified by site/receiver type/receiver number.



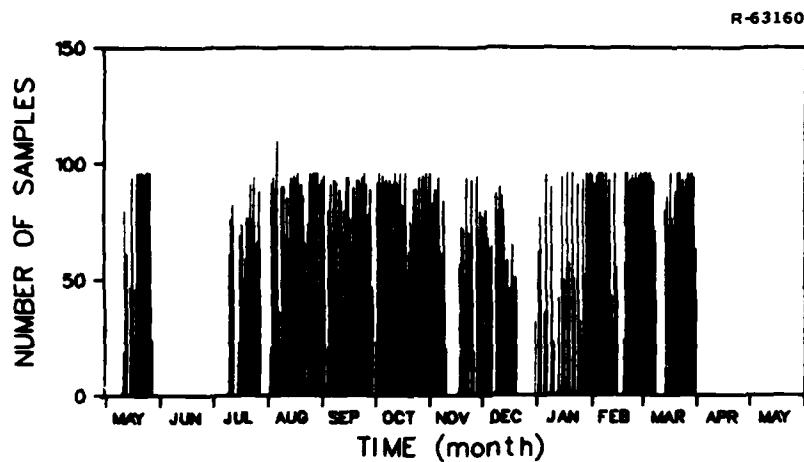


a) Time Difference X

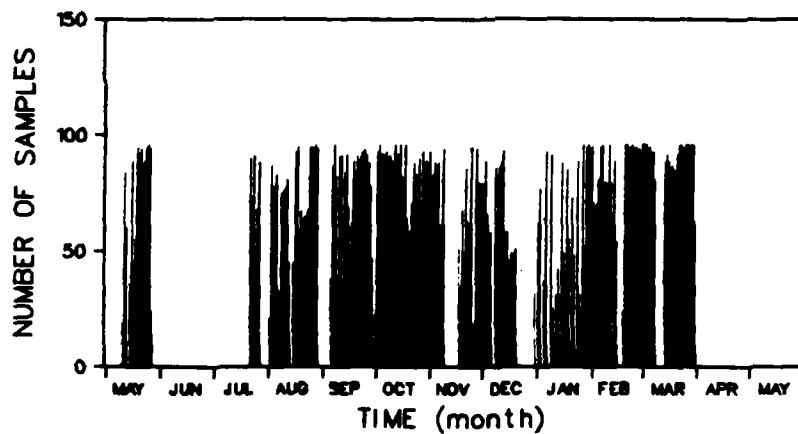


b) Time Difference Y

Figure 2.3-1 TD Data Inventory for DeTour/LC-204/1



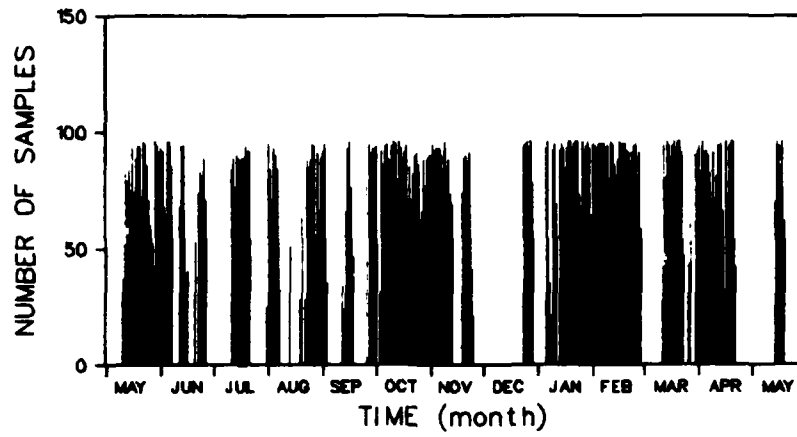
a) Time Difference Y



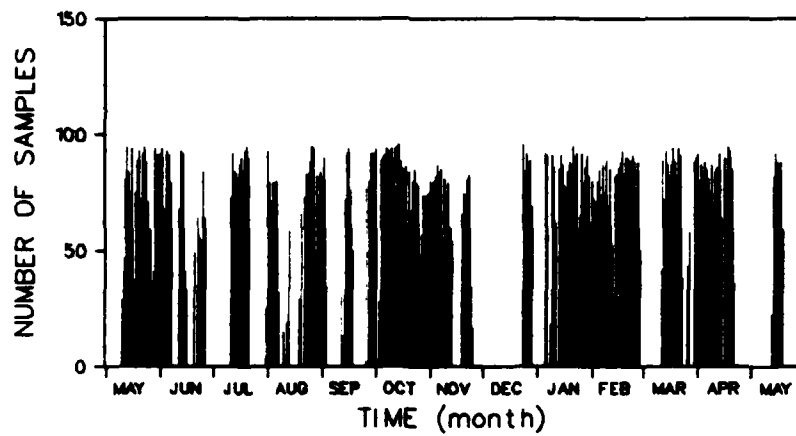
b) Time Difference Z

Figure 2.3-2 TD Data Inventory for DeTour/LC-204/2

R63161

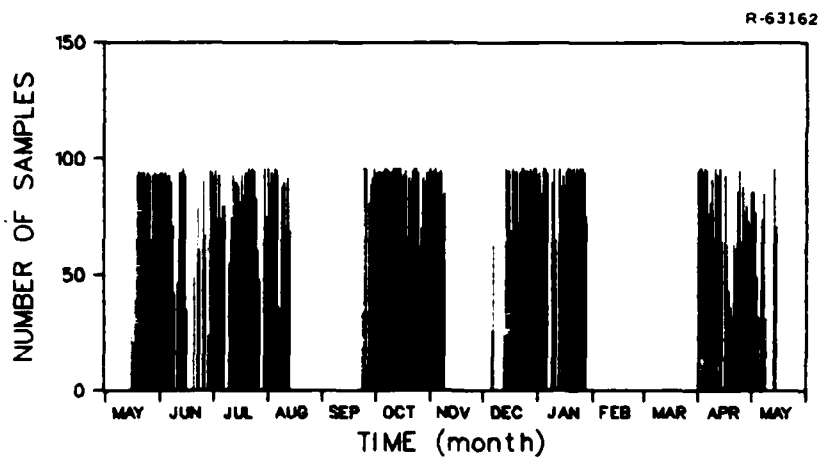


a) Time Difference X

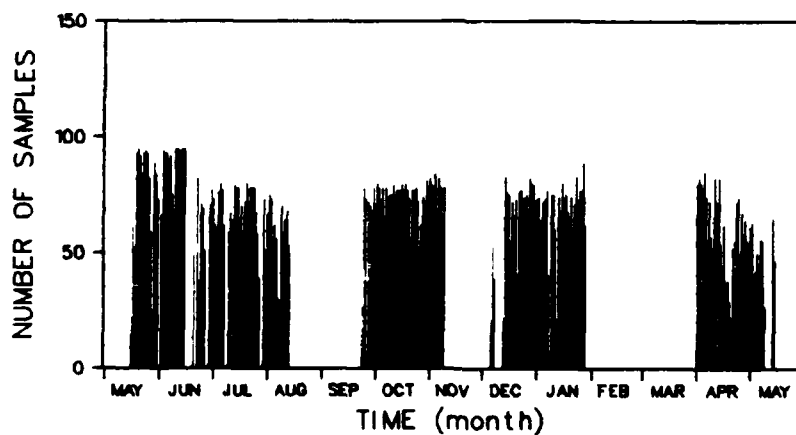


b) Time Difference Y

Figure 2.3-3 TD Data Inventory for Dunbar/BRN-5/1

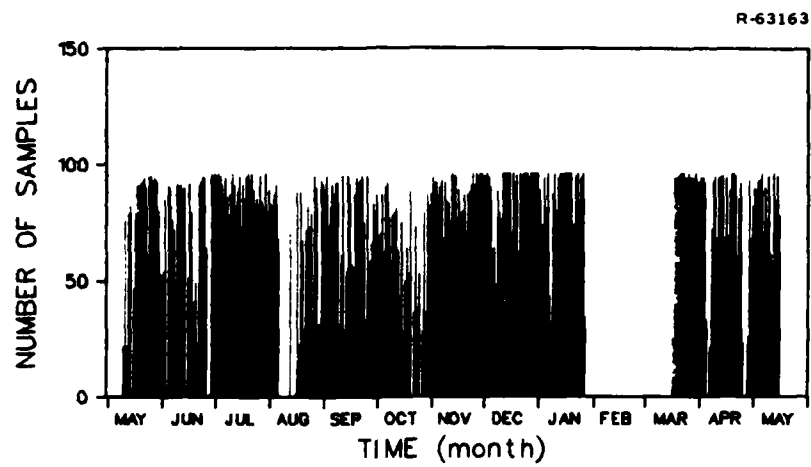


a) Time Difference Y

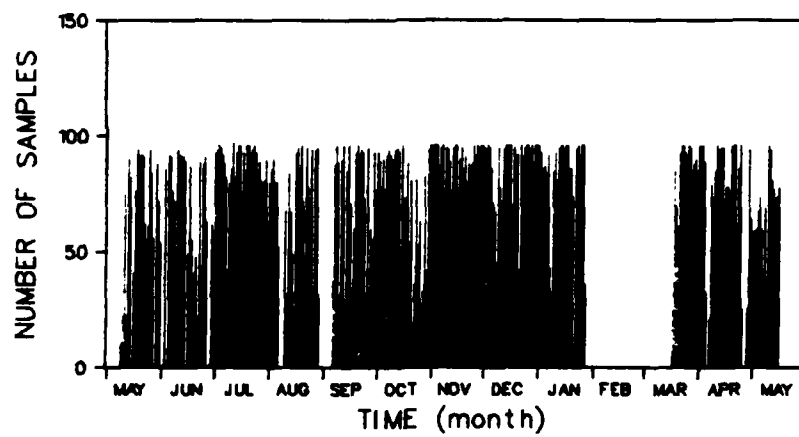


b) Time Difference Z

Figure 2.3-4 TD Data Inventory for Dunbar/LC-204/2



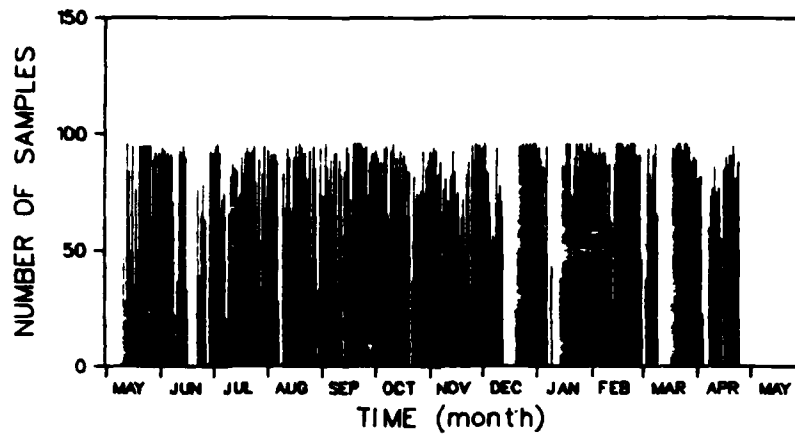
a) Time Difference X



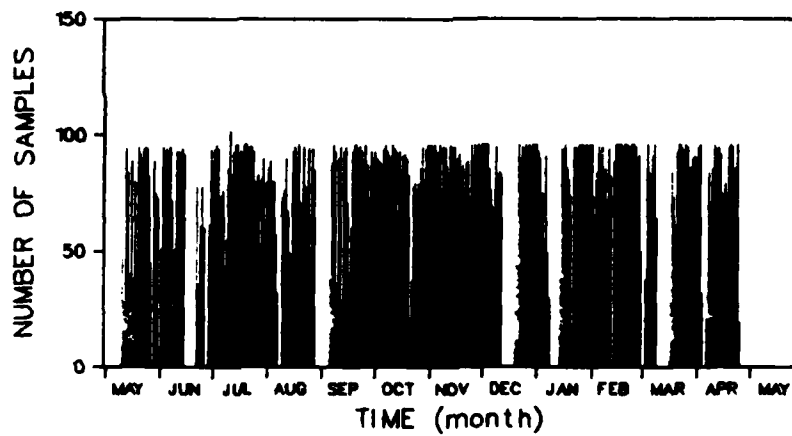
b) Time Difference Z

Figure 2.3-5 TD Data Inventory for Iroquois/LC-204/1

R-63164

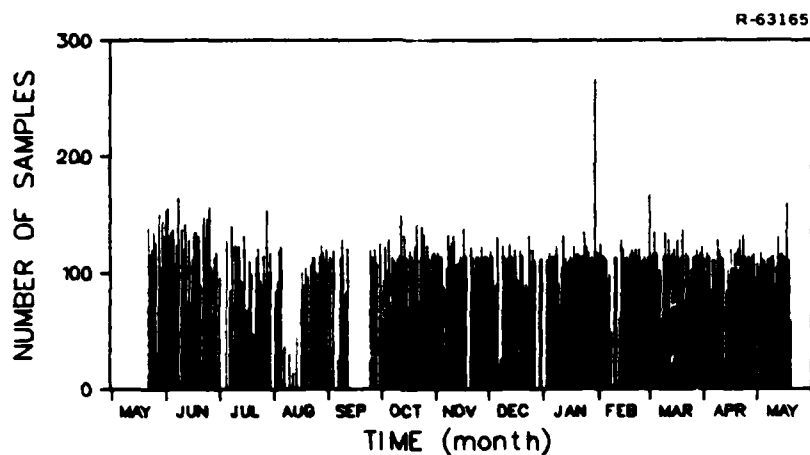


a) Time Difference Y

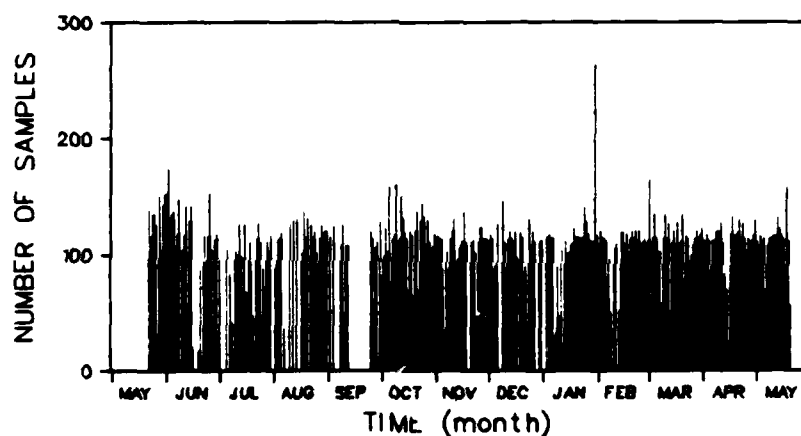


b) Time Difference Z

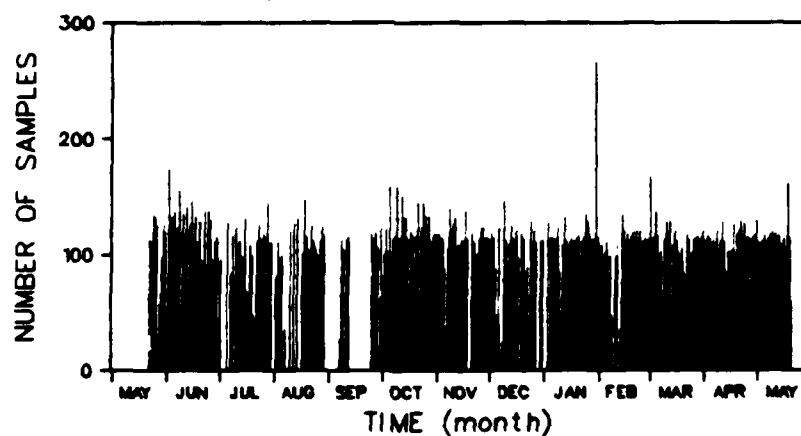
Figure 2.3-6 TD Data Inventory for Iroquois/LC-204/2



a) Time Difference X



b) Time Difference Y



c) Time Difference Z

Figure 2.3-7 TD Data Inventory for SAM/Austron/1

in many time series are associated with missing cassette tapes, rather than edited data. The U.S. Coast Guard low-density data can be used to fill these gaps and provide additional low-frequency (seasonal) detail. However, inclusion of low-density data is beyond the scope of the current effort and would not significantly affect the analysis results.

#### 2.4 TOA DATA BASE

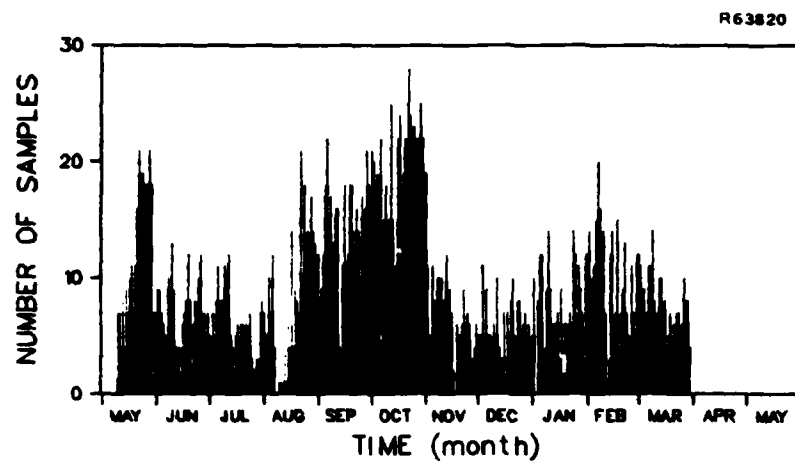
Master, Secondary X, and Secondary Y TOA data are measured with the BRN-5 receiver at the Dunbar site. An inspection of the TOA data shows that the clock was reset periodically to keep the master TOA near a value of 1000  $\mu$ sec. The numerous TOA jumps introduced by this procedure make it infeasible to remove clock effects from the data. Identification of the jumps is further complicated by large gaps in the TOA time series, coincident with the TD time series gaps shown in Fig. 2.3-3.

Because clock effects cannot be removed, the TOA data are not analyzed in the current study. TOA Editing Marks 1, 2, and 4 are set by the Data-Base Management Software, but the remaining editing marks require prior compensation for clock phase variations.

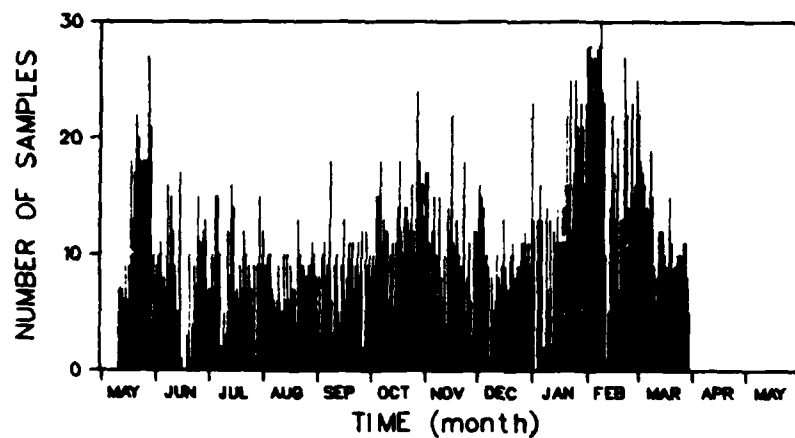
#### 2.5 LPA DATA INVENTORY

LPA data are manually entered into the data base by TASC, from the CALOC system printout. The number of LPA samples per day for each secondary transmitter is shown in Fig. 2.5-1. Approximately 10 LPAs per day, on the average, are required to satisfy the 0.015- $\mu$ sec control tolerance.

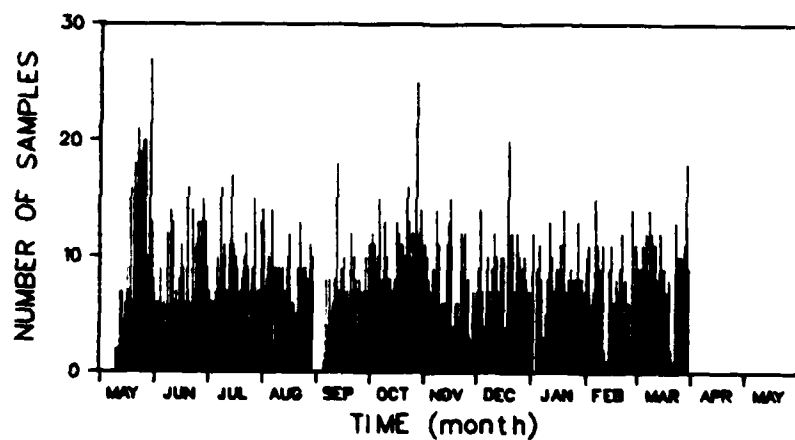




a) Transmitter X



b) Transmitter Y



c) Transmitter Z

Figure 2.5-1 LPA Data Inventory  
2-16

## 2.6 DATA-BASE TAPES DELIVERED TO U.S. COAST GUARD

The 46-megabyte St. Marys River Loran-C data base, with editing marks included, is delivered to the U.S. Coast Guard on three half-inch magnetic tapes (9-track, 800 BPI, ASCII code). The tapes are arranged as shown in Table 2.6-1, with one file for each receiver except the BRN-5, which requires a separate file for secondary and master records. The block size in each receiver file is 8190, which includes 63 records with 130 characters each. The block size for the LPA file is 8160, which includes 204 records with 40 characters each. The record formats are given in Appendices B and C.

TABLE 2.6-1  
SUMMARY OF DATA-BASE TAPES  
DELIVERED TO U.S. COAST GUARD \*

TAPE NUMBER	FILE NUMBER	SITE NUMBER†	RECEIVER TYPE	RECEIVER NUMBER	NUMBER OF DATA RECORDS
1	2	1	BRN5 SEC	1	2,589
1	3	1	BRN5 MAS	1	1,292
1	4	1	LC204	1	19,579
1	5	1	LC204	2	20,629
1	6	2	BRN5 SEC	1	48,017
1	7	2	BRN5 MAS	1	23,251
2	1	2	LC204	2	20,495
2	2	3	LC204	1	28,936
2	3	3	LC204	2	30,040
2	4	—	LPAs	—	9,517
3	1	8	AUSTRON	1	151,179

\*This table is repeated on Tape 1/File 1.

†1 = DeTour, 2 = Dunbar, 3 = Iroquois, and 8 = SAM.

Each file is identified by lead and final records with the following formats:

\*\*\* BEGIN: SITE=\_ REC.TYPE=\_ REC.NUM=\_ \*\*\*

\*\*\* END: SITE=\_ REC.TYPE=\_ REC.NUM=\_ \*\*\*

The BRN-5 secondary and master files are further distinguished by the following second and next-to-last records:

\*\*\* BEGIN: MASTER \*\*\*

\*\*\* END: MASTER \*\*\*

\*\*\* BEGIN: SECONDARY \*\*\*

\*\*\* END: SECONDARY \*\*\*

In addition, each record has a unique "signature," consisting of the record number, site number, receiver type, and receiver number (see Appendix B).

### 3. QUANTIFICATION OF ST. MARYS RIVER LORAN-C TD GRID INSTABILITY

#### 3.1 INTRODUCTION

The edited data base described in Section 2.3 is employed in this chapter to quantify TD grid instability in the St. Marys River Loran-C mini-chain. Quantification is based on the following non-parametric descriptions of the data:

- TD time series plots and related statistics to exhibit seasonal, monthly, and diurnal variations
- Autocorrelation and cross-correlation functions to identify TD/TD, TD/temperature, and TD/refractive index relationships
- Power spectral densities to examine the frequency content of the TD variations
- LPA statistics to quantify SAM TD variations in the case of no chain control
- Comparison of theoretical and measured TD variations to provide a basis for possible future studies.

The high-density analyses parallel the low-density analyses conducted by the U.S. Coast Guard, where possible.

#### 3.2 TD TIME SERIES PLOTS AND RELATED STATISTICS

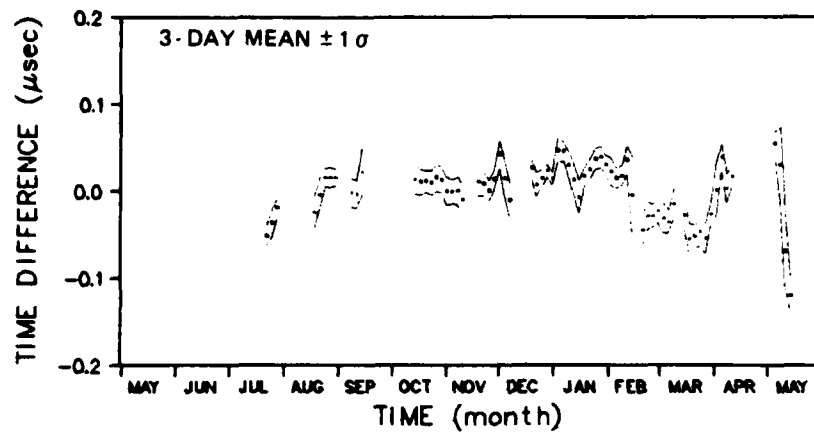
##### 3.2.1 Seasonal Variations

Seasonal TD variations are quantified by the mean and standard deviation of the data in 3-day time windows (see

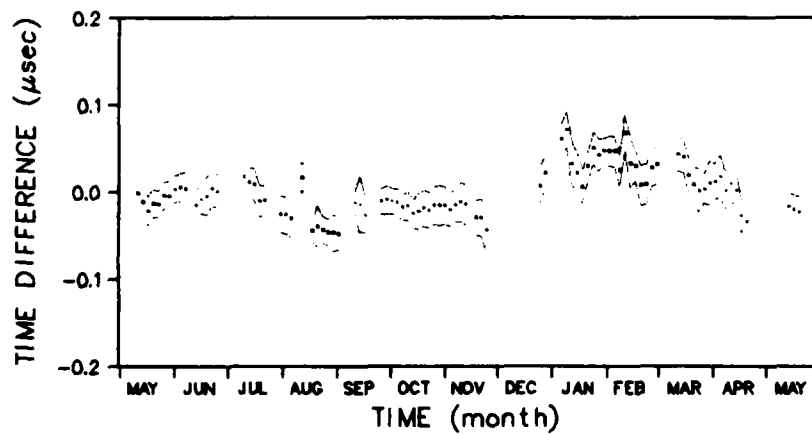
Figs. 3.2-1 to 3.2-4). In this study, seasonal variations are defined as the variation in the 3-day mean over the data collection period. The standard deviation gives an indication of shorter-term TD variations relative to the seasonal variations. To avoid misinterpretation of the results, no point is plotted for 3-day windows which contain fewer than 20 samples. The TD is shown relative to the average value of the time series, i.e., the mean of the 3-day means (see Table 3.2-1). The three redundant TDs -- TDY for DeTour/LC-204/1, TDY for Dunbar/BRN-5/1, and TDZ for Iroquois/LC-204/1 -- are not included here, but are discussed in Section 3.3.2.

An examination of Figs. 3.2-1 to 3.2-4 leads to the following conclusions:

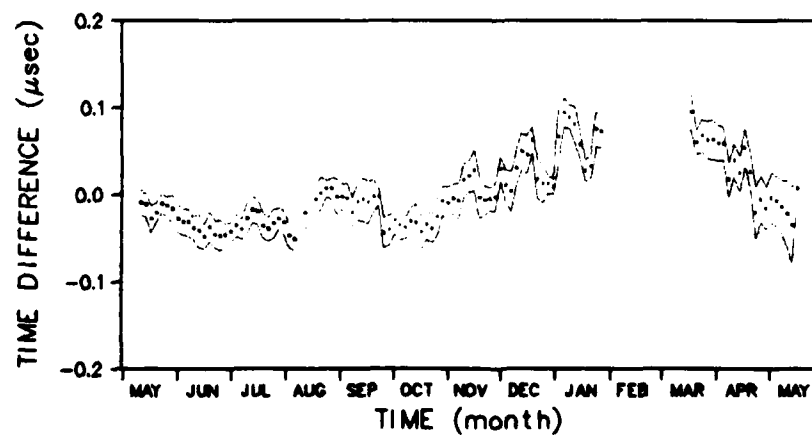
- Seasonal TD variations are less than 0.4  $\mu\text{sec}$  peak-to-peak (p-p) at the DeTour, Dunbar, and Iroquois sites, consistent with previous observations (Refs. 2 and 3)
- TD values in May 1979 and May 1980 are approximately equal, suggesting that the seasonal meteorological cycle causes the variations
- TD variations during monthly periods are larger in the winter than in the summer, consistent with signal propagation theory (Refs. 3 and 9)
- The 3-day standard deviations (shown by dotted curves in Figs. 3.2-1 to 3.2-4) are less than 0.025  $\mu\text{sec}$ , which is small relative to the variation of the 3-day means
- The standard deviation of the 3-day means (see Table 3.2-1) is larger for TDY than for TDX and TDZ, i.e., 0.069  $\mu\text{sec}$  average compared to 0.032  $\mu\text{sec}$  average
- SAM TD variations are less than 0.02  $\mu\text{sec}$  p-p except for TDY in February (see Fig. 3.2-4), indicating that chain control tolerances are satisfied.



a) DeTour/LC-204/1



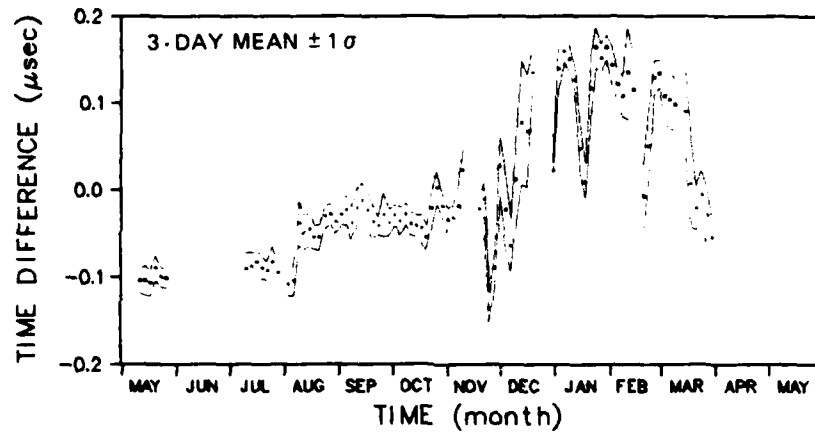
b) Dunbar/BRN-5/1



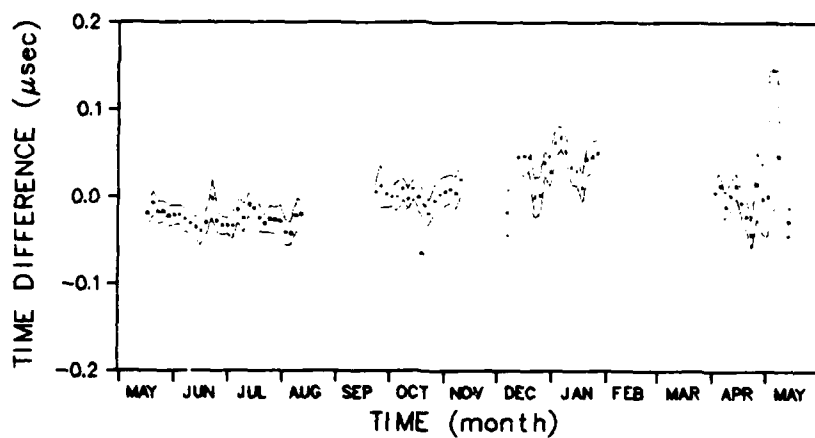
c) Iroquois/LC-204/1

Figure 3.2-1 TDX Seasonal Time Series

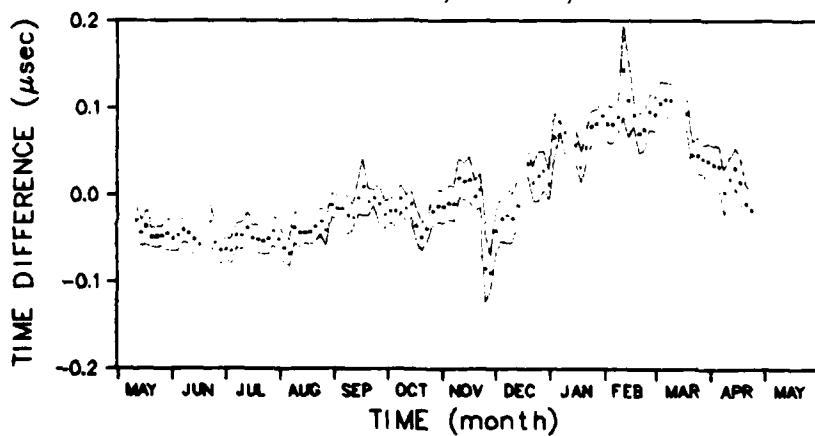
R-63167



a) DeTour/LC-204/2



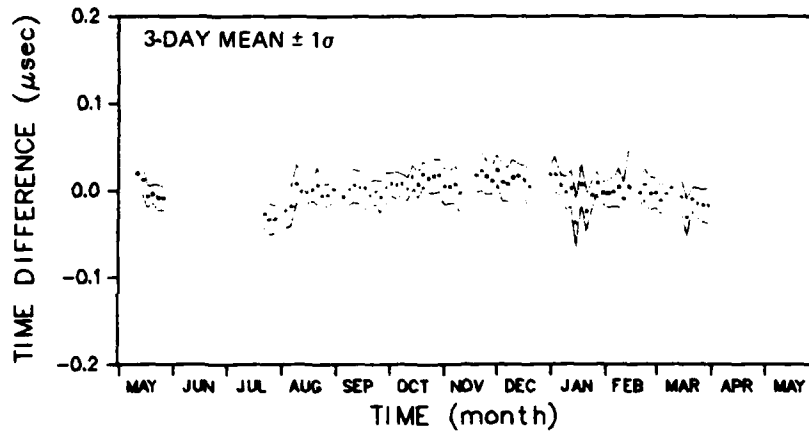
b) Dunbar/LC-204/2



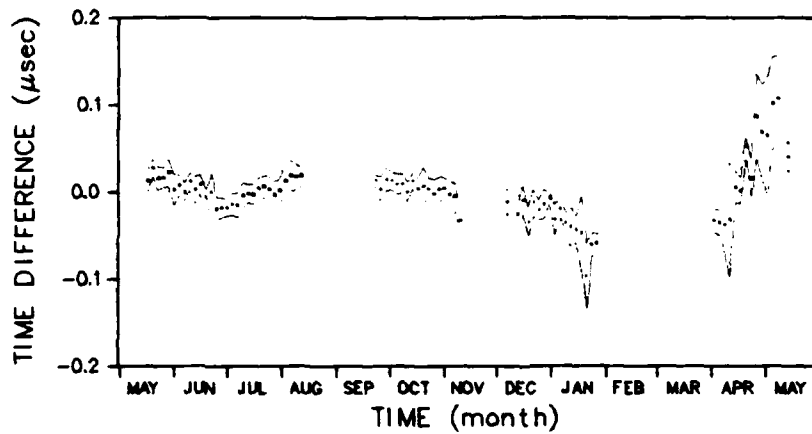
c) Iroquois/LC-204/2

Figure 3.2-2 TDY Seasonal Time Series

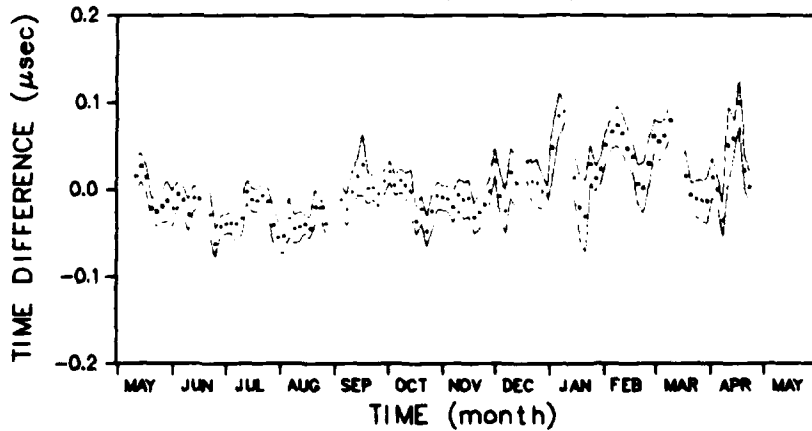
R-63168



a) DeTour/LC-204/2



b) Dunbar/LC-204/2

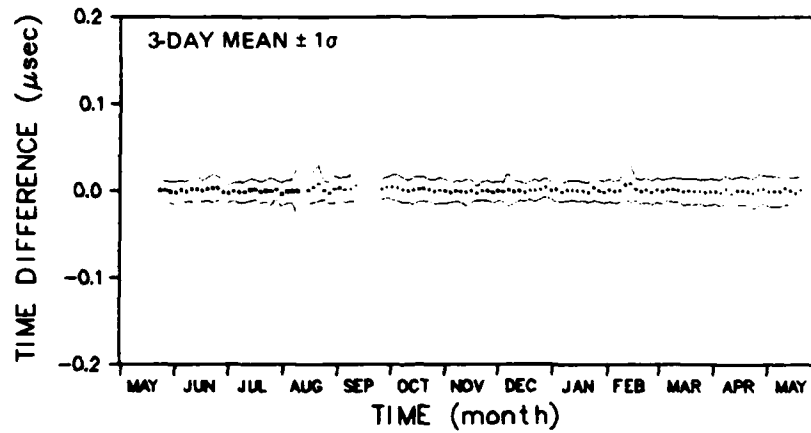


c) Iroquois/LC-204/2

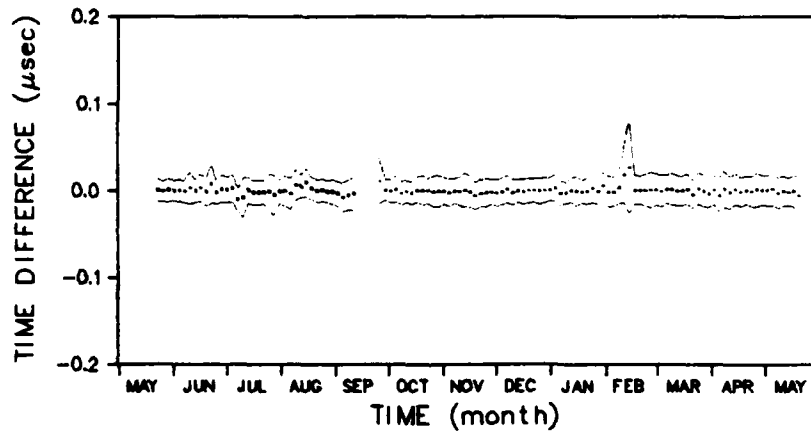
Figure 3.2-3 TDZ Seasonal Time Series



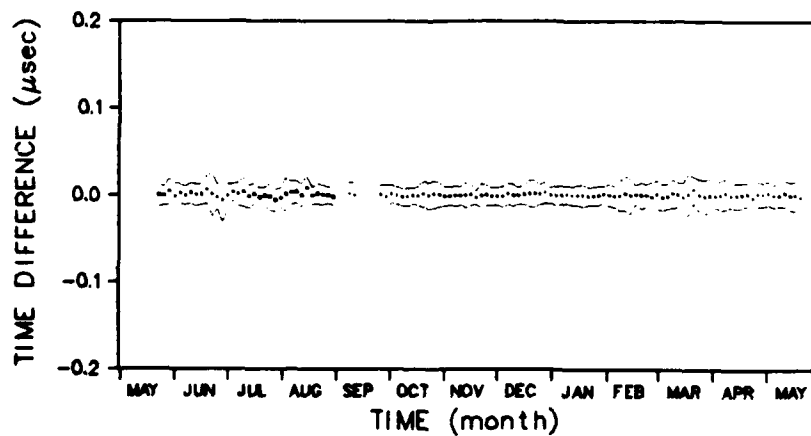
R-63169



a) Time Difference X



b) Time Difference Y



c) Time Difference Z

Figure 3.2-4 SAM Seasonal Time Series

TABLE 3.2-1  
SEASONAL TD STATISTICS

SITE	RECEIVER TYPE/ NUMBER	TIME DIFFERENCE	STATISTICS OF 3-DAY TD MEANS ( $\mu$ sec)		
			MEAN	STANDARD DEVIATION	PEAK-TO-PEAK
DeTour	LC-204/1	X	11328.261	0.032	0.174
		Y	22210.351	0.106	0.532
DeTour	LC-204/2	Y	22210.346	0.082	0.300
		Z	33416.693	0.013	0.061
Dunbar	BRN-5/1	X	11293.276	0.027	0.119
		Y	22363.361	0.045	0.180
Dunbar	LC-204/2	Y	22363.369	0.032	0.189
		Z	33290.870	0.033	0.204
Iroquois	LC-204/1	X	11325.374	0.037	0.146
		Z	33156.894	0.044	0.235
Iroquois	LC-204/2	Y	22413.893	0.052	0.232
		Z	33156.915	0.034	0.162
SAM	Austron/1	X	11259.695	0.002	0.013
		Y	22363.866	0.005	0.037
		Z	33200.397	0.003	0.015

The seasonal component of TD variations dominates the monthly and diurnal components, as expected for Loran-C groundwave propagation.

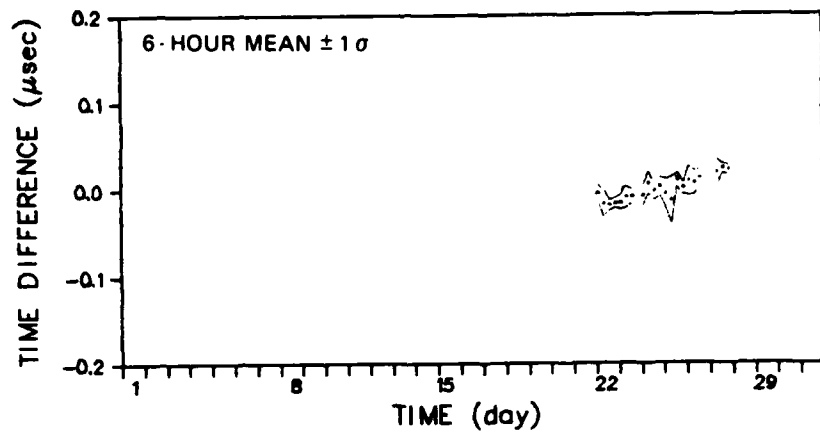
### 3.2.2 Monthly Variations

The distinct difference between summer and winter TD variations is analyzed by focusing on the months of July and January. Monthly TD variations are quantified by the mean and standard deviation of the data in 6-hr time windows (see Figs. 3.2-5 to 3.2-8 for July and Figs. 3.2-9 to 3.2-12 for January). No point is plotted for 6-hr windows which contain fewer than 10 samples.

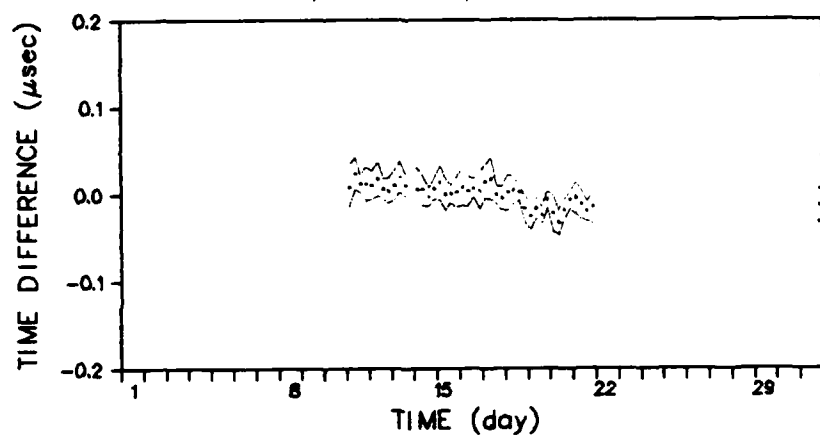
An examination of the monthly time series leads to the following conclusions:

- TD variations are less than 0.10  $\mu$ sec p-p for July, but as large as 0.20  $\mu$ sec p-p for January
- TDs often change very abruptly in January, -- e.g., 0.10  $\mu$ sec during a one- or two-day period
- Diurnal variations are smaller in July than in January, but represent a greater proportion of the overall monthly variation in July
- The 6-hr standard deviations are small relative to the variation of the 6-hr means
- The chain is controlled more effectively by the SAM in January than in July (compare Figs. 3.2-8 and 3.2-12).

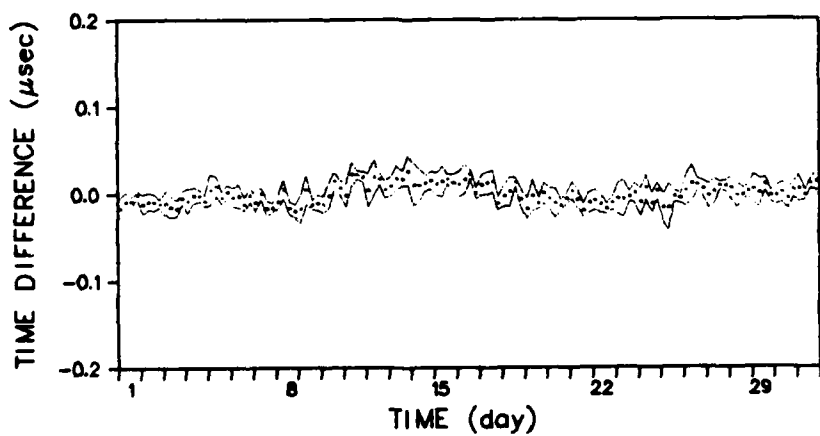
Confirmation of the expected differences between summer and winter TD variations is an important contribution of the St. Marys River Loran-C data collection/analysis effort.



a) DeTour/LC-204/1

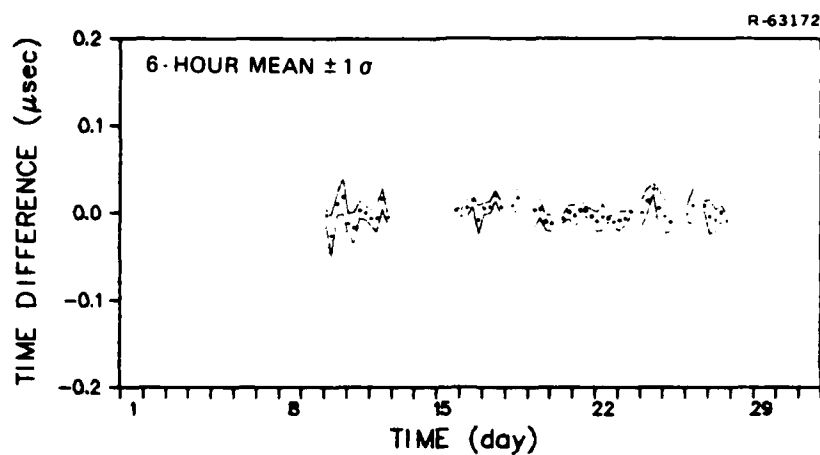


b) Dunbar/BRN-5/1

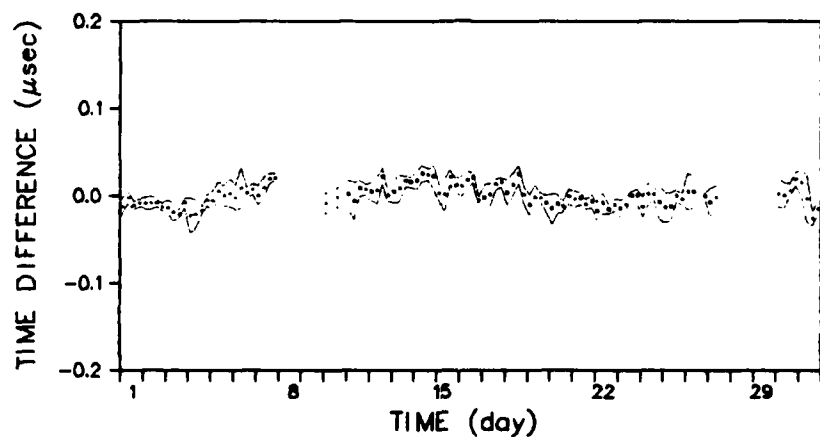


c) Iroquois/LC-204/1

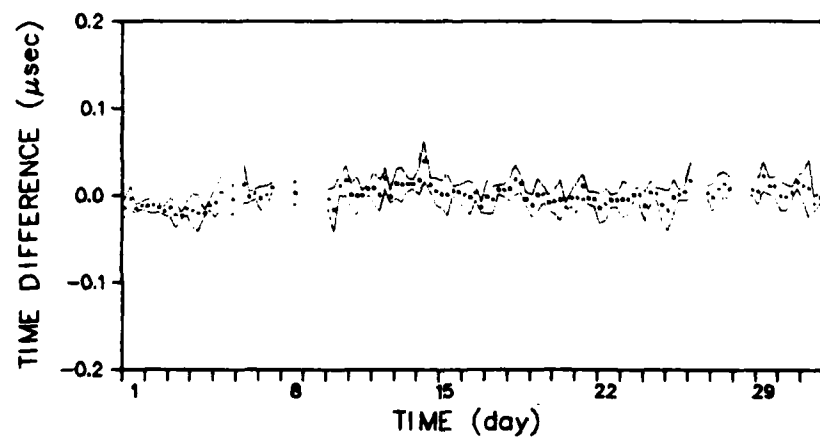
Figure 3.2-5 TDX Monthly Time Series for July



a) DeTour/LC-204/2

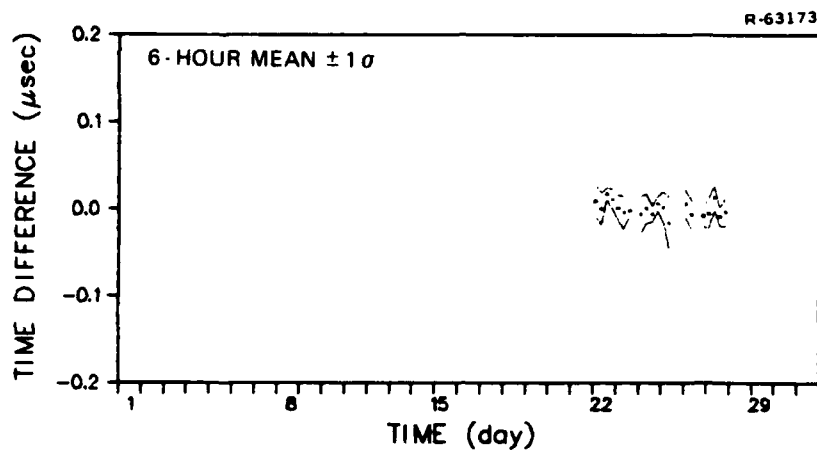


b) Dunbar/LC-204/2

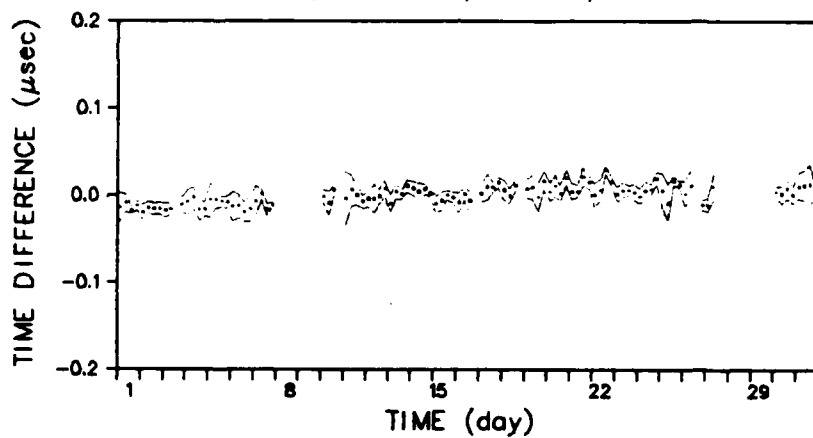


c) Iroquois/LC-204/2

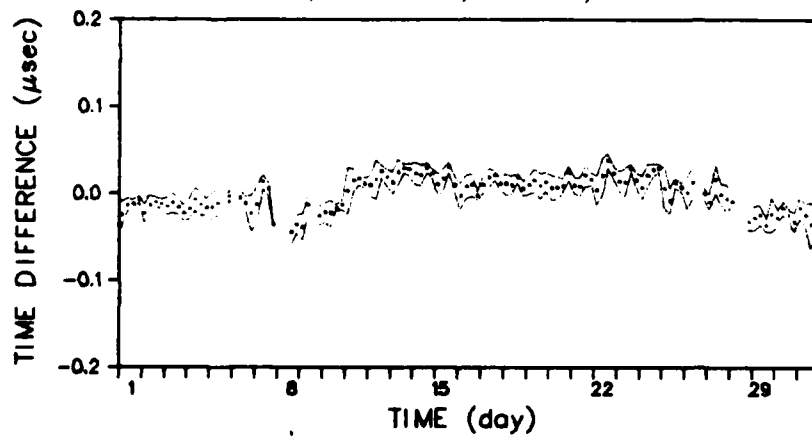
Figure 3.2-6 TDY Monthly Time Series for July



a) DeTour/LC-204/2

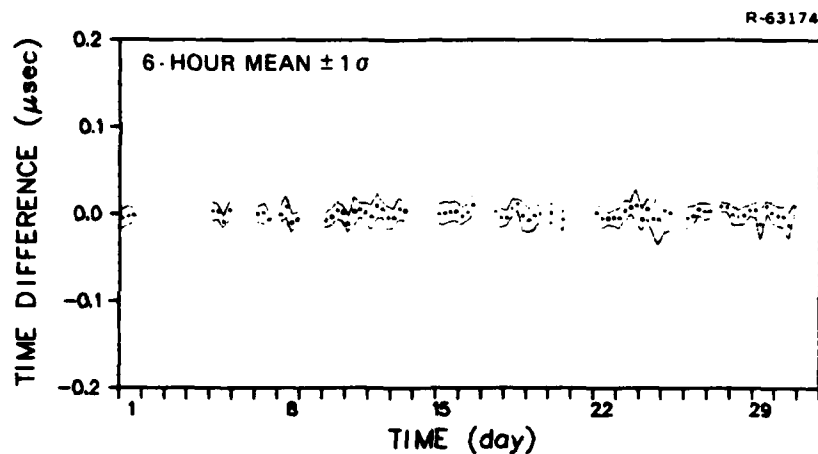


b) Dunbar/LC-204/2

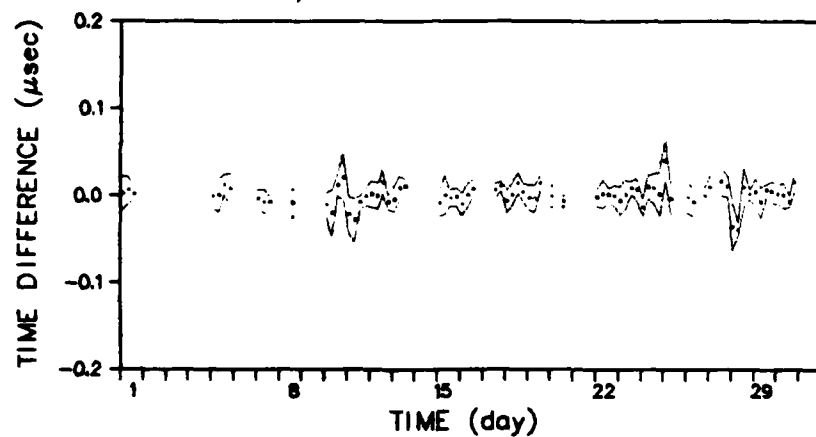


c) Iroquois/LC-204/2

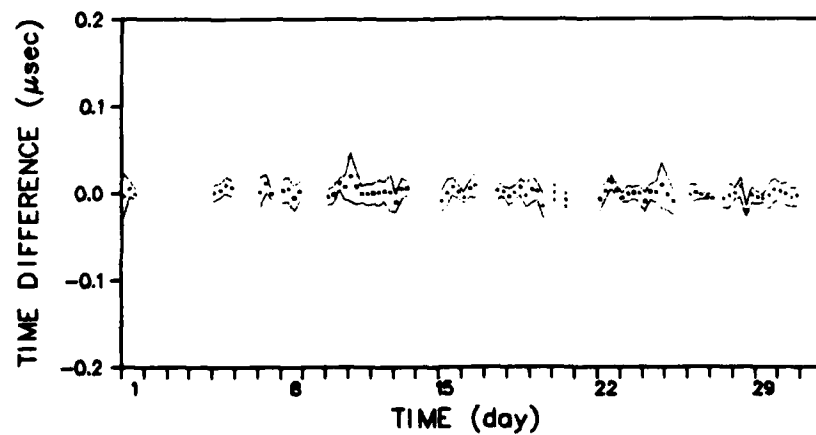
Figure 3.2-7 TDZ Monthly Time Series for July



a) Time Difference X

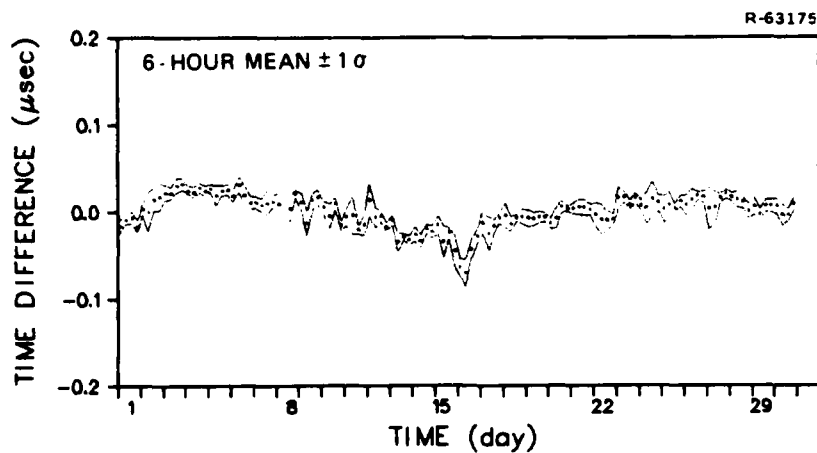


b) Time Difference Y

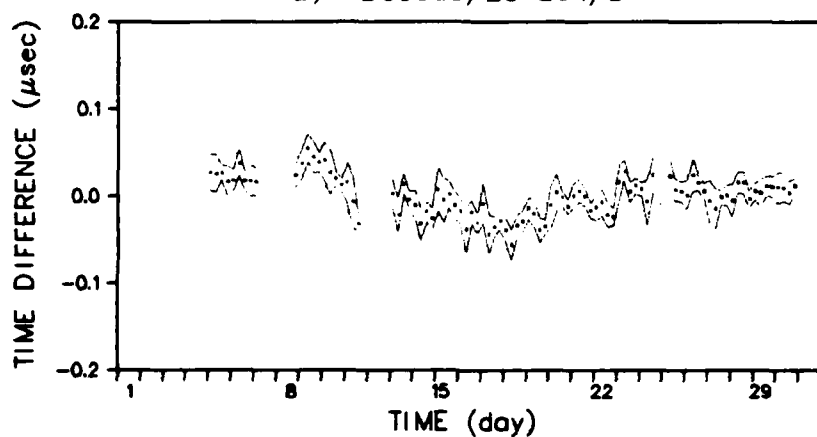


c) Time Difference Z

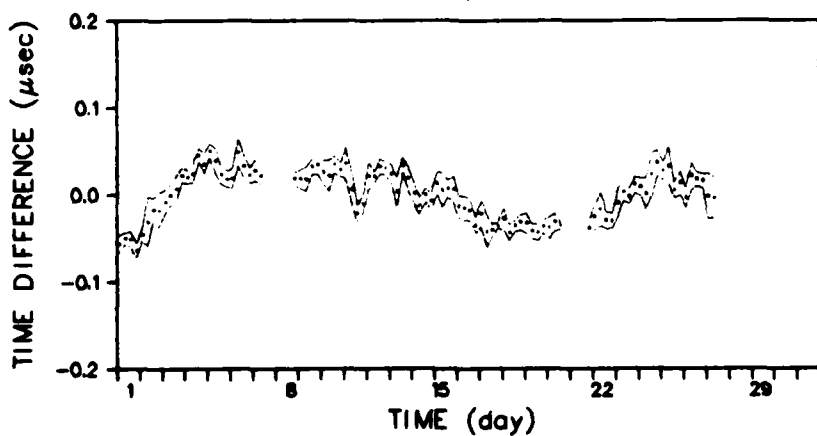
Figure 3.2-8 SAM Monthly Time Series for July



a) DeTour/LC-204/1



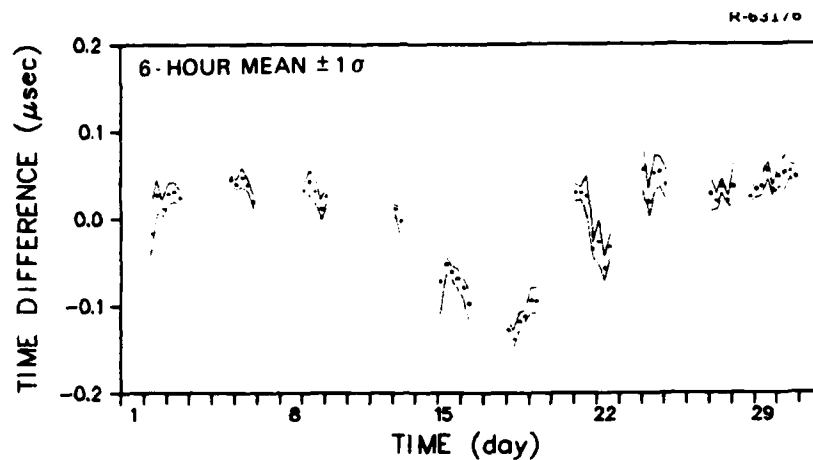
b) Dunbar/BRN-5/1



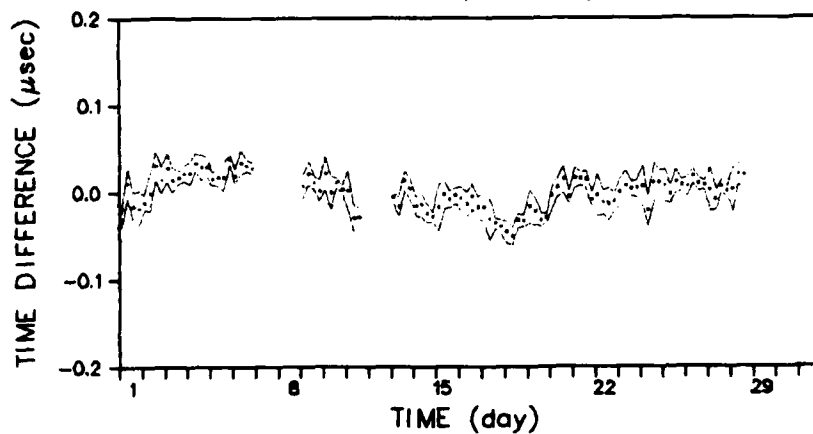
c) Iroquois/LC-204/1

Figure 3.2-9 TDX Monthly Time Series for January

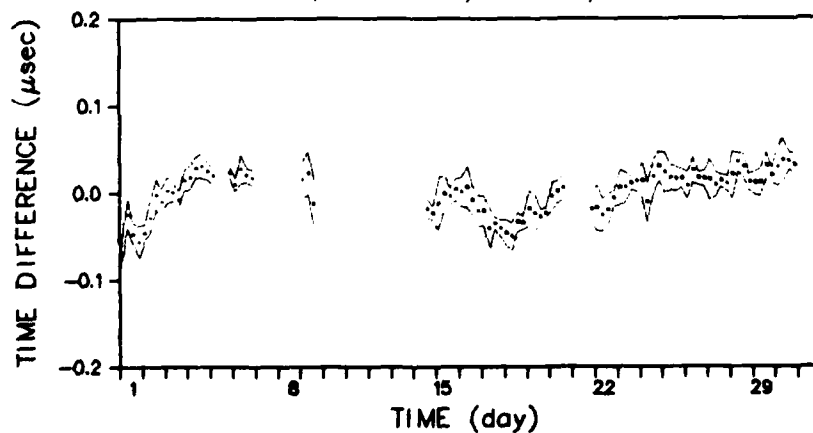




a) DeTour/LC-204/2

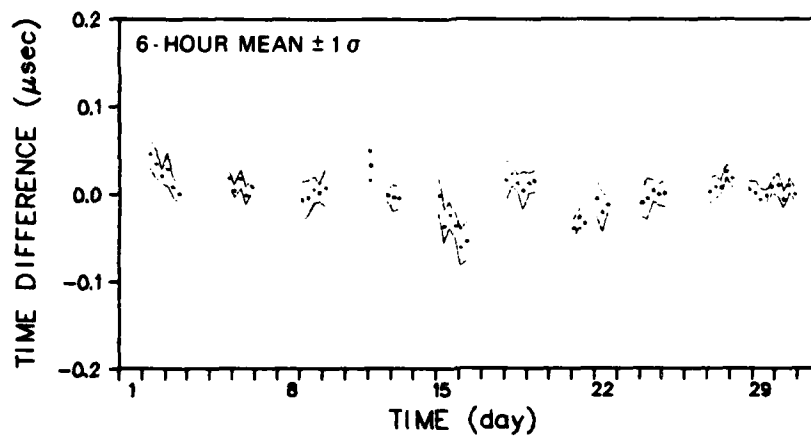


b) Dunbar/LC-204/2

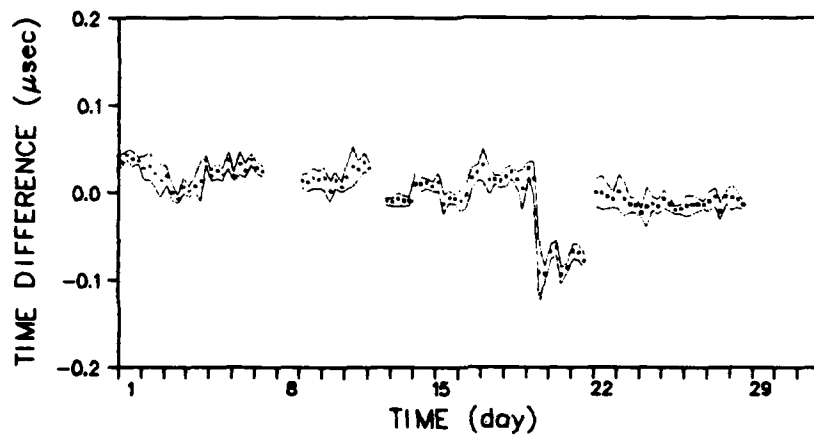


c) Iroquois/LC-204/2

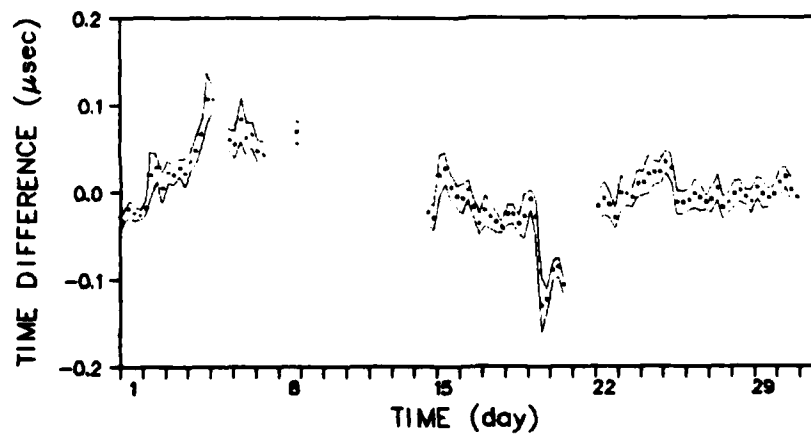
Figure 3.2-10 TDY Monthly Time Series for January



a) DeTour/LC-204/2

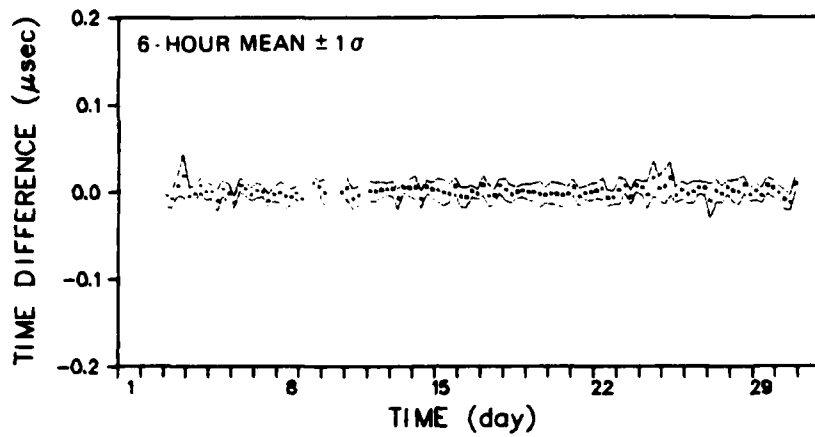


b) Dunbar/LC-204/2

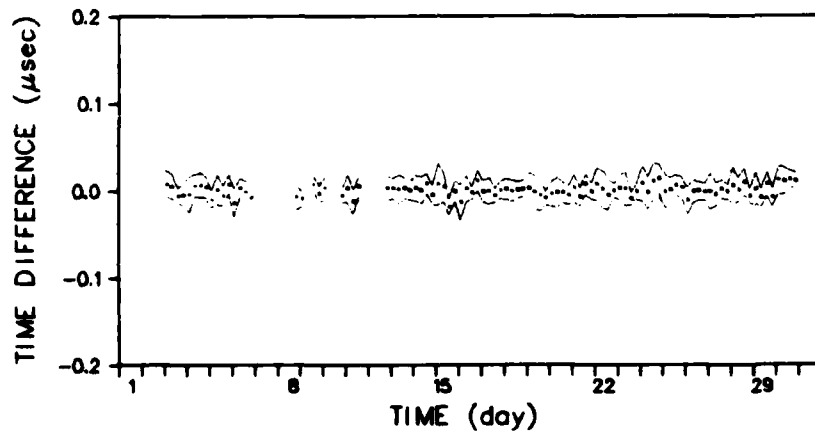


c) Iroquois/LC-204/2

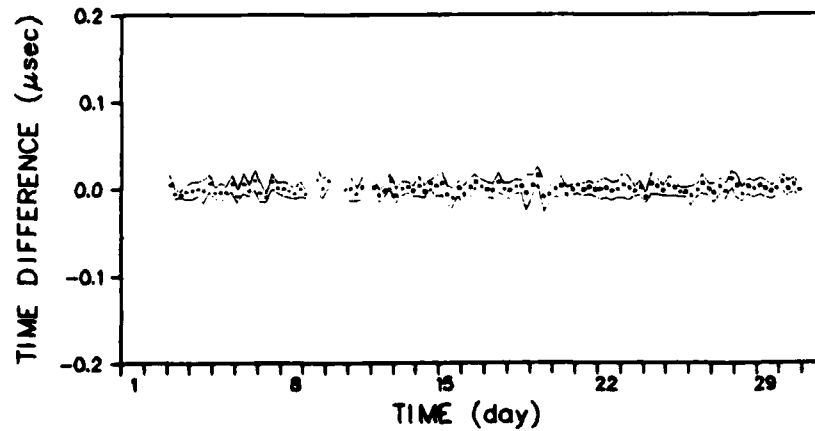
Figure 3.2-11 TDZ Monthly Time Series for January



a) Time Difference X



b) Time Difference Y



c) Time Difference Z

Figure 3.2-12 SAM Monthly Time Series for January

### 3.2.3 Diurnal Variations

Although diurnal variations are small compared to longer-term TD variations, their magnitude is important in selecting pattern monitor sampling rates and user update rates for differential Loran-C. The diurnal TD variations for July and January are analyzed separately herein, using the following procedure:

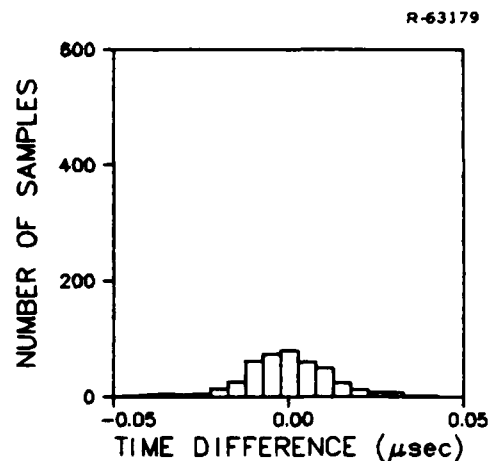
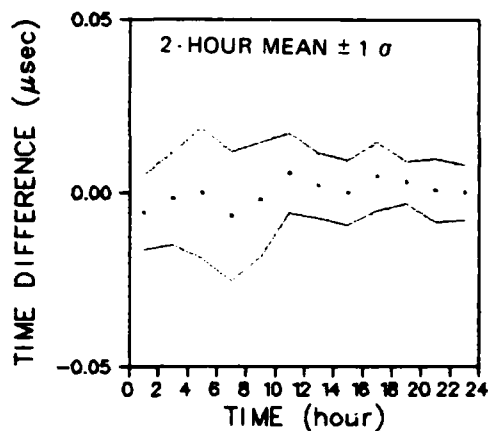
- Sort the data by day and subtract the daily mean to form TD residuals, thus removing the day-to-day variation
- Sort the TD residuals by time-of-day, irrespective of day-of-month, and compute the mean and standard deviation of the residuals in 2-hr time windows (the mean is the diurnal cycle)
- Construct a histogram of the differences between the residuals and the diurnal cycle.

The resulting diurnal cycles and histograms are presented in Figs. 3.2-13 to 3.2-15 for July and in Figs. 3.2-16 to 3.2-18 for January.\*

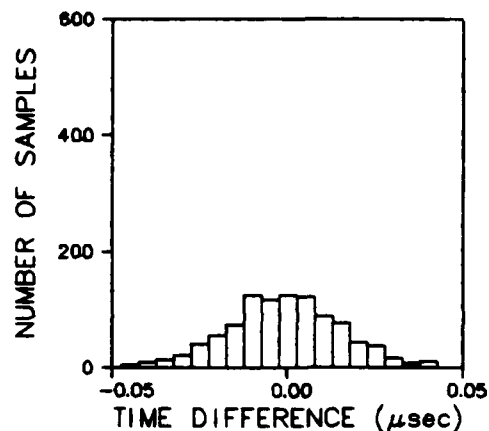
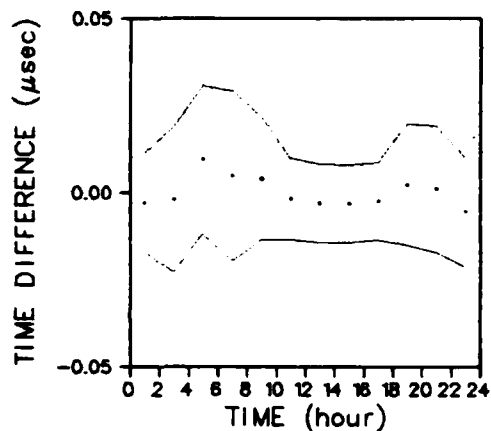
An examination of these results leads to the following conclusions:

- The diurnal cycles are small, generally less than 0.02  $\mu\text{sec}$  p-p

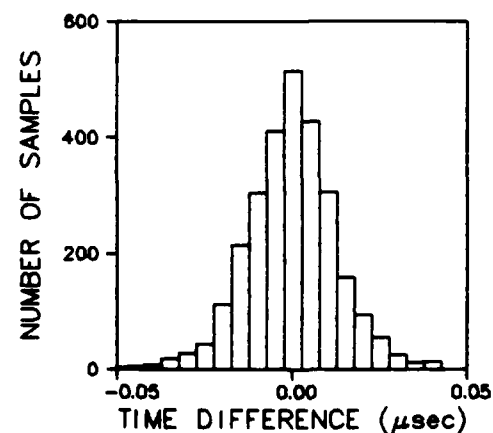
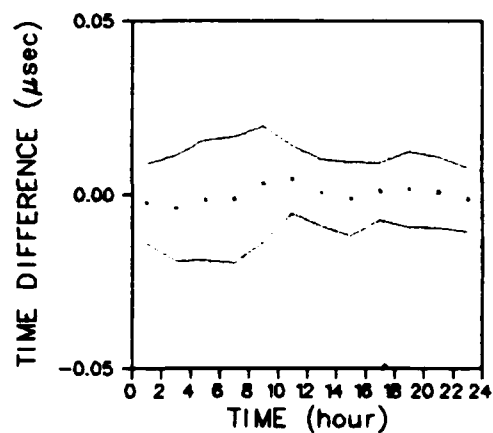
\*The time shown is Greenwich Mean Time (GMT), where 0 hours GMT is 7 p.m. Sault Sainte Marie local time.



a) DeTour/LC-204/1

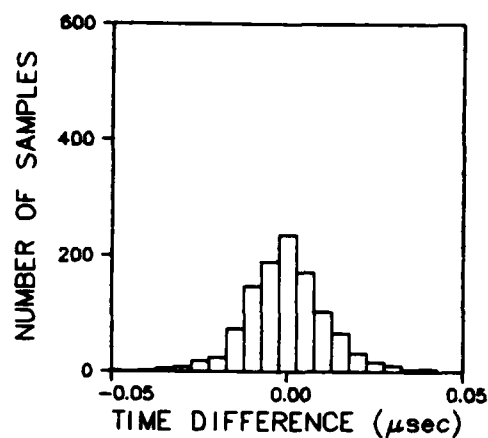
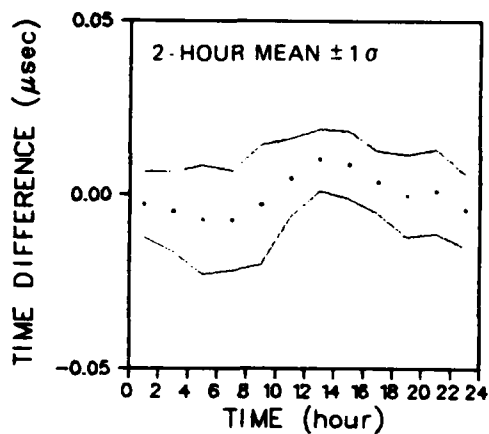


b) Dunbar/BRN-5/1

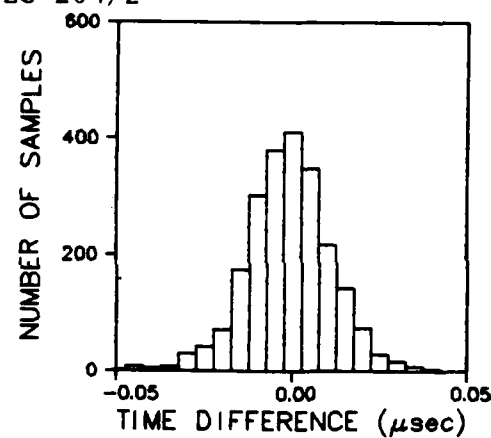
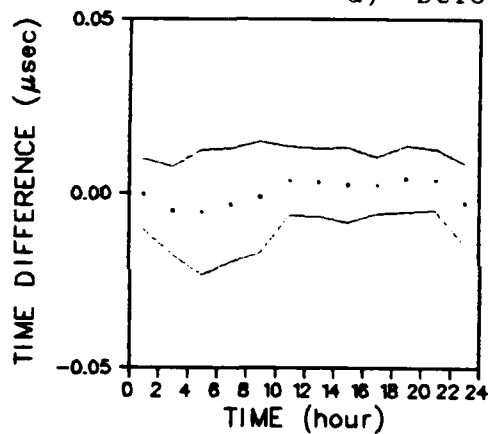


c) Iroquois/LC-204/1

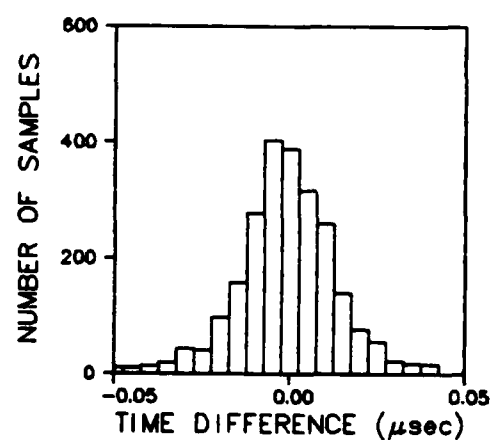
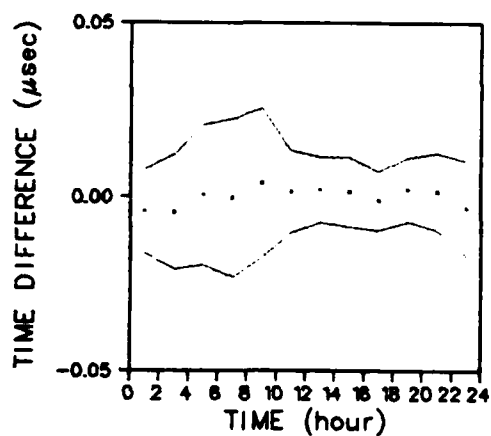
FIG. 3.2-13 TDX Diurnal Cycles and Histograms for July



a) DeTour/LC-204/2

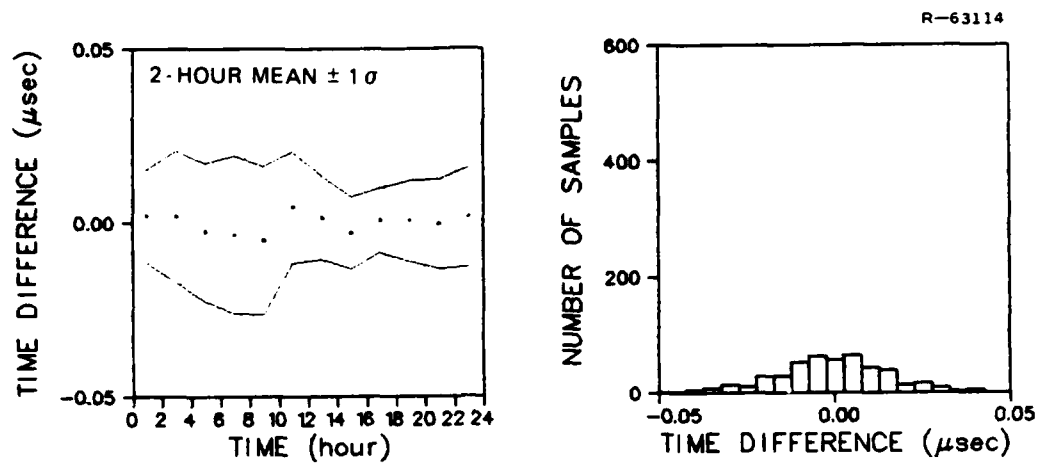


b) Dunbar/LC-204/2

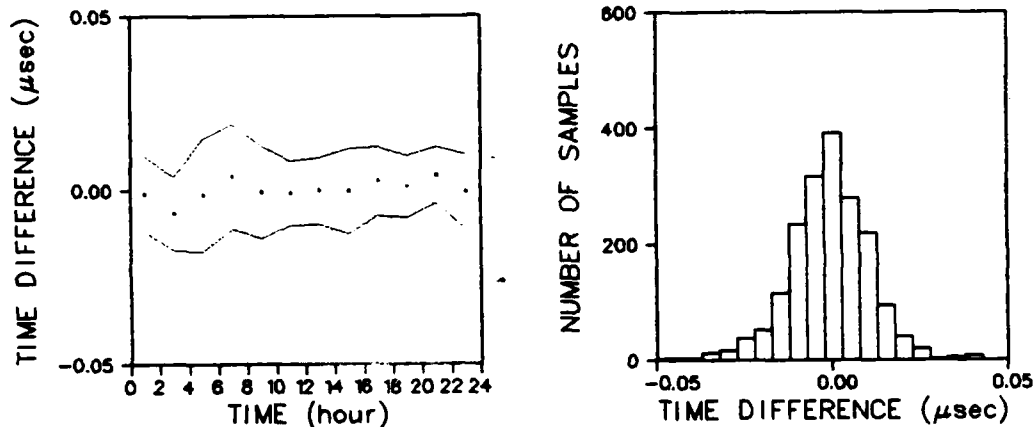


c) Iroquois/LC-204/2

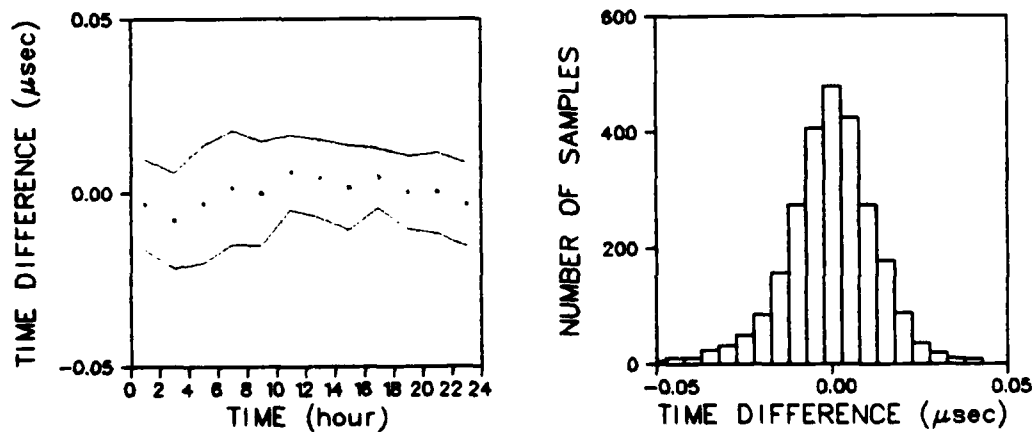
Figure 3.2-14 TDY Diurnal Cycles and Histograms for July



a) DeTour/LC-204/2

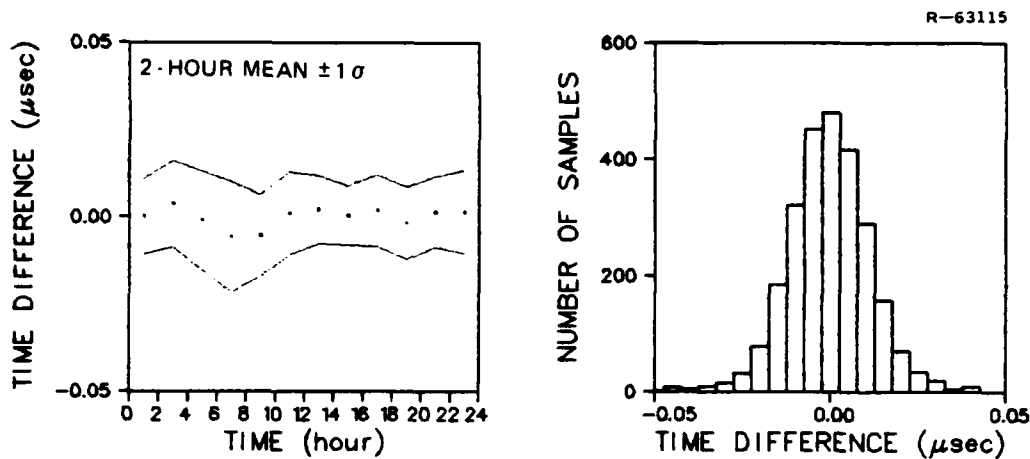


b) Dunbar/LC-204/2

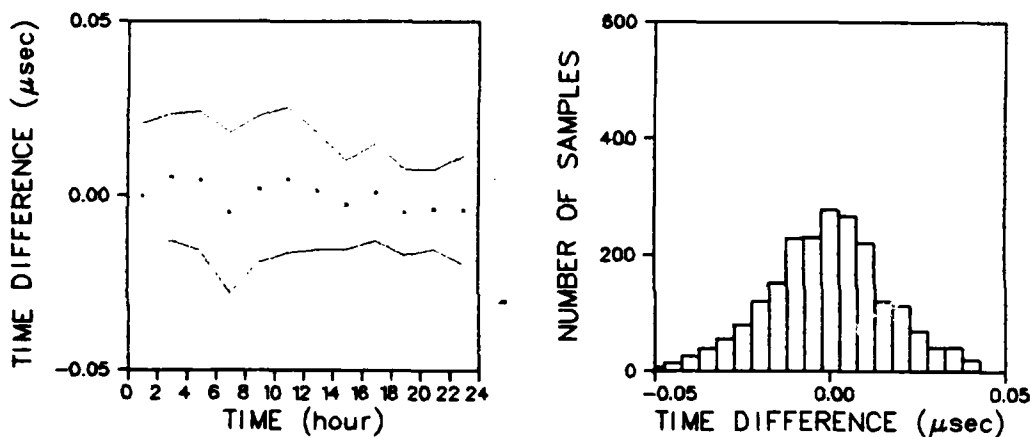


c) Iroquois/LC-204/2

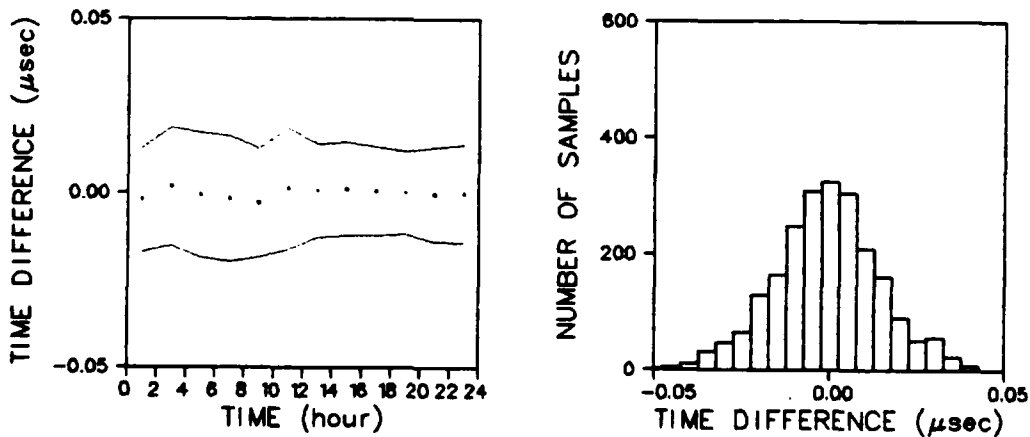
Figure 3.2-15 TDZ Diurnal Cycles and Histograms for July



a) DeTour/LC-204/1



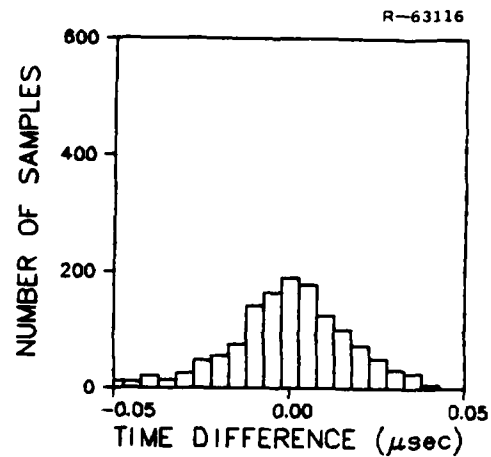
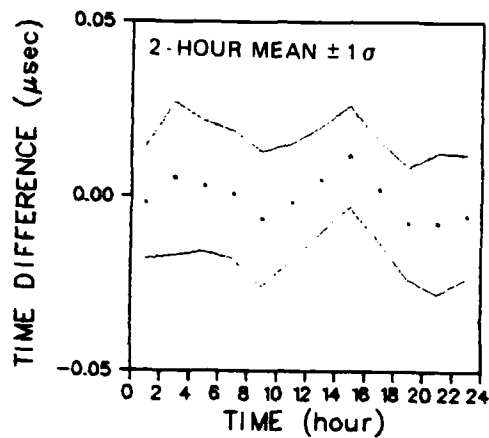
b) Dunbar/BRN-5/1



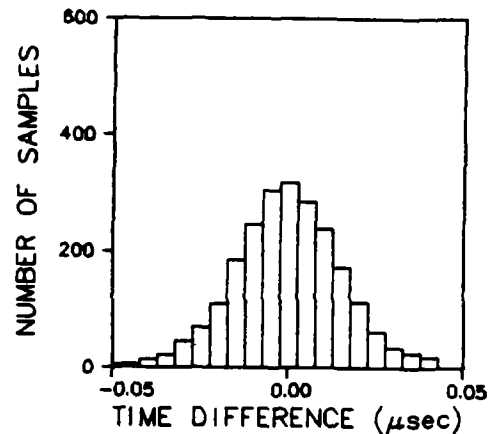
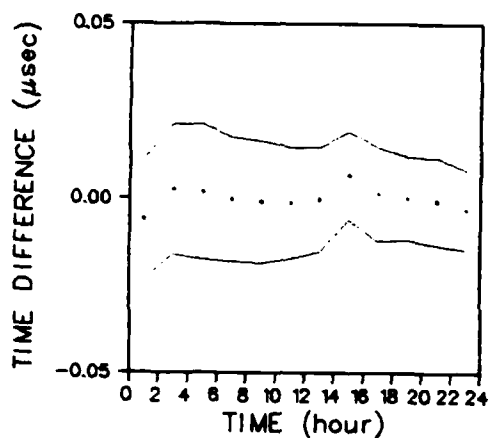
c) Iroquois/LC-204/1

Figure 3.2-16 TDX Diurnal Cycles and Histograms for January

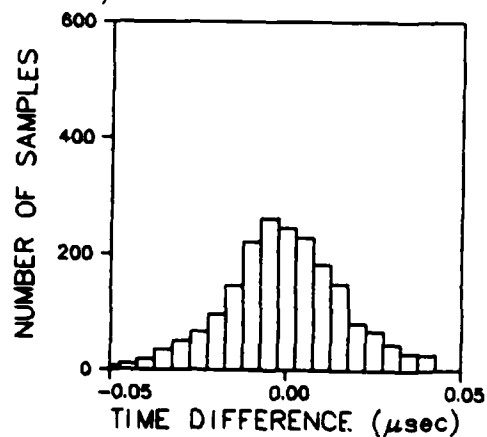
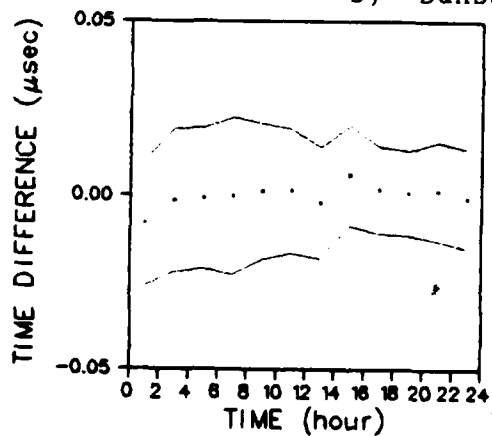




a) DeTour/LC-204/2

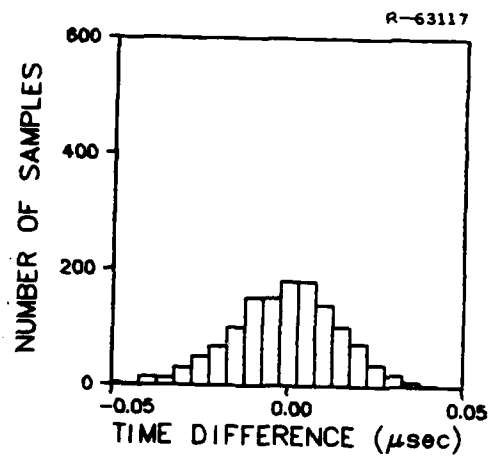
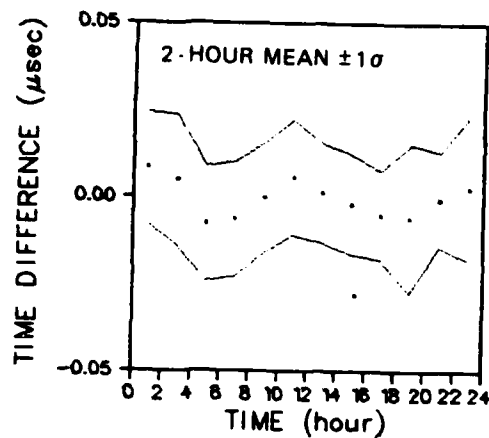


b) Dunbar/LC-204/2

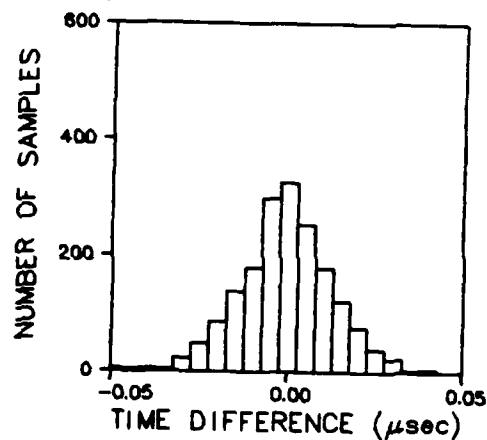
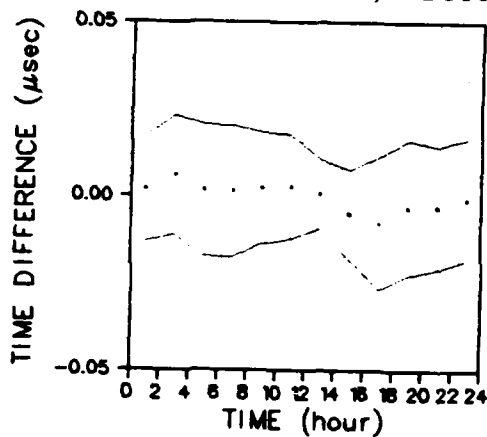


c) Iroquois/LC-204/2

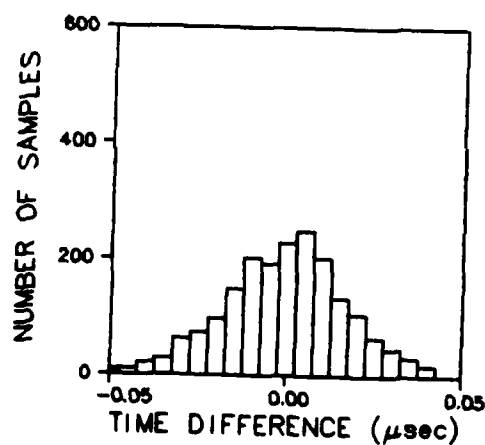
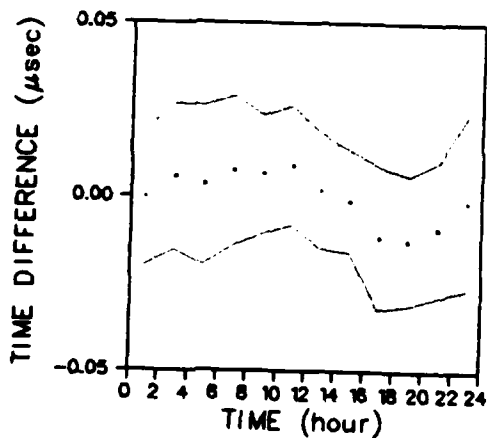
Figure 3.2-17 TDY Diurnal Cycles and Histograms for January



a) DeTour/LC-204/2



b) Dunbar/LC-204/2



c) Iroquois/LC-204/2

Figure 3.2-18 TDZ Diurnal Cycles and Histograms for January

- The diurnal cycle is obscured by random variations (i.e., a large standard deviation) for many time series, but is very distinct for others (e.g., see Fig. 3.2-14a)
- Some diurnal cycles exhibit a bimodal behavior, indicating a 12-hr period (e.g., see Fig. 3.2-17a)
- The 2-hr standard deviations are larger for January than for July, which is inconsistent with the lower atmospheric noise level known to occur in January (Ref. 10)
- The 2-hr standard deviations for July are generally larger at night (0 to 12 hours GMT) than during the day, which is inconsistent with the lower noise levels known to occur at night (Ref. 10)
- The random variations around the diurnal cycle can be characterized by a normal distribution with a standard deviation of approximately 0.02  $\mu$ sec.

The high-frequency detail afforded by the 15-min sampling interval makes the St. Marys River Loran-C data base an important resource for future cause/effect analyses of diurnal variations.

### 3.3 CORRELATION AND SPECTRAL ANALYSES

#### 3.3.1 Autocorrelation Functions and Power Spectral Densities

The relative contribution of seasonal, monthly, and diurnal TD variations is given by the Power Spectral Density (PSD), which is discussed in detail in Refs. 11 to 13. The following procedure is used to compute the PSD in the present study:

- Construct a smoothed time series, consisting of 2-hr averages of the original data, to reduce computer-processing requirements
- Synthesize TD data by linear interpolation to fill any time series gaps
- Remove the mean and trend (i.e., a straight-line fit) from the time series to minimize non-stationarity\*
- Compute the Autocorrelation Function (ACF) of the time series by the technique described in Ref. 13, which involves the Fast Fourier Transform
- Multiply the ACF by a Kaiser window (Ref. 14), which has the effect of smoothing the PSD
- Compute the PSD as the Fast Fourier Transform of the ACF.

This procedure is adopted based on previous TASC experience in data processing, after conducting various tests on the present data.

The 2-hr averaging time is chosen because no significant spectral peaks are found to occur for periods<sup>†</sup> less than 10 hr. A 2-hr averaging time guarantees that the computed PSD is meaningful for periods greater than 4 hr, i.e., the Nyquist sampling period. Linear interpolation is selected for data synthesis, based on a comparison with two alternative techniques:

---

\*Non-stationarity occurs when the length of the time series is short compared to the period of the low-frequency components (Ref. 12).

†The period of a spectral component is the inverse of the cyclical frequency.

placing zeroes in the gaps and ignoring the gaps (i.e., "squeezing" the time series). Interpolation preserves the low-frequency content of the data, and does not introduce discontinuities into the time series or associated spurious frequencies into the spectrum. Detrending is an important aspect of the PSD-computation procedure in cases where the TD values in May 1979 and May 1980 differ significantly. If the TD trend is not removed, the PSD and ACF are distorted by the occurrence of high energy near zero frequency.

ACFs and PSDs computed by the aforementioned procedure are presented in Figs. 3.3-1 to 3.3-3. The time series all contain spectral peaks at the 24-hr and 12-hr periods (0.042 cycle/hr and 0.083 cycle/hr, respectively, in the PSD plots). The 24-hr diurnal peak is 10 to 20 dB below the zero-frequency spectral level and, in some cases, is more than 10 dB above the spectral level at adjacent frequencies (e.g., see Fig. 3.3-3b). The ACF generally decreases with increasing time lag, and contains a sinusoid-like component with a period of 24 hr.

The width of the 24-hr "hump" in the PSD depends on the seasonal variation (i.e., modulation) of the diurnal-cycle amplitude. The hump would be a "spike" if the diurnal cycle were a pure sinusoid with constant amplitude. The 12-hr component in the PSD may be partly due to the bimodal diurnal cycle identified in Section 3.2.3. However, such a component is expected to arise even for a unimodal diurnal cycle, if the cycle is not a pure amplitude-modulated sinusoid. Indeed, the 12-hr component is the first harmonic of the fundamental 24-hr component.

The slope of the ACF differs significantly for the various time series. The slope is governed largely by the

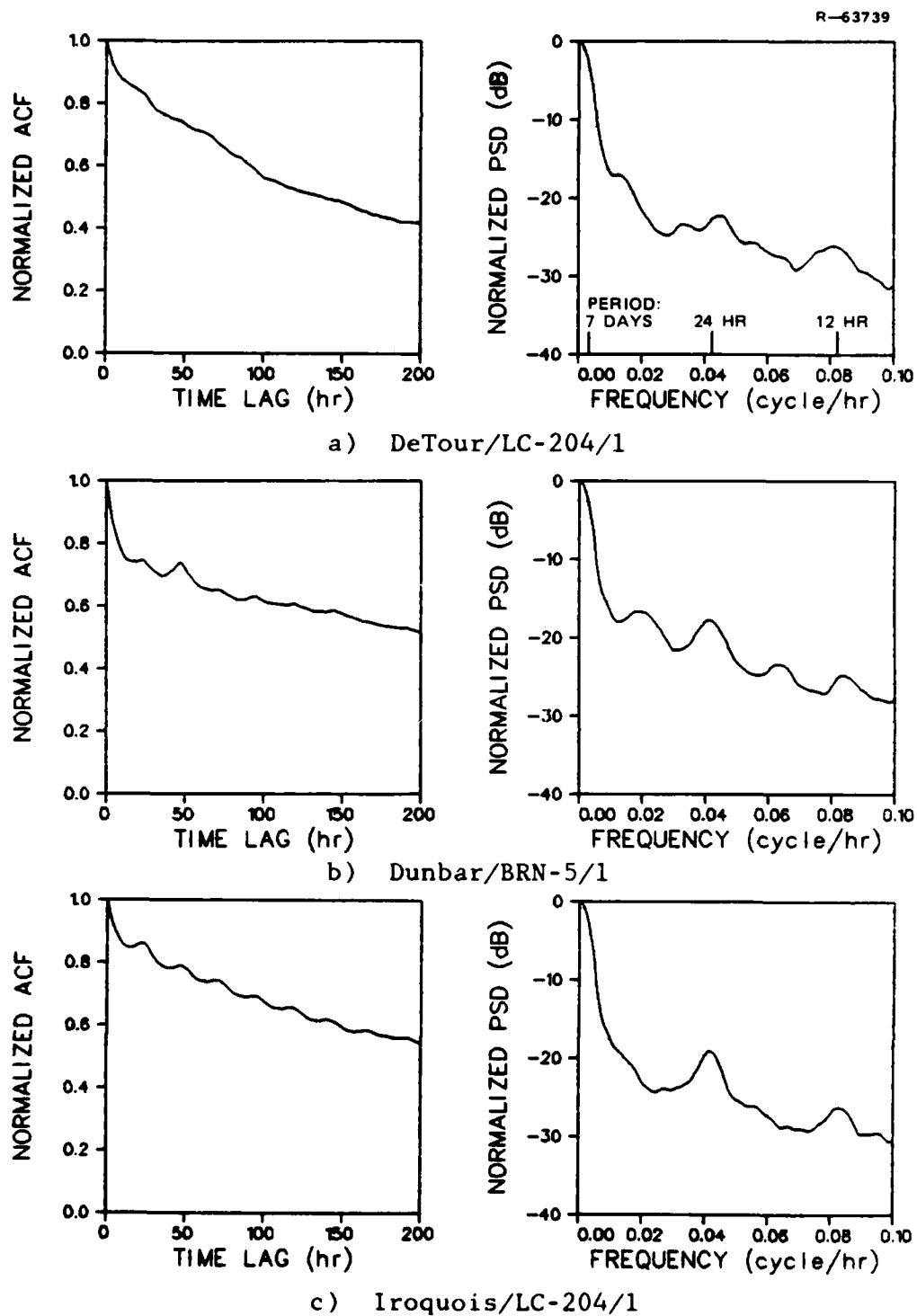
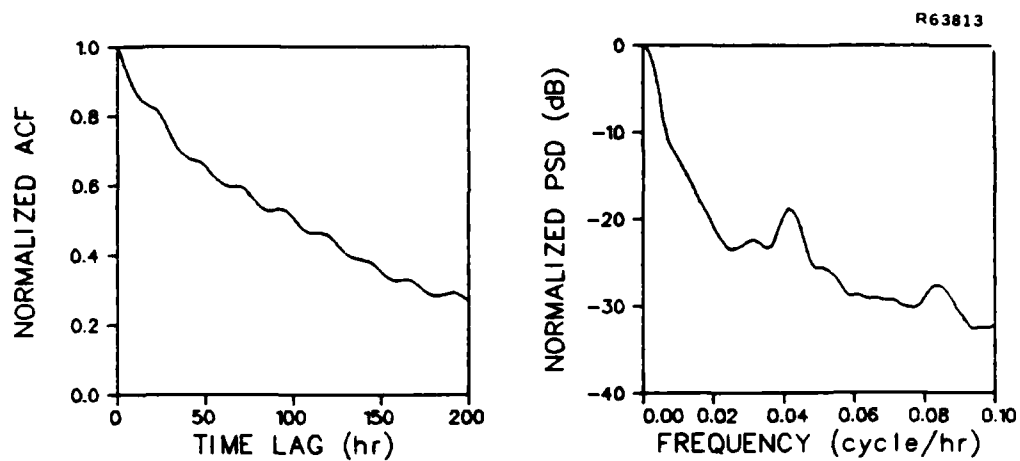
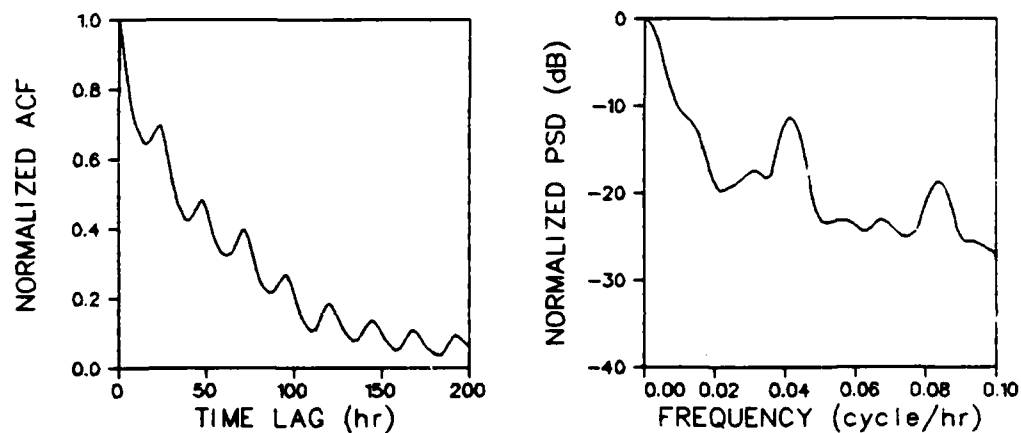


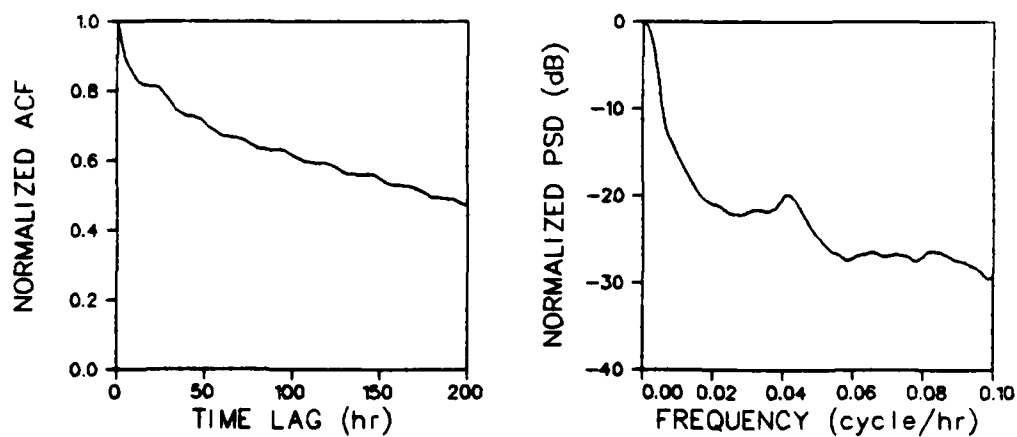
Figure 3.3-1 Autocorrelation Functions and Power Spectral Densities for TDX



a) DeTour/LC-204/2



b) Dunbar/LC-204/2



c) Iroquois/LC-204/2

Figure 3.3-2 Autocorrelation Functions and Power Spectral Densities for TDY

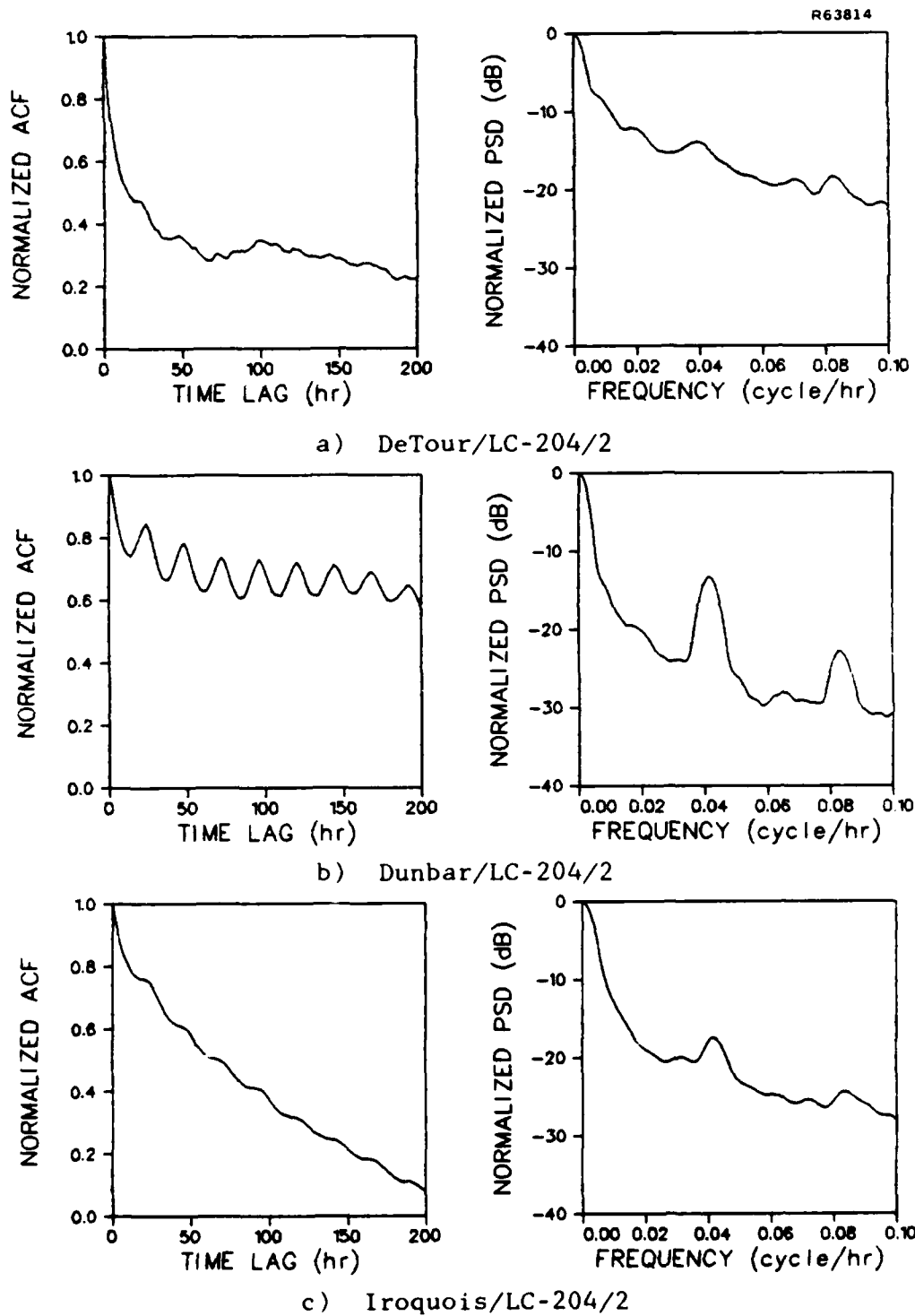


Figure 3.3-3 Autocorrelation Functions and Power Spectral Densities for TDZ



nature of the low-frequency (seasonal) variations. Because the seasonal variations may differ from year to year and the ACF is based on one year of data, the ACFs are not particularly useful for comparison purposes. In other words, the time series are not strictly stationary. Some improvement in stationarity can be achieved by high-pass filtering the data to remove seasonal variations which can not be removed by simple detrending. A comparison of ACFs, with and without filtering, is presented in Fig. 3.3-4 to illustrate this point. The ACF with filtering crosses zero at a time lag of approximately 3 days, which is consistent with U.S. Coast Guard analyses of one-month segments of low-density data (e.g., Ref. 16). Filtering is not performed in the ACF/PSD analyses in this study, to permit a comparison between the actual spectral levels at zero and diurnal frequencies. However, it should be kept in mind that the relative spectral levels may be different in other years.

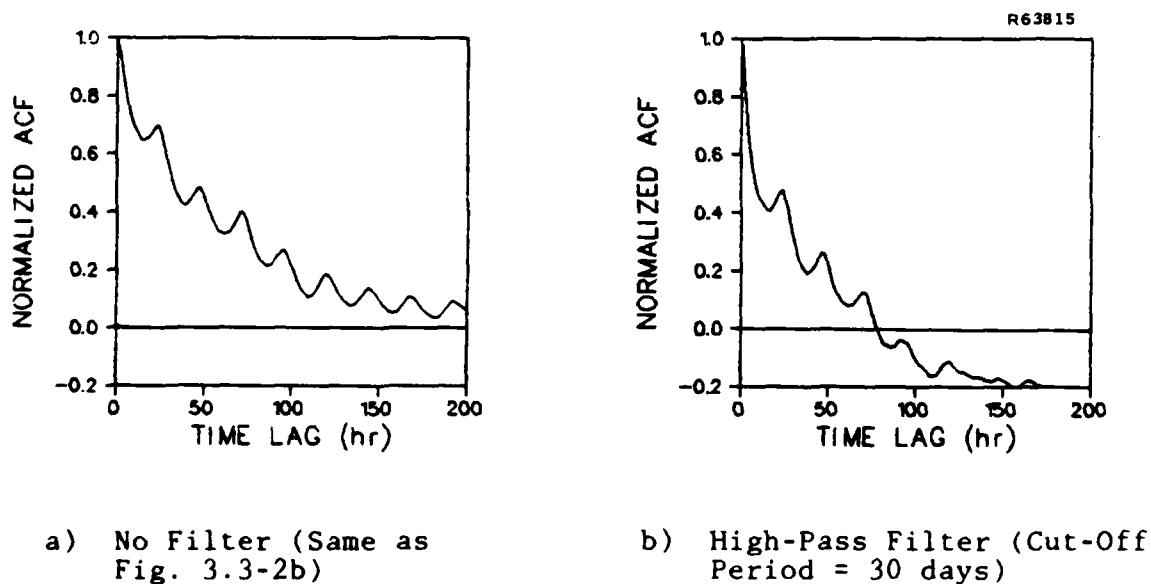


Figure 3.3-4 Effect of High-Pass Filtering on the ACF  
(TDY for Dunbar/LC-204/2)

### 3.3.2 Correlation of TD Pairs

Relationships among the various TDs are identified by correlating pairs of time series. The 3-day smoothed seasonal time series presented in Section 3.2.1 are used for this purpose.

Correlation coefficients ( $\rho$ ) for TD pairs arranged by site are presented in Tables 3.3-1 to 3.3-3. Of particular interest is the correlation of redundant TDs, i.e., those measured at the same site with different receivers. Redundant TDY data collected with the two LC-204 receivers at DeTour exhibit a correlation coefficient of 0.94 and, therefore, are nearly identical. However, the redundant TDY data collected with the BRN-5 and LC-204 receivers at Dunbar are less highly correlated ( $\rho = 0.80$ ). The smaller correlation may be caused by differences in the Magnavox and Internav signal-processing techniques or notch-filter settings. The low correlation between the TDZ data collected with the two LC-204 receivers at Iroquois ( $\rho = 0.61$ ) suggests that at least one of these receivers may not be functioning properly.

Correlation coefficients for TD pairs arranged by station are presented in Tables 3.3-4 to 3.3-6. These results reveal that TDY data for the three sites are highly correlated ( $\rho = 0.87$  to  $0.94$ ). This high correlation, together with the low correlation for TDX and TDZ, suggests that TDY variations are caused by a common non-propagation mechanism. The mechanism is necessarily associated with either the TDY channel of the Austron-5000 receiver at the SAM or with transmitter Y itself. The relationship between TDY and temperature variations is explored in Section 3.3.3.

TABLE 3.3-1  
CORRELATION COEFFICIENTS FOR DETOUR

		LC-204/1		LC-204/2	
		TDX	TDY	TDY	TDZ
LC-204/1	TDX	+1.00	—	—	—
	TDY	+0.66	+1.00	—	—
LC-204/2	TDY	+0.36	+0.94	+1.00	—
	TDZ	+0.53	+0.07	+0.05	+1.00

TABLE 3.3-2  
CORRELATION COEFFICIENTS FOR DUNBAR

		BRN-5/1		LC-204/2	
		TDX	TDY	TDY	TDZ
BRN-5/1	TDX	+1.00	—	—	—
	TDY	+0.89	+1.00	—	—
LC-204/2	TDY	+0.69	+0.80	+1.00	—
	TDZ	-0.69	-0.83	-0.08	+1.00

TABLE 3.3-3  
CORRELATION COEFFICIENTS FOR IROQUOIS

		LC-204/1		LC-204/2	
		TDX	TDZ	TDY	TDZ
LC-204/1	TDX	+1.00	—	—	—
	TDZ	+0.41	+1.00	—	—
LC-204/2	TDY	+0.84	+0.40	+1.00	—
	TDZ	+0.59	+0.61	+0.71	+1.00

TABLE 3.3-4  
CORRELATION COEFFICIENTS FOR TDY

		DETOUR	DUNBAR	IROQUOIS
		LC-204/1	BRN-5/1	LC-204/1
DETOUR	LC-204/1	+1.00	-	-
DUNBAR	BRN-5/1	+0.22	+1.00	-
IROQUOIS	LC-204/1	+0.18	+0.56	+1.00

TABLE 3.3-5  
CORRELATION COEFFICIENTS FOR TDY

		DETOUR	DUNBAR	IROQUOIS
		LC-204/2	LC-204/2	LC-204/2
DETOUR	LC-204/2	+1.00	-	-
DUNBAR	LC-204/2	+0.94	+1.00	-
IROQUOIS	LC-204/2	+0.87	+0.88	+1.00

TABLE 3.3-6  
CORRELATION COEFFICIENTS FOR TDZ

		DETOUR	DUNBAR	IROQUOIS
		LC-204/2	LC-204/2	LC-204/2
DETOUR	LC-204/2	+1.00	-	-
DUNBAR	LC-204/2	+0.10	+1.00	-
IROQUOIS	LC-204/2	+0.07	-0.17	+1.00

Each correlation coefficient presented above is a measure of the relationship between two seasonal time series. It is also of interest to determine the short-term correlation, by employing a more refined time scale. The coherency spectrum, which in effect shows the correlation coefficient as a function of frequency, is very useful in this regard. The coherency spectrum is related to the cross PSD, which in turn is computed as the Fast Fourier Transform of the cross-correlation function (Ref. 12). Examples of the cross-correlation function and coherency spectrum are given in Fig. 3.3-5 for TDX vs TDY data from the Dunbar/BRN-5/1 receiver. The coherency at zero frequency is approximately 0.89, the same as the correlation coefficient previously given in Table 3.3-2. However, the coherency decreases rapidly and is less than 0.50 for frequencies greater than 0.01 cycle/hr (i.e., periods less than 4 days). Based on these results, TD/TD relationships are expected to be more pronounced on a seasonal rather than diurnal time scale. The value of the cross-correlation function at zero time lag (0.75; see Fig. 3.3-5) can be interpreted as an "ensemble average" correlation coefficient over all frequencies. However, it should be recognized that this average value is weighted by the energy at each frequency and, thus, is closer to the zero-frequency coherency than otherwise expected.

### 3.3.3 Correlation of TDs with Temperature and Refractive Index

Meteorological data from the National Weather Service Station at Sault Sainte Marie, Michigan were provided to TASC on magnetic tape by the U.S. Coast Guard. The data include the dry-bulb, wet-bulb, and dew-point temperatures and the relative humidity, all recorded at 3-hr intervals. The 3-day

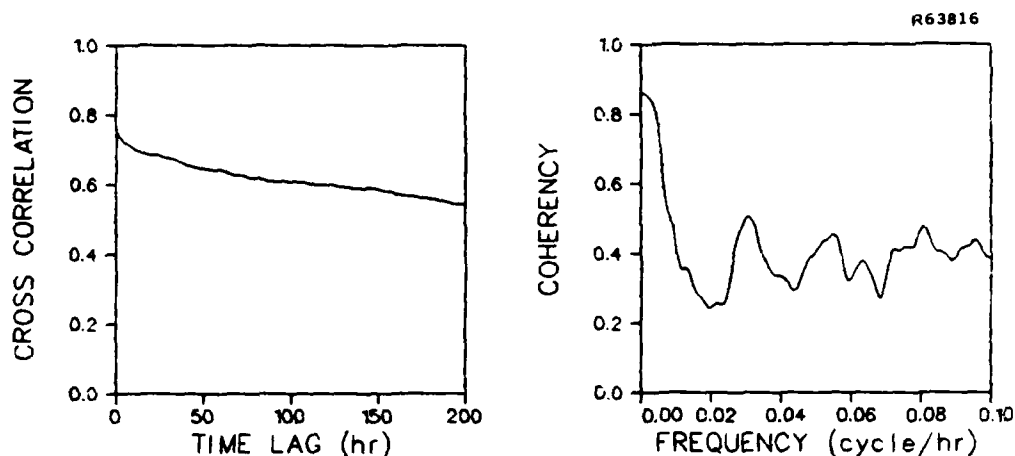


Figure 3.3-5 Cross-Correlation Function and Coherency Spectrum for TDX vs TDY Data (Dunbar/BRN-5/1)

smoothed dry-bulb temperature is shown in Fig. 3.3-6 and refractivity\*, computed by the formula in Refs. 3 and 8, is presented in Fig. 3.3-7.

Correlation coefficients for TDs vs temperature and TDs vs refractivity are given in Table 3.3-7. These results indicate a relatively strong negative correlation ( $\rho = -0.77$  to  $-0.85$ ) between TDY and temperature for all sites and receivers. Because the TD/temperature correlation is generally weaker for TDY than for TDX and TDZ, it appears that the temperature effect is not related to chain-wide propagation conditions. This contention is further justified by the TD/refractivity correlation coefficients presented in Table 3.3-7, which are all less than or equal to 0.61 in absolute value. The order of the TD/refractivity correlation coefficients is the same as for the TD/temperature correlation coefficients, because of the dependence of refractivity on temperature. However, the fundamental parameter is clearly temperature.

\*Refractivity = (refractive index - 1.0)  $\times 10^6$ .  
3-35

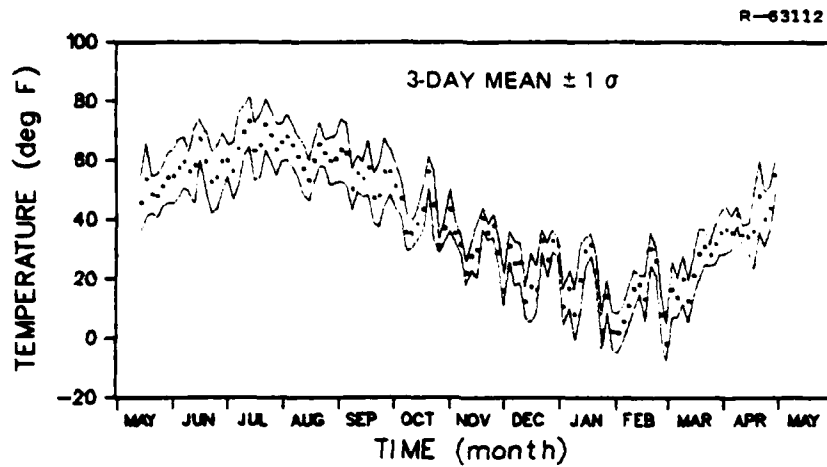


Figure 3.3-6 Temperature Seasonal Time Series

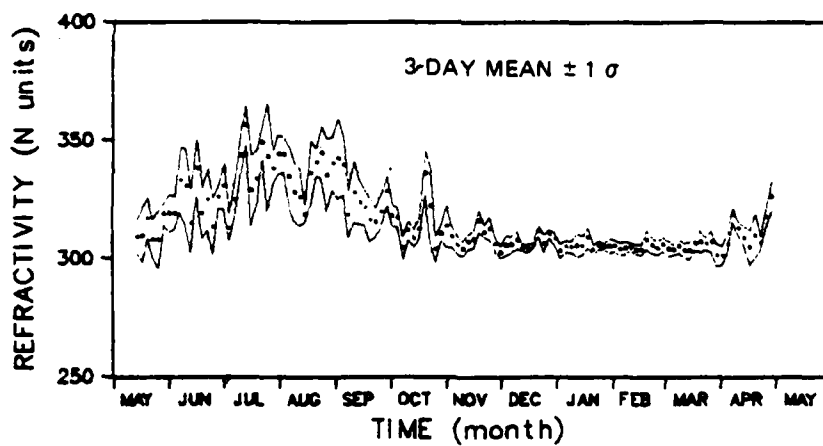


Figure 3.3-7 Refractivity Seasonal Time Series

TABLE 3.3-7  
CORRELATION OF TDs WITH TEMPERATURE AND REFRACTIVITY

SITE	RECEIVER TYPE/ NUMBER	TIME DIFFERENCE	CORRELATION COEFFICIENTS	
			TD vs TEMPERATURE	TD vs REFRACTIVITY
DeTour	LC-204/1	X	-0.22	-0.14
		Y	-0.77	-0.55
DeTour	LC-204/2	Y	-0.84	-0.57
		Z	-0.19	-0.24
Dunbar	BRN-5/1	X	-0.70	-0.50
		Y	-0.80	-0.61
Dunbar	LC-204/2	Y	-0.85	-0.61
		Z	+0.54	+0.35
Iroquois	LC-204/1	X	-0.76	-0.56
		Z	-0.51	-0.31
Iroquois	LC-204/2	Y	-0.80	-0.60
		Z	-0.66	-0.51

The correlation between TDY and temperature is further explored by computing the cross-correlation function and coherency spectrum in the case of the Iroquois/LC-204/2 data (see Fig. 3.3-8). The coherency is approximately 0.80 at zero frequency, consistent with the correlation coefficient presented in Table 3.3-7. However, the coherency falls off rapidly with increasing frequency, suggesting that the effect of temperature is primarily seasonal. The U.S. Coast Guard has computed TD/temperature correlation coefficients based on 14-day smoothing (Ref. 21). The results show larger TDZ/temperature correlation coefficients for the Dunbar and Iroquois sites than those computed based on 3-day smoothing in the present study. The discrepancy is consistent with the coherency spectrum.



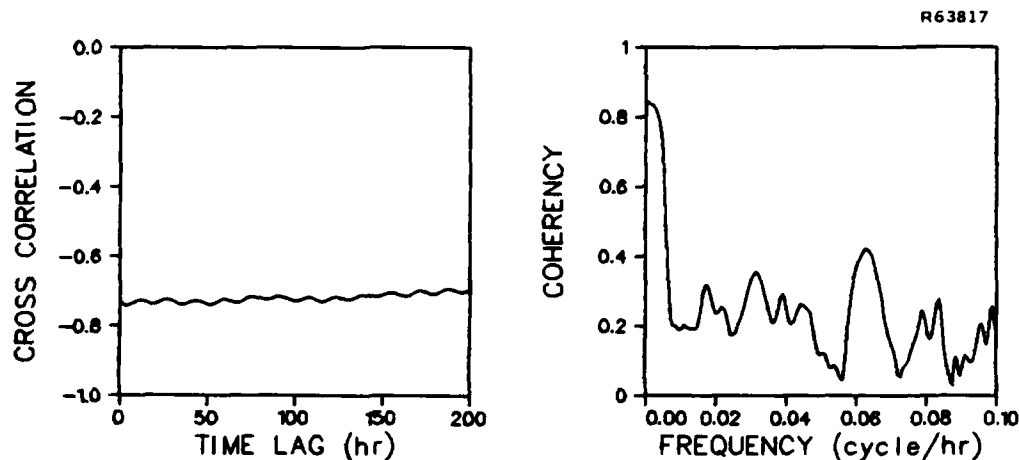


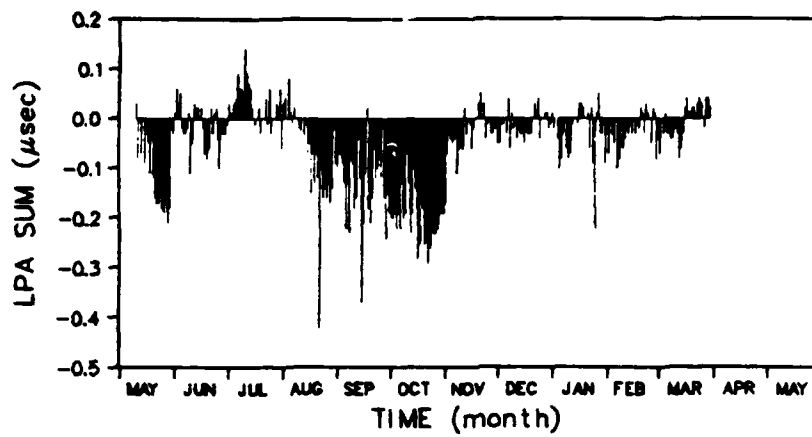
Figure 3.3-8 Cross-Correlation Function and Coherency Spectrum for TDY (Iroquois/LC-204/2) vs Temperature Data

#### 3.4 LPA STATISTICS

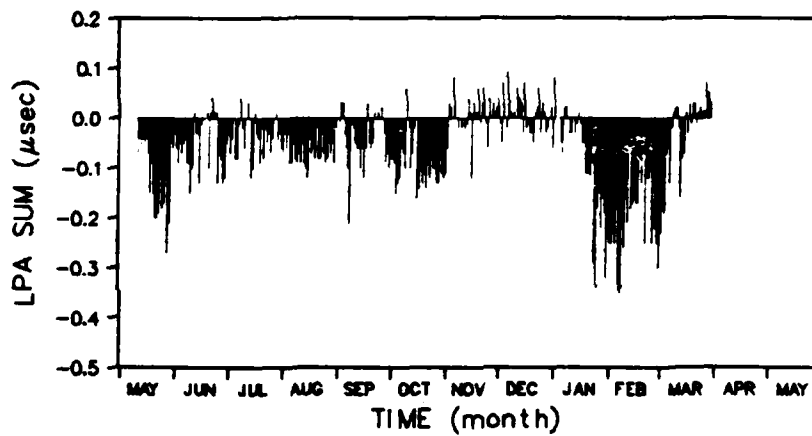
The LPA data contain information regarding the propagation variations which occur along transmitter-to-SAM signal paths. However, extraction of the information requires careful removal of clock phase drift caused by differences in the frequencies of the secondary and master cesium standards.

To illustrate this point, the daily sum of the LPAs is presented in Fig. 3.4-1 for each secondary transmitter. Inspection of the results for transmitter X might lead to the conclusion that propagation variations are larger in September than in January. However, a graph of the cumulative LPA sum vs time (see Fig. 3.4-2) shows that the large difference in

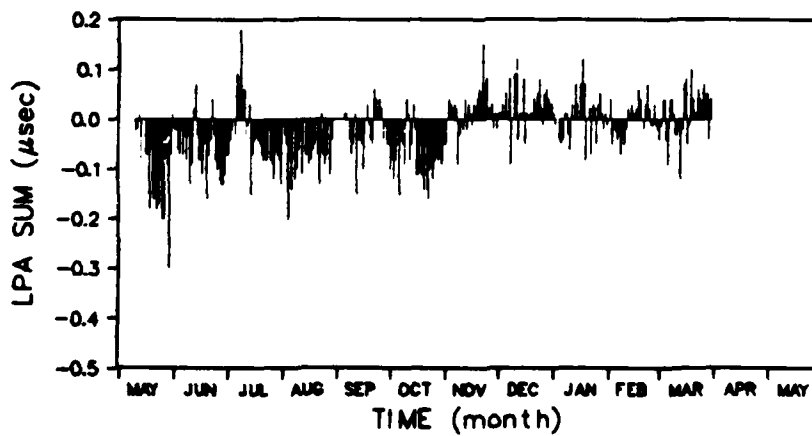
R63818



a) Transmitter X



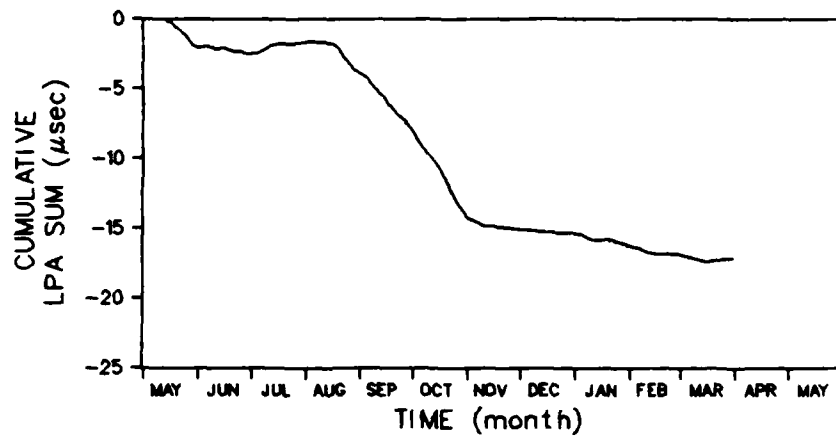
b) Transmitter Y



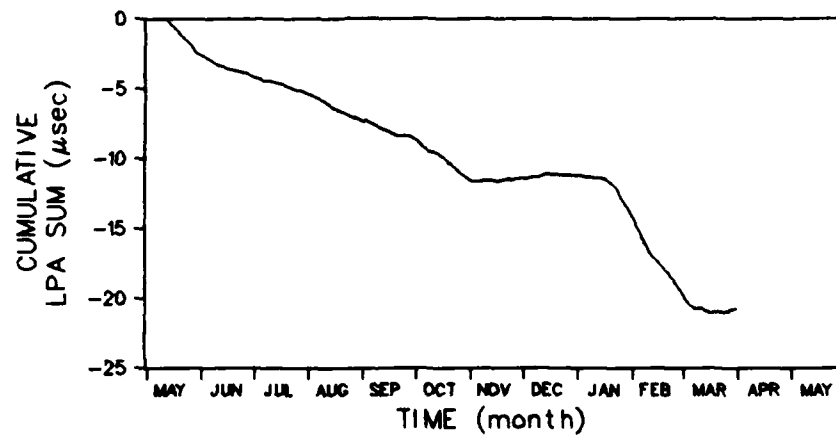
c) Transmitter Z

Figure 3.4-1 Daily Sum of LPAs

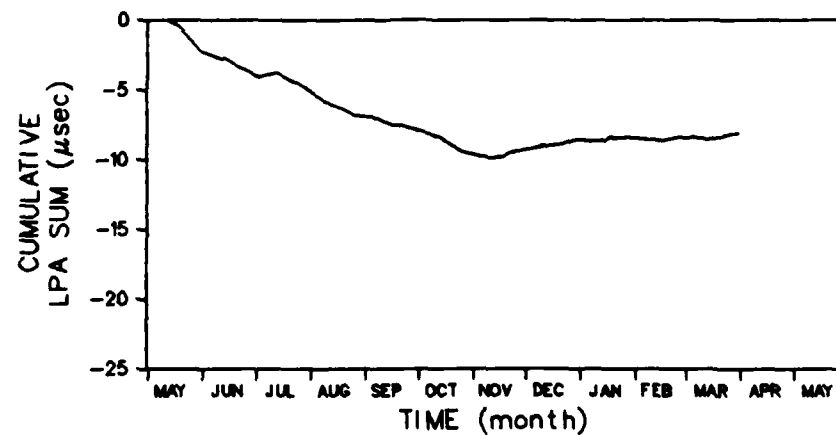
R63819



a) Transmitter X



b) Transmitter Y



c) Transmitter Z

Figure 3.4-2 Cumulative Sum of LPAs

daily LPA sums is caused by a difference in clock drift rates for the two months. The drift rate in September is approximately 0.17  $\mu\text{sec/day}$ , but after clock adjustments made in November the drift rate is only -0.02  $\mu\text{sec/day}$ . Therefore, the daily LPA sums for September shown in Fig. 3.4-1a are primarily associated with clock synchronization, rather than propagation. Separation of synchronization and propagation effects is beyond the scope of the current effort.

### 3.5 COMPARISON OF THEORETICAL AND OBSERVED TD VARIATIONS

Signal propagation theory is employed in Ref. 3 to estimate the magnitude of St. Marys River Loran-C TD grid instability. Because the mini-chain coverage area is less than 60 nm in diameter, the propagation medium is assumed to be homogeneous. This simplifying assumption is consistent with the goal of estimating temporal TD variations, although it is not necessarily appropriate for a model of spatial variations (Refs. 1 and 2).

The sensitivity of TDs to temporal variations in three propagation parameters -- atmospheric refractive index, vertical lapse rate of refractive index, and ground conductivity -- is analyzed in Ref. 3. It is shown that TD sensitivity to refractive index and vertical lapse rate variations is proportional to the "Double Range Difference"

$$\text{DRD} = (R_s - R_m) - (R'_s - R'_m) \quad (3.5-1)$$

where  $R_s$  and  $R_m$  are the secondary-to-site master-to-site ranges, respectively, and  $R'_s$  and  $R'_m$  are the corresponding ranges to

the SAM. DRD contours are hyperbolas, as shown in Figs. 3.5-1 to 3.5-3. The contour of zero sensitivity (DRD = 0) passes through the SAM location, because the SAM maintains its TD at a constant level. TD sensitivity to conductivity variations is given by a Modified Double Range Difference

$$\text{Modified DRD} = (R_s^a - R_m^a) - (R_s'^a - R_m'^a) \quad (3.5-2)$$

where the exponent "a" approximately equals 0.5. This modification accounts for the nonlinearity in the secondary phase delay vs. range function for ranges less than 100 nm (Ref. 15).

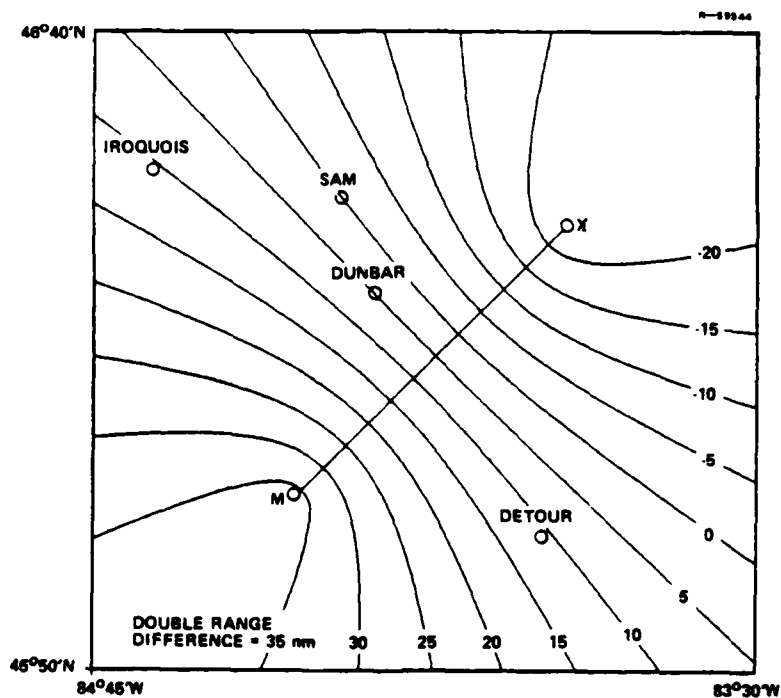


Figure 3.5-1 TDX Temporal Variation Sensitivity

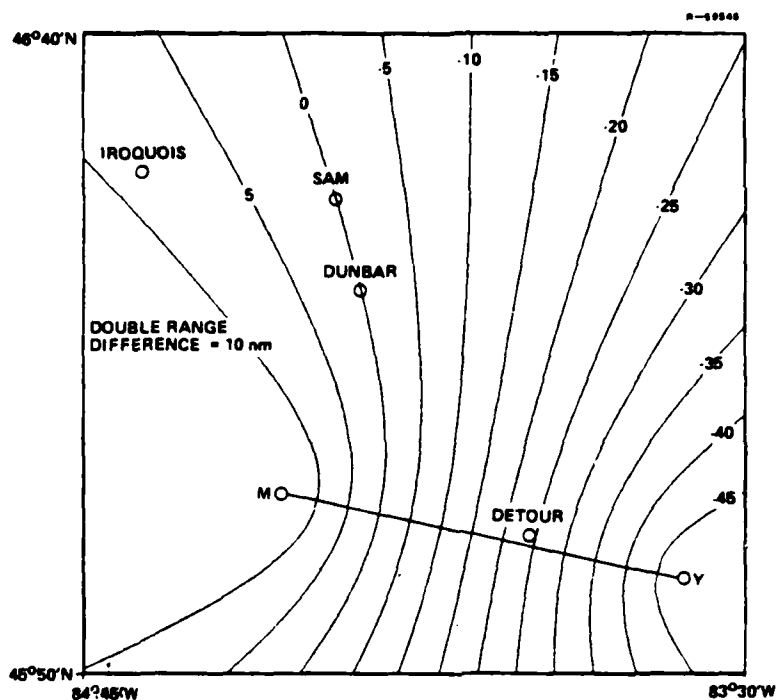


Figure 3.5-2 TDY Temporal Variation Sensitivity

The theoretical TD variations associated with particular variations in the propagation parameters are indicated below:

- Refractive Index --  $6 \times 10^{-6} \mu\text{sec/nm}^*$  per N-unit
- Vertical Lapse Rate --  $3 \times 10^{-5} \mu\text{sec/nm}$  per 0.01  $\alpha$ -units
- Conductivity --  $4 \times 10^{-3} \mu\text{sec/nm}$  per doubling of conductivity.

\*TD variation per nm of DRD. For conductivity, a linear approximation is used to permit the DRD to replace the Modified DRD.

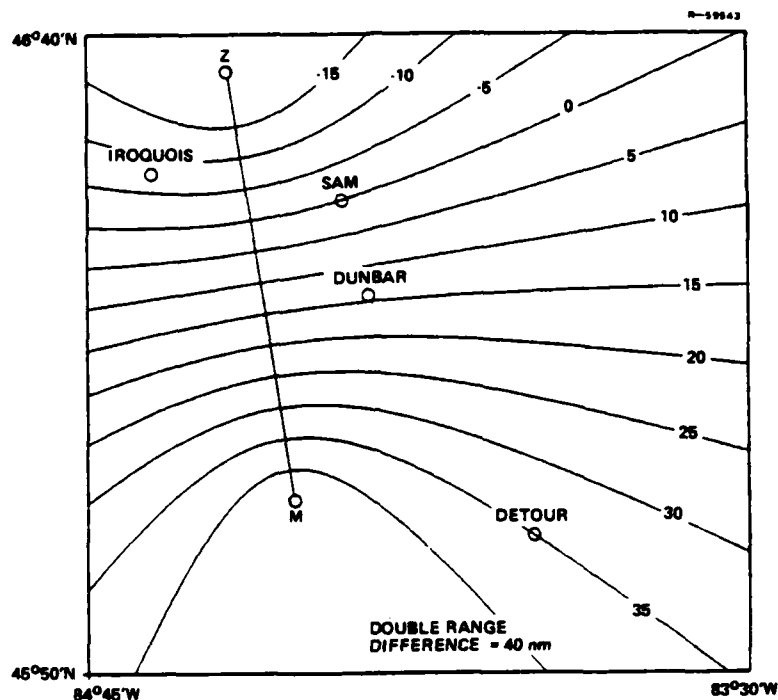


Figure 3.5-3 TDZ Temporal Variation Sensitivity

The maximum DRD for the St. Marys River Loran-C data collection sites is 35 nm (see Figs. 3.5-1 to 3.5-3). Therefore, the maximum seasonal TD variation expected for a 50 N-unit refractive index variation (see Fig. 3.3-7) is only 0.010  $\mu\text{sec}$ . Similarly, the maximum seasonal TD variation expected for a 0.25  $\alpha$ -unit vertical lapse rate variation (Refs. 3 and 9) is 0.026  $\mu\text{sec}$ . Clearly, the  $\pm 0.2$ - $\mu\text{sec}$  seasonal TD variations shown in Section 3.2.1, if propagation-related, are necessarily caused by conductivity variations. The maximum TD variation expected for a doubling of conductivity from winter to summer (Ref. 3) is 0.14  $\mu\text{sec}$  for the three data collection sites.

Although the maximum magnitude of the observed TD variations is consistent with propagation theory, the relative variations of the individual time series are not consistent with the DRD. This is illustrated in Fig. 3.5-4, a comparison of the seasonal time series and the corresponding DRDs. The following are among the obvious discrepancies:

- Dunbar TDY variations are 0.189  $\mu\text{sec}$  peak-to-peak, but the DRD equals zero
- DeTour TDZ variations are only 0.061  $\mu\text{sec}$  peak-to-peak, but the DRD equals +35 nm
- DeTour and Iroquois TDY variations are in the same direction, but the DRDs are of opposite sign (-25 nm vs +8 nm)
- DeTour and Iroquois TDX variations differ significantly, but the DRDs are both equal to +11 nm.

For the data collection sites considered, the Modified DRD is nearly proportional to the DRD and, therefore, does not contribute to resolving the discrepancies.

It is possible that seasonal conductivity variations are spatially heterogeneous, thereby violating the assumptions inherent in the DRD model. However, it is more likely that the observed TD variations are caused by a transmitter- and/or receiver-related mechanism, which dominates or disguises the propagation mechanism.



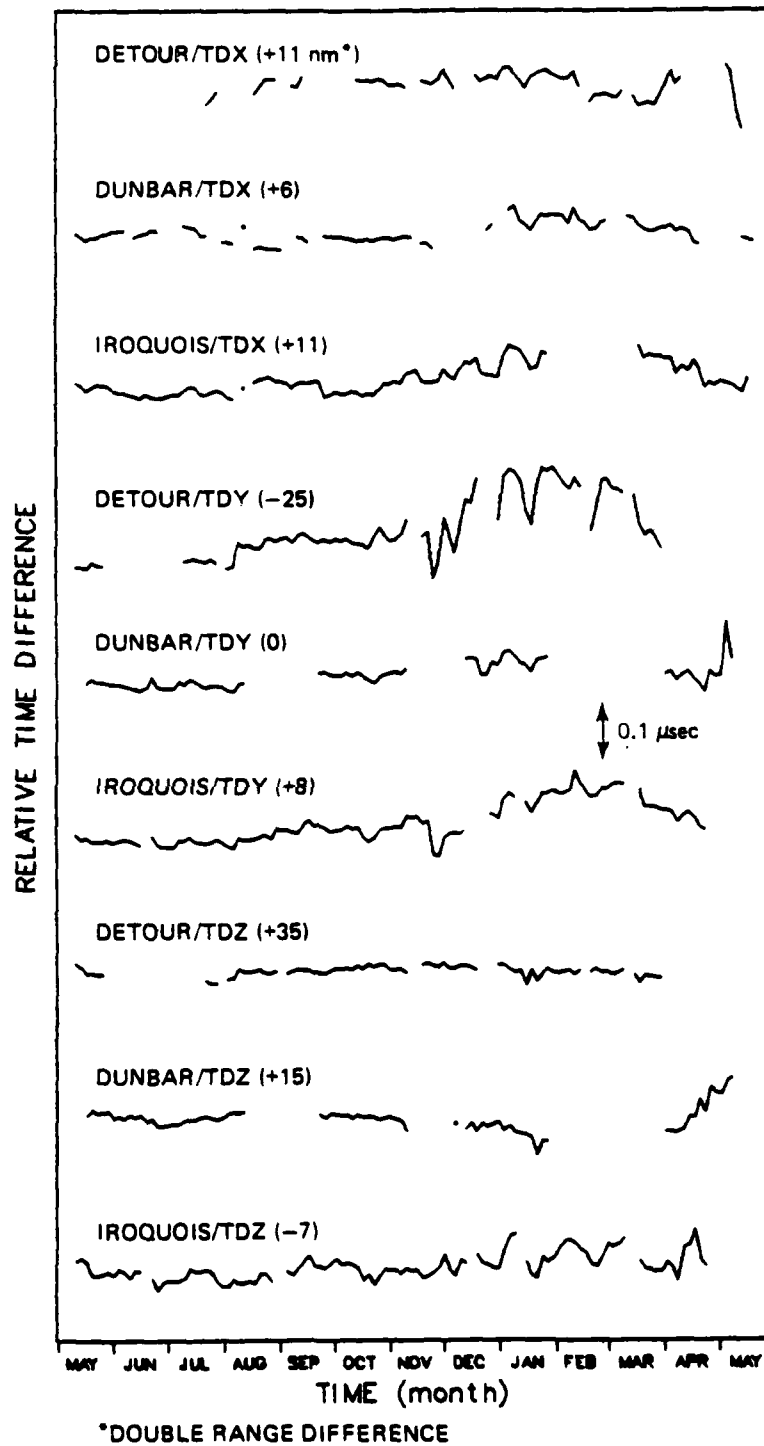


Figure 3.5-4 Comparison of Seasonal TD Time Series

4.

EVALUATION OF  
LOW-DENSITY DATA ANALYSIS APPROACH

4.1 INTRODUCTION

The U.S. Coast Guard has conducted low-density data analyses, which closely parallel the high-density analyses presented in this report. The low-density approach is motivated by the desire of the U.S. Coast Guard to have a quick-response, in-house analysis capability. Specifically, the reduced data volume has enabled monthly internal reports to be issued, which summarize the analysis results (e.g., Ref. 6). A statistical evaluation of the low-density approach is presented in this chapter to validate the monthly reports and to establish an efficient Loran-C monitoring strategy for harbors.

4.2 COMPARISON OF EDITED LOW-DENSITY AND  
HIGH-DENSITY DATA

Potential errors in the low-density TD data, compared to the high-density data, can be categorized as follows:

- Relatively small errors associated with computing mean TD values based on a reduced sample size
- Relatively large errors resulting from the inability to detect outliers in short segments of a time series.

The first error category is addressed in this section, by employing low-density data extracted from the edited high-density data base. Such low-density data would result if

there were no outliers in the measured time series. The contribution of outliers is explored in Section 4.3.

"Generic" low-density sampling strategies are employed to investigate the effect of sample size. Each generic strategy is defined by three parameters:

- Number of equally-spaced time windows per day, during which 15-min samples are recorded
- Width of time windows
- Phase of time windows, i.e., the time-of-day at the beginning of the first window.

The nominal U.S. Coast Guard sampling strategy involves two time windows of width equal to 1 hr, beginning at 0 hr and 7 hr GMT. Because the windows are not equally-spaced (i.e., 12 hr apart), this strategy is addressed separately from the generic strategies.

#### 4.2.1 Seasonal Variations

The utility of the low-density data in quantifying seasonal TD variations depends on the difference between the low- and high-density 3-day smoothed time series. The rms differences (i.e., errors) for the generic sampling strategies are presented as a function of window width in Fig. 4.2-1a and as a function of window phase in Fig. 4.2-1b. These results are obtained by processing TDY data from the Iroquois/LC-204/2 receiver, which is selected to represent worst-case seasonal variations. A direct comparison of the high-density and U.S. Coast Guard low-density time series is given in Fig. 4.2-1c.

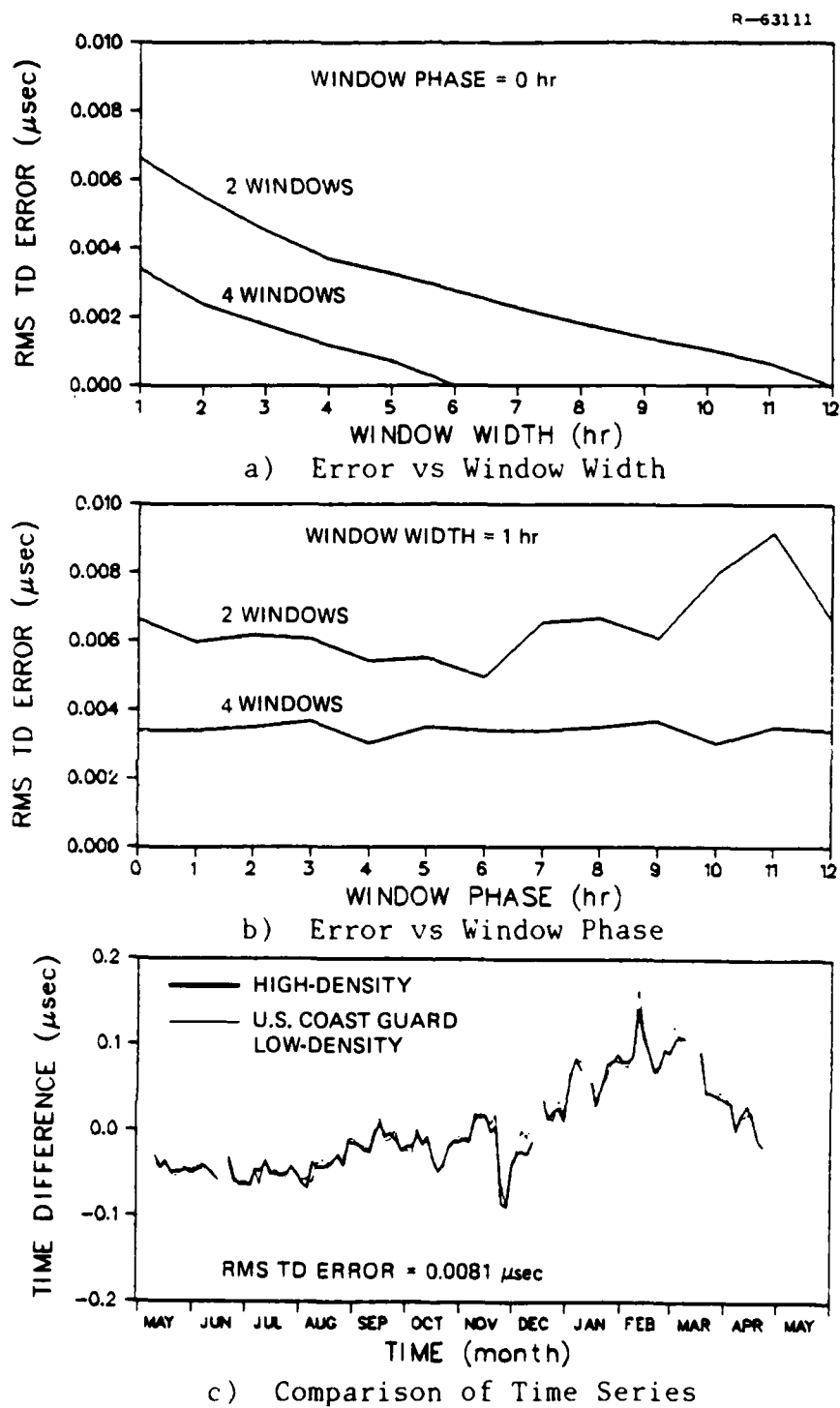


Figure 4.2-1 Accuracy of Edited Low-Density Seasonal Time Series (TDY for Iroquois/LC-204/2)

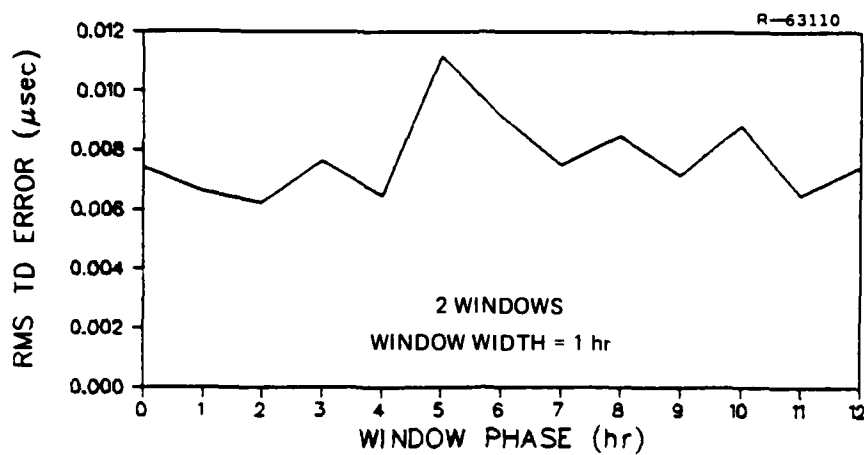
The following conclusions can be drawn, regarding the accuracy of the low-density seasonal time series:

- TD errors are less than 0.01  $\mu$ sec rms for all strategies considered
- Four 1-hr windows are more effective than two 2-hr windows, although they contain the same number of samples
- TD errors are more sensitive to window phase for two windows than for four windows
- The U.S. Coast Guard sampling strategy could be improved only slightly (0.0081  $\mu$ sec error to 0.0067  $\mu$ sec error) by placing the windows at 0 hr and 12 hr GMT.

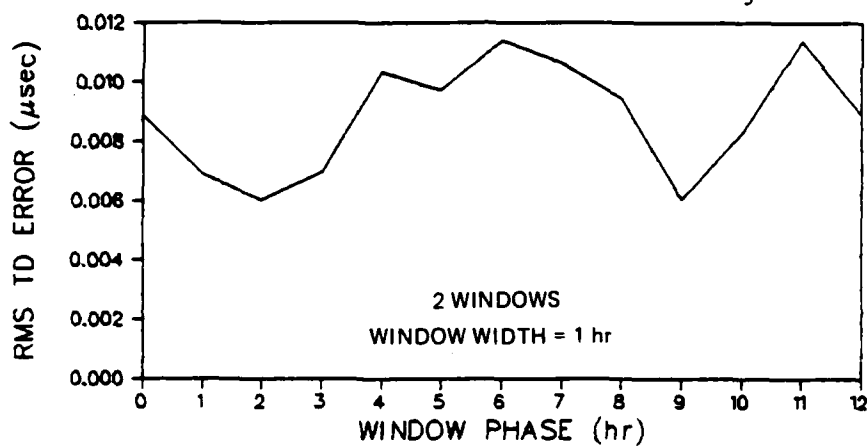
If TD errors are less than 0.01  $\mu$ sec rms, as is the case for the U.S. Coast Guard sampling strategy, seasonal variations can be adequately identified. Although a significant reduction in TD errors can be achieved by using four 1-hr windows instead of two, the additional detail does not contribute significantly to the quantification of seasonal variations.

#### 4.2.2 Monthly Variations

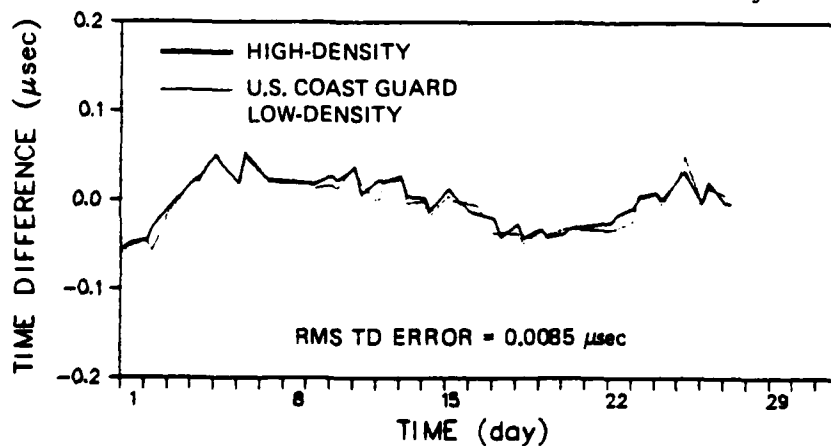
The utility of the low-density data in quantifying monthly TD variations depends on the difference between the low- and high-density 6-hr smoothed time series. The rms TD errors for the generic sampling strategies are presented as a function of window phase for July and January, in Figs. 4.2-2a and 4.2-2b, respectively. These graphs are based on TDX data from the Iroquois/LC-204/1 receiver, which exhibits worst-case TD variations for January. A comparison of the high-density and U.S. Coast Guard low-density time series for January is presented in Fig. 4.2-2c.



a) Error vs Window Phase for July



b) Error vs Window Phase for January



c) Comparison of Time Series for January

Figure 4.2-2 Accuracy of Edited Low-Density Monthly Time Series (TDX for Iroquois/LC-204/1)

The low-density monthly time series is somewhat less accurate than the low-density seasonal time series but, nevertheless, is in error by less than 0.012  $\mu$ sec rms. Consequently, the U.S. Coast Guard sampling strategy is judged to be adequate for measuring monthly TD variations. The large sensitivity of TD errors to window phase, especially for the January data (see Fig. 4.2-2b), is apparently not related to the diurnal TD cycle. Indeed, the TDX diurnal cycle for January for the Iroquois/LC-204/1 receiver is less than 0.005  $\mu$ sec peak-to-peak (see Fig. 3.2-16c). Rather, the two minima in the TD-error vs window-phase graph arise from the assumed definition of a monthly time series. Specifically, the best estimate of the 6-hr means is obtained by sampling in the center of the 6-hr intervals, i.e., at 3 hr, 9 hr, 15 hr, and 21 hr GMT.

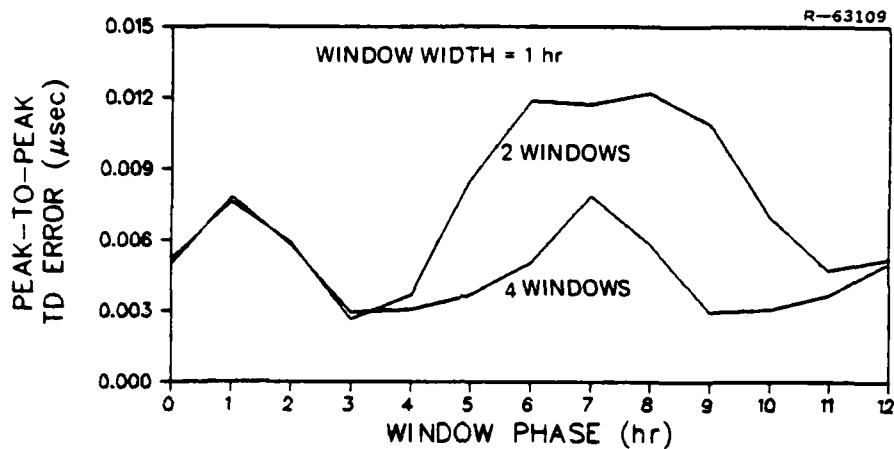
#### 4.2.3 Diurnal Variations

Intuitively, it is difficult to accurately measure the peak-to-peak value of the diurnal TD cycle by using only two 1-hr windows. The phase of the windows is a critical parameter in this case, more so than in the measurement of seasonal and monthly TD variations.

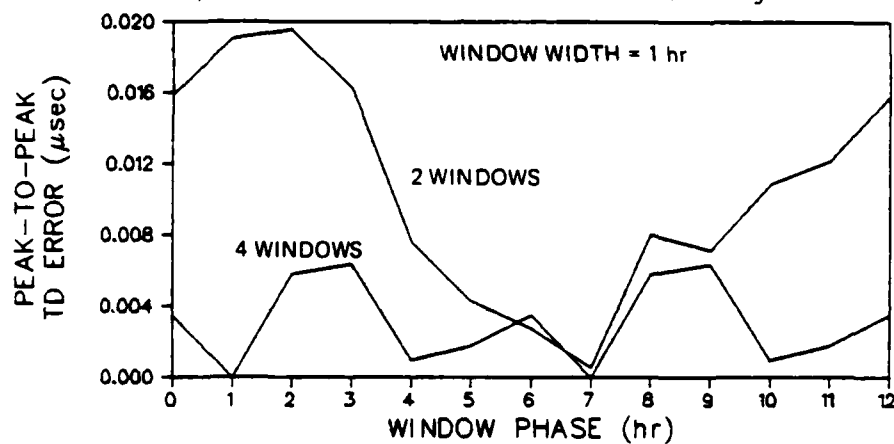
The error in the peak-to-peak value of the low-density diurnal cycle<sup>\*</sup> is presented as a function of window phase for July and January, in Figs. 4.2-3a and 4.2-3b, respectively. TDZ data from the Iroquois/LC-204/2 receiver are selected for the analyses, because they exhibit a distinct diurnal cycle. The high-density and U.S. Coast Guard low-density diurnal cycles are compared for July and January, in Figs. 4.2-3c and 4.2-3d, respectively.

---

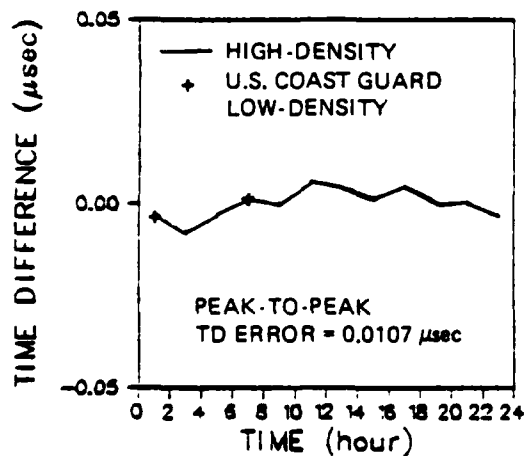
<sup>\*</sup>For two 1-hr windows, the "diurnal cycle" consists of two points, each computed as described in Section 3.2.3.



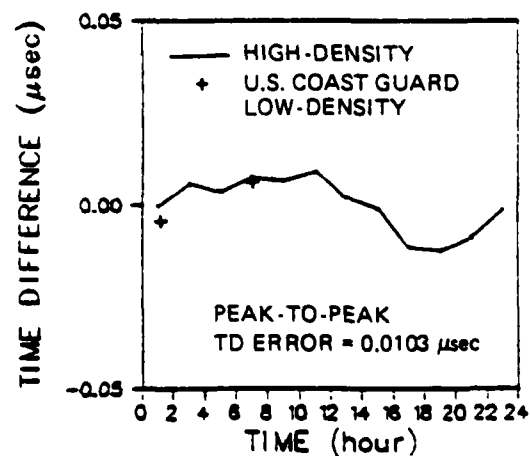
a) Error vs Window Phase for July



b) Error vs Window Phase for January



c) July Comparison



d) January Comparison

Figure 4.2-3 Accuracy of Edited Low-Density Diurnal Cycle (TDZ for Iroquois/LC-204/2)



The following conclusions are drawn regarding the accuracy of the low-density diurnal cycle:

- TD cycle errors are more sensitive to window phase in January than in July, because the diurnal cycle amplitude is larger in January
- The optimal window phase is different in July than in January, because the phase of the diurnal cycle is different in the two months
- TD cycle errors for January, range from less than 0.001  $\mu$ sec to 0.020  $\mu$ sec, depending on the choice of window phase
- Sensitivity to window phase is greatly reduced by using four windows instead of two
- The "peak" in the July diurnal cycle and the "trough" in the January diurnal cycle are not observable with the U.S. Coast Guard sampling strategy, thereby resulting in a 50-percent error in the measured cycle amplitudes.

It is important to recognize that the optimal window phase is generally different for the other TD time series (see Figs. 3.2-13 to 3.2-18).

Clearly, the U.S. Coast Guard low-density data should not be employed for diurnal analyses. Use of the data to identify spectral components for periods less than or equal to 24 hr leads to an aliasing error (Ref. 13). To minimize this problem, it is recommended that four or more time windows per day be employed in the Loran-C harbor monitor program.

#### 4.3 EFFECT OF OUTLIERS ON LOW-DENSITY DATA

The high-density editing procedure described in Chapter 2 consists of three steps: signal-quality check (Editing Mark 2), tolerance check (Editing Mark 3), and outlier editing (Editing Mark 6). A signal-quality check is performed in the microprocessors of the low-density data-recording system, and a tolerance check is performed by the U.S. Coast Guard upon receipt of the data. However, the ability to detect outliers is limited by the short (1-hr) contiguous time periods during which 15-min samples are available. In particular, there are not enough samples to compute a reliable daily trend line (see Section 2.2.6).

Outliers occur in a small percentage of the 1-hr windows: only 1.9 to 10.8 percent of the high density-data are outliers, and only one-twelfth (8.3 percent) of the high-density data are involved in the low-density analyses. Therefore, a comparison of time series, analogous to the comparisons presented in Section 4.2, is not particularly useful for showing the effect of outliers. The following alternative approach is selected and applied to the TDY time series for the DeTour/LC-204/1 receiver:

- Partition the time series into 1-hr intervals and consider only those intervals which contain outliers
- Calculate the differences (errors) between the 1-hr TD means computed with and without outliers
- Construct a histogram of the TD errors.

The histogram shows the distribution of all potential errors encountered in a low-density monthly time series<sup>\*</sup>, due to the presence of outliers. However, very few of the errors are actually encountered, because very few 1-hr intervals with outliers are involved in the low-density data.

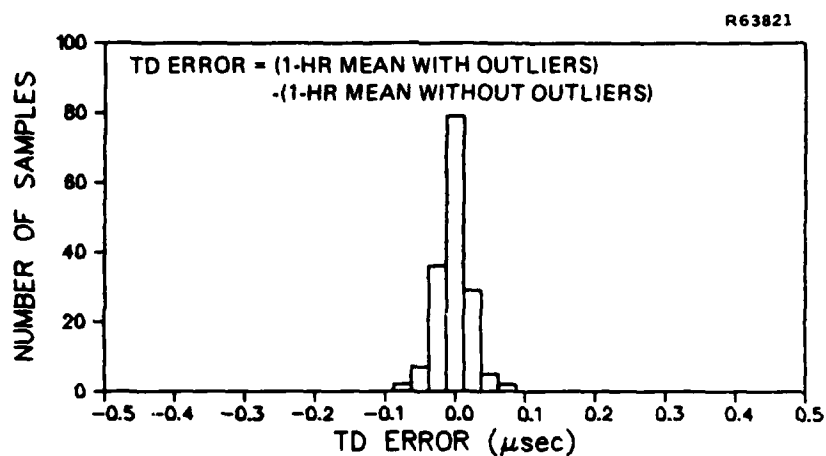
Histograms are presented in Fig. 4.3-1 for three definitions of outliers: Editing Mark 6 = "1", "1" to "4", or "1" to "6". It is unlikely that outliers with Editing Mark 6 = "1" can be detected in the low-density data. However, the potential TD errors introduced by these outliers are typically less than 0.04  $\mu$ sec, not a major concern. Outliers with Editing Mark 6 = "2" to "4" can be detected by a careful inspection of the low-density data, except when multiple outliers occur in a 1-hr window. Such an inspection is warranted because the TD errors can be as large as 0.10  $\mu$ sec. As indicated in Fig. 4.3-1c, outliers with Editing Mark 6 = "5" or "6" can cause TD errors as large as 0.2  $\mu$ sec. Fortunately, these gross outliers are easily detected and removed from the low-density data. The implication of the skewed histogram in Fig. 4.3-1c is that gross outliers consistently lie below the daily trend line, suggesting a possible anomaly in the DeTour/ LC-204/1 receiver.

#### 4.4 ASSESSMENT OF LOW-DENSITY DATA ANALYSIS TECHNIQUES

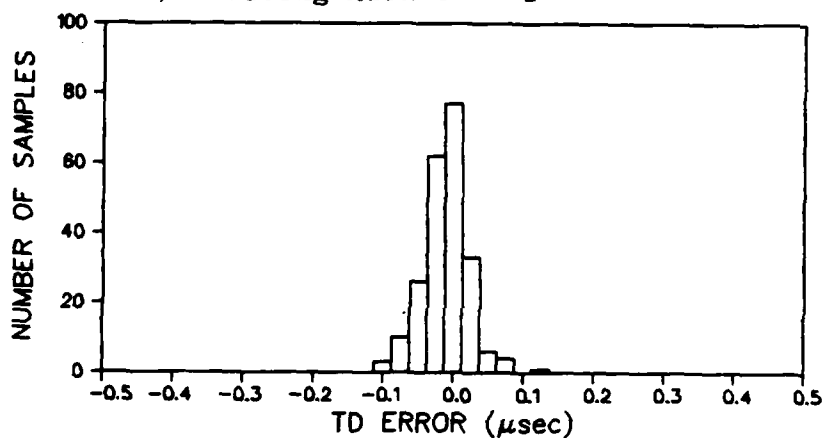
The following are among the low-density data analysis techniques used by the U.S. Coast Guard (Refs. 17 and 18):

- K-Factor Analysis -- used to predict relative TD variations in an assumed homogeneous chain coverage area

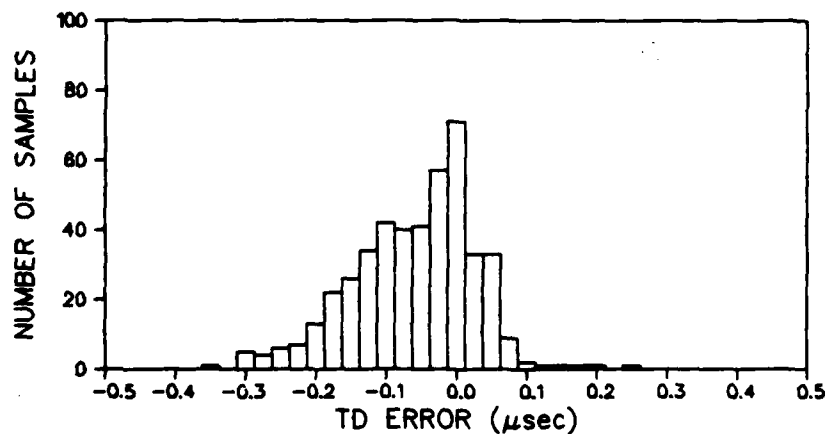
<sup>\*</sup>The low-density monthly time series necessarily consists of 1-hr means, rather than 6-hr means.



a) Editing Mark 6 = "1"



b) Editing Mark 6 = "1" to "4"



c) Editing Mark 6 = "1" to "6"

Figure 4.3-1 Effect of Outliers on Low-Density Monthly Time Series (TDY for DeTour/LC-204/1)

- Uniform Propagation Velocity Model -- used to extract propagation velocity and common SAM-induced errors from the TD data
- Radial Position Error Estimation --used to project propagation velocity variations, SAM-induced errors, and measurement noise into Loran-C user position errors
- TD/Temperature Correlation Analysis -- used to confirm the TD/vertical lapse rate relationship expected by the U.S. Coast Guard.

TASC believes these analysis techniques are appropriately and correctly applied, except as noted below.

K-factor analysis is equivalent to the Double Range Difference analysis presented in Section 3.5. The technique is based on the assumption that the propagation delay increases linearly with range. If conductivity variations are more important than vertical lapse rate variations, however, the dependence is nonlinear in range. In this case, a modified K-factor, analogous to the Modified Double Range Difference (see Eq. 3.5-2), is a more accurate index.

A similar modification to the geometry matrix of the uniform propagation velocity model is required to accommodate conductivity variations. It is also cautioned that the "common SAM-induced error" appearing in the model includes a zero-range bias in the propagation velocity vs range function. This artificial bias occurs because the data cover a limited set of ranges and the assumed velocity vs range function is an approximation. The "bias" varies with time, in conjunction with the modeled propagation velocity variations.

It is shown in Ref. 1 that the cross-channel position error is significantly smaller than the radial (specifically, the 2d rms) position error, in certain areas of the St. Marys River navigation channel. Therefore, it is recommended that both the cross-channel and radial position errors, or the cross-channel and along-channel position errors, be included in comparisons with the channel width (Ref. 17).

TD/temperature correlation analyses, similar to those presented in Section 3.3.3, are an important part of the U.S. Coast Guard low-density approach. It is recommended that the analyses be limited to correlation coefficients. The cross-correlation function is very sensitive to the nature of low-frequency effects and, therefore, cannot be relied on for comparison purposes. Although agreeing that TD/temperature relationships must be identified, TASC is not in agreement with the U.S. Coast Guard contention that such relationships are primarily a vertical lapse rate effect (Ref. 17). The theoretical results in Refs. 3 and 9 show clearly that the TD variations induced by vertical lapse rate variations are negligible ( $<0.03 \mu\text{sec}$ ) in a short-baseline chain. It appears from the results presented in this report that the high TD/temperature correlation observed in the data is not related to propagation. To further test this hypothesis, it is recommended that vertical lapse rate data from the National Weather Service Station at Sault Sainte Marie, Michigan be correlated against the TD data. In computing the vertical lapse rate from radiosonde data, it should be kept in mind that the results may be sensitive to the altitudes selected for the computation (Ref. 20). Various altitudes in addition to the surface/1-km standards should be tested.

5.

## CONCLUSIONS AND RECOMMENDATIONS

Results of a detailed analysis of St. Marys River temporal Loran-C data, collected by the U.S. Coast Guard from May 1979 to May 1980, are documented in this report. The following objectives are met by the data analysis effort:

- Quantification of Time Difference (TD) grid instability in the St. Marys River Loran-C mini-chain, based on high-density (15-min) data
- Establishment of an efficient Loran-C monitoring strategy for harbors, based on an evaluation of the U.S. Coast Guard low-density<sup>\*</sup> data analysis approach.

Data-organizing and -editing capabilities, needed to support the analyses, are provided by the TASC Loran-C Data-Base Management Software developed in a previous effort (Ref. 5). Conclusions and recommendations related to the two study objectives are presented below.

### 5.1 QUANTIFICATION OF ST. MARYS RIVER LORAN-C TD GRID INSTABILITY

The following principal conclusions are drawn from analyses of the high-density TD time series data:

---

<sup>\*</sup>Low-density data consist of five 15-min samples recorded twice daily.

- Seasonal TD variations (i.e., variations in 3-day means over the data collection period) are less than 0.4  $\mu$ sec peak-to-peak at the three data collection sites, consistent with previous observations (Refs. 2 and 3)
- TD variations during monthly periods are larger in the winter than in the summer (e.g., see Fig. 5.1-1), consistent with signal propagation theory (Refs. 3 and 9)
- Diurnal TD cycles are generally less than 0.02  $\mu$ sec peak-to-peak, which is small relative to longer-term variations (e.g., see Fig. 5.1-2)
- Power Spectral Densities (PSDs) computed from the data show that the diurnal TD cycle is 10 to 20 dB below the zero-frequency spectral component (e.g., see Fig. 5.1-3)
- TDZ data measured at the Pt. Iroquois site differ significantly for the two Internav LC-204 receivers (the correlation coefficient,  $\rho$ , is 0.61)
- TDY data from the three sites are highly correlated ( $\rho = 0.87$  to  $0.94$ )
- TDY data exhibit a relatively high negative correlation with Sault Sainte Marie temperature data ( $\rho = -0.77$  to  $-0.85$ ).

A comparison of the data analysis results to the theoretical predictions given in Ref. 3 shows that the maximum observed TD variation is consistent with expected seasonal conductivity variations. However, the relative variations of the individual time series are not consistent with propagation theory for a homogeneous medium.

It is possible that seasonal conductivity variations are spatially heterogeneous, thereby violating the assumptions made in Ref. 3. However, it appears more likely that the observed TD variations are caused by a transmitter- and/or



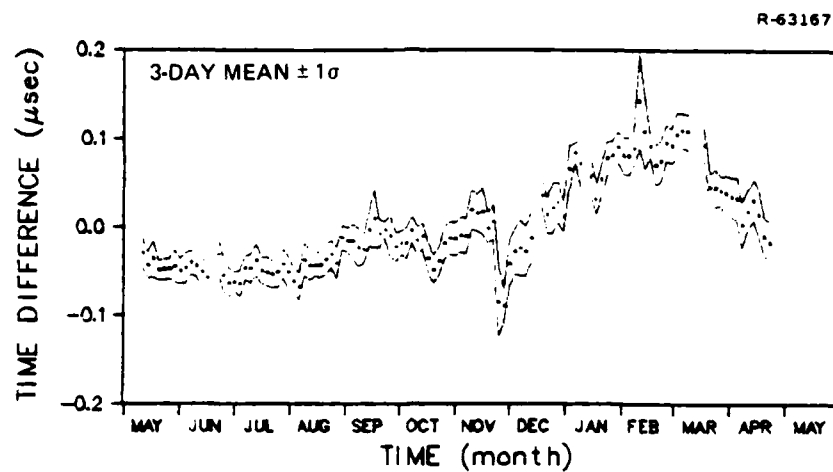


Figure 5.1-1 TDY Seasonal Time Series for Iroquois/LC-204/2

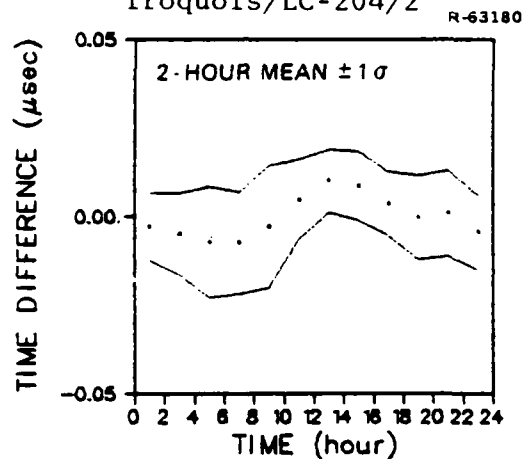


Figure 5.1-2 TDY Diurnal Cycle for DeTour/LC-204/2

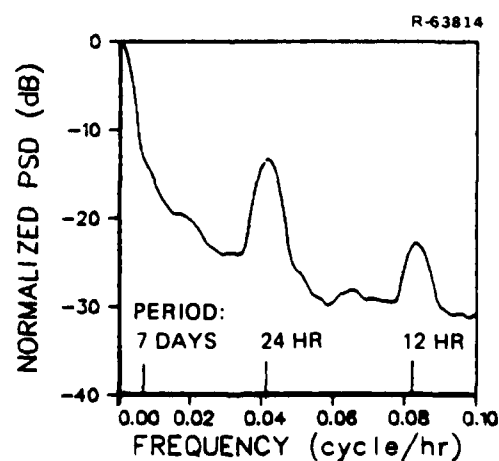


Figure 5.1-3 TDZ Power Spectral Density for Dunbar/LC-204/2

receiver-related mechanism, which disguises the propagation effect. It is important to establish the nature of this mechanism, because of its potential impact on the Loran-C harbor monitor program. Therefore, it is recommended that additional data analyses be conducted, to search for possible cause/effect relationships, whether they be propagation- or transmitter/receiver-induced (Ref. 19). The data base described herein is the most comprehensive of its kind ever assembled and provides a strong nucleus for such an effort.

## 5.2 EVALUATION OF LOW-DENSITY DATA ANALYSIS APPROACH

The following principal conclusions are drawn from the evaluation of the U.S. Coast Guard low-density data analysis approach:

- Errors in the low-density seasonal TD time series, relative to the high-density time series, are less than 0.01  $\mu$ sec rms
- A reduction in the low-density seasonal time series errors can be realized by increasing the number of samples collected per day, but the reduction results in only a slight improvement in data utility
- The above conclusions also hold for the low-density monthly time series
- Significant errors (as large as 50 percent) result if the low-density data are used to compute the peak-to-peak value of the diurnal TD cycle
- The low-density diurnal-cycle errors are very sensitive to the times-of-day selected for sampling
- The optimal sampling times for diurnal-cycle resolution generally differ for different months and different receiver/TD combinations

AD-A108 074

ANALYTIC SCIENCES CORP READING MA

QUANTIFICATION OF ST. MARYS RIVER LORAN-C TIME DIFFERENCE GRID --ETC(U)

F/G 17/7

AUG 80

DOT-CB-A1-77-1785

NL

UNCLASSIFIED

USCG-D-92-81

2 2



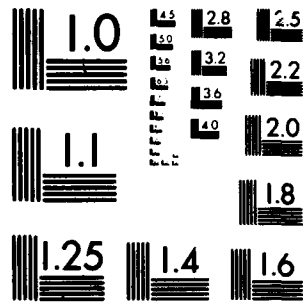
END

DATE

FILED

1 82

DTIC



MICROCOPY RESOLUTION TEST CHART  
NATIONAL BUREAU OF STANDARDS-1963-A<sub>1</sub>

- Moderate data outliers are not a problem in the low-density data, but gross outliers must be removed by inspection.

Based on these conclusions, it is recommended that the U.S. Coast Guard low-density data not be employed for diurnal analyses. To permit diurnal analyses in the Loran-C harbor monitor program, the number of 1-hr time windows per day should be increased from two, to at least four. Furthermore, it must be recognized that the analysis results herein pertain specifically to the St. Marys River mini-chain. In anticipation that different results may apply to a long-baseline chain, it is recommended that high-density harbor monitor data be collected during both a summer month and a winter month and analyzed prior to standardizing a low-density sampling strategy.

The U.S. Coast Guard low-density data analysis techniques described in Ref. 17 are judged to be appropriately and correctly applied, with a few minor exceptions (see Section 4.4). However, TASC is not in agreement with the U.S. Coast Guard contention that the high TD/temperature correlation observed in the data is primarily a vertical lapse rate effect. Based on signal propagation theory, the vertical lapse rate effect is expected to be negligible in a mini-chain. To resolve this issue, it is recommended that vertical lapse rate data from the National Weather Service Station at Sault Sainte Marie, Michigan be correlated against the TD data.

APPENDIX A  
FORMATS FOR LORAN-C DATA SUPPLIED TO TASC

Formats for Loran-C data supplied to TASC on half-inch magnetic tape by the U.S. Coast Guard are presented in Tables A-1 to A-4. The record lengths are 80 characters for the LC-204 and BRN-5 formats and 40 characters for the Austron-5000 format. All characters which are not included in the tables are "blanks."

TABLE A-1  
INTERNAV LC-204 FORMAT FOR DATA SUPPLIED TO TASC

T3484

CHARACTERS	DATA ITEM	DESCRIPTION
1	SWITCH	Control unit switch setting (G for valid, B for invalid)
2-4	DAY	Julian day (Greenwich Mean Time)
5-6	HR	Hours
7-8	MIN	Minutes
9-10	SEC	Seconds
11-14	SNRECDM	Master Signal-to-Noise Ratio (SNR) or Envelope-to-Cycle Difference (ECD) (See char. 38)
15-18	SNRECD1	Secondary 1 SNR or ECD
20-28	TD1	Time difference 1 (0.1 nsec)
33	SITE	Site number
34	---	(1)
35-37	DATAID	Experiment number
38	IDSNRECD	Indicates whether SNR(0) or ECD(1) is printed this record
41-44	SNRECD2	Secondary 2 SNR or ECD
45	ECSM	Master Envelope Command Signal (ECS) indicates whether no cycle jump (0), positive jump (1), or negative jump (2) is commanded by receiver
46	ECS1	Secondary 1 ECS
47	ECS2	Secondary 2 ECS
48	SUFFSIG	Sufficient signal indicator: When converted to a binary number, the 3 digits indicate whether master, secondary 1 and secondary 2 signals are insufficient (0) or sufficient (1)
50-58	TD2	Time difference 2 (0.1 nsec)

TABLE A-2  
MAGNAVOX AN/BRN-5 FORMAT (SECONDARY) FOR DATA  
SUPPLIED TO TASC

T3487

CHARACTERS	DATA ITEM	DESCRIPTION
1	IDENT	Record type indicator: secondary 1 (2) or secondary 2 (3)
2-4	DAY	Julian day (Greenwich Mean Time)
5-6	HR	Hours
7-8	MIN	Minutes
9-10	SEC	Seconds
12	SITE	Site number
13-15	DATAID	Experiment number
17	SUFSIG	Secondary 1 or 2 signal status: When converted to a binary number, first digit indicates whether (1) or not (0) signal is present and second digit whether (1) or not (0) station is blinking
19-27	TD	Time difference 1 or 2 (0.1 nsec)
29-37	TOA	Time of arrival 1 or 2 (0.1 nsec)
39-42	RMSTOA	RMS time of arrival 1 or 2 (nsec)
44-46	ETE	Secondary 1 or 2 envelope time estimate (0.1 $\mu$ sec). Similar to ECD
48-53	SIGLEV	Secondary 1 or 2 signal level (0.24414 mv)
55-58	FRQNT12	Notch filter frequency (0.1 KHz). For notch 1 if char. 1 = 2; for notch 2 if char. 1 = 3
60-61	RECATTEN	Receiver attenuation (dB) for secondary 1 or 2 signal
63-66	SNR	Secondary 1 or 2 signal-to-noise ratio (0.1 dB)



TABLE A-3  
MAGNAVOX AN/BRN-5 FORMAT (MASTER) FOR  
DATA SUPPLIED TO TASC

T3486

CHARACTERS	DATA ITEM	DESCRIPTION
1	IDENT	Master record type indicator (1)
2-4	DAY	Julian day (Greenwich Mean Time)
5-6	HR	Hours
7-8	MIN	Minutes
9-10	SEC	Seconds
12	SITE	Site number
13-15	DATAID	Experiment number
17	SUFSIG	Master signal status: When converted to a binary number, first digit indicates whether (1) or not (0) signal is present and second digit whether (1) or not (0) station is blinking
19	ENVSky	When converted to a binary number, first digit indicates whether (0) or not (1) envelope servo is enabled and second digit whether (1) or not (0) skywave detection is enabled
20	SYNINTER	No synchronous interference (0), even synchronous harmonic present (1), or odd synchronous harmonic present (2)
21	TEMPCOMP	Temperature compensation performed (1) or not performed (0) in last 100-sec interval
23-27	DELAY	Relative receiver time delay (nsec)
29-37	TOA	Master time of arrival (0.1 nsec)
39-42	RMSTOA	Master RMS time of arrival (nsec)
44-46	ETE	Master envelope time estimate (0.1 $\mu$ sec) (Similar to ECD)
48-53	SIGLEV	Master signal level (0.24414 mv)
56-58	COUPATTE	Antenna coupler attenuation (dB)
60-61	RECATTEN	Receiver attenuation (dB) for master signal
63-66	SNR	Master signal-to-noise ratio (0.1 dB)

TABLE A-4  
AUSTRON-5000 FORMAT FOR DATA SUPPLIED TO TASC\*

CHARACTERS	DATA ITEM	DESCRIPTION
2	STATION	Station designator (M, X, Y, or Z)
4-5	MODE	Receiver operating mode (AC, AV, AF, AW, AS, AT, or K)
8-10	GAIN	Receiver gain number
12-15	SNR	S gnal-to-noise ratio
17-21	CYCLE	Receiver cycle number
23-30	TOA	Time-of-arrival relative to internal oscillator (μsec)
32-39	TD	Time difference (μsec)

\*Time is contained in a separate record with the following format: DAY(3-5), HR(7-8), MIN(10-11), and SEC(13-14)

APPENDIX B  
FORMATS FOR LORAN-C DATA DELIVERED TO U.S. COAST GUARD

Formats for Loran-C data delivered to the U.S. Coast Guard on half-inch magnetic tape are presented in Tables B-1 to B-5. The record lengths are 130 characters for all receiver formats and 40 characters for the LPA format. All characters which are not included in the tables are "blanks."

TABLE B-1  
INTERNAV LC-204 FORMAT FOR DATA DELIVERED  
TO U.S. COAST GUARD

T3488

CHARACTERS	DATA ITEM	DESCRIPTION
1-5	OBS	Record Number
7	SITE	*
9-13	RECTYPE	Receiver type (LC204)
15	RECNUM	Receiver number
17-19	DAY	*
21-22	HR	*
24-25	MIN	*
27-28	SEC	*
30-39	TD1	Time difference 1 ( $\mu$ sec)
41-46	DIFCORR1	Differential correction for TD1 ( $\mu$ sec)
48-57	TD2	Time difference 2 ( $\mu$ sec)
59-64	DIFCORR2	Differential correction for TD2 ( $\mu$ sec)
66	IDSNRECD	*
68-71	SNRECDM	*
73-76	SNRECD1	*
78-81	SNRECD2	*
83	SWITCH	*
85-87	DATAID	*
89	ECSM	*
91	ECS1	*
93	ECS2	*
95	SUFFSIG	*
97-102	TD1MARKS	Editing Marks for TD1
104-109	TD2MARKS	Editing Marks for TD2
111-118	TIME	Time in sec since beginning of 1979

\* These data items are described in Table A-1

TABLE B-2  
MAGNAVOX AN/BRN-5 FORMAT (SECONDARY) FOR DATA DELIVERED  
TO U.S. COAST GUARD

T-3491

CHARACTERS	DATA ITEM	DESCRIPTION
1-5	OBS	Record number
7	SITE	*
9-13	RECTYPE	Receiver type (BRN5)
15	RECNUM	Receiver number
17-19	DAY	*
21-22	HR	*
24-25	MIN	*
27-28	SEC	*
30-39	TD	Time difference 1 or 2 ( $\mu$ sec)
41-46	DIFCORR1	Differential correction for TD ( $\mu$ sec)
48-57	TOA	Time of arrival 1 or 2 ( $\mu$ sec)
59-64	DIFCORR2	Differential correction for TOA ( $\mu$ sec)
66-69	RMSTOA	*
71-74	SNR	*
76-78	ETE	*
80-82	DATAID	*
84	SUFSIG	*
86-91	SIGLEV	*
93-94	RECATTEN	*
96-99	FRQNT12	*
101	IDENT	*
103-108	TDMARKS	Editing marks for TD
110-115	TOAMARKS	Editing marks for TOA
117-124	TIME	Time in sec since beginning of 1979

\*These data items are described in Table A-2

TABLE B-3  
MAGNAVOX AN/BRN-5 FORMAT (MASTER) FOR DATA DELIVERED  
TO U.S. COAST GUARD

T3490

CHARACTERS	DATA ITEM	DESCRIPTION
1-5	OBS	Record Number
7	SITE	*
9-13	RECTYPE	Receiver Type (BRN5)
15	RECNUM	Receiver number
17-19	DAY	*
21-22	HR	*
24-25	MIN	*
27-28	SEC	*
30-39	TOA	Master time of arrival ( $\mu$ sec)
41-44	RMSTOA	*
46-49	SNR	*
51-53	ETE	*
55-57	DATAID	*
59	SUFSIG	*
61	ENVSKY	*
63	SYNINTER	*
65	TEMPCOMP	*
67-71	DELAY	*
73-78	SIGLEV	*
80-82	COUPATTE	*
84-85	RECATTEN	*
87	IDENT	*
89-94	TOAMARKS	Editing marks for TOA
96-103	TIME	Time in sec since beginning of 1979

\*These data items are described in Table A-3

TABLE B-4  
AUSTRON-5000 FORMAT FOR DATA DELIVERED  
TO U.S. COAST GUARD

CHARACTERS	DATA ITEM	DESCRIPTION
1-6	OBS	Record number
8	SITE	Site number
10-13	RECTYPE	Receiver type (AUST)
15	RECNUM	Receiver number
17-19	DAY	*
21-22	HR	*
24-25	MIN	*
27-28	SEC	*
30-37	TD	*
39-44	DIFCORR	Differential correction for TD ( $\mu$ sec)
46-47	MODE	*
49-51	GAIN	*
53-56	SNR	*
58-62	CYCLE	*
64-71	TOA	*
73-78	TDMARKS	Editing marks for TD
80-87	TIME	Time in sec since beginning of 1979

\*These data items are described in Table A-4.

TABLE B-5  
FORMAT FOR LPA DATA DELIVERED  
TO U.S. COAST GUARD

CHARACTERS	DATA ITEM	DESCRIPTION
1-5	OBS	Record number
7-9	DAY	Julian day (Greenwich Mean Time)
11-12	HR	Hours
14-15	MIN	Minutes
17-18	SEC	Seconds
20-23	LPA	Local phase adjustment (nsec)
25	STATION	Loran-C transmitter (X, Y, Z), or "B" or "E" to indicate beginning or end of segment of LPAs for which time is uncertain *
27	MASTER	Set to "*" if LPA is applied through master and other two secondaries
29-36	TIME	Time in sec since beginning of 1979

\*The LPA times are known to lie between the B-time and E-time.  
LPA times for the records between the B- and E-records are  
set to the B-time.



APPENDIX C  
PARTIAL LISTING OF LORAN-C DATA BASE

Examples of the data formats described in Appendix B are presented in Figs. C-1 to C-5. Lead and final file records are not included in these listings, but are included on the magnetic tapes. Column labels are provided here for convenience, but are not included on the magnetic tapes.

C-2

**Figure C-1 Partial Listing of Internav LC-204 Data**

QBS	SITE	REC TYPE	REC NUM	DAY	HR	MIN	SEC	TIME	DO	DO DIFF	DO	DO DIFF	RMS	SNR	EFF	DATE	SIG	SEC	FRONT	IDENT	MARKS	MARKS	TIME
1	2	5MB	1	00	00	00	00	000															

Figure C-2 Partial Listing of Magnavox AN/BRN-5 Secondary Data

QBS	S I E	REC T Y P E	REC N D R	Q A V	M H N	M I N	S E C	T O R	R M S I O R	S Z R	E F E	D A T E	S U B S Y S	S Y N M C O R	D E L A Y	S I C L E	C O U P A T I V E	R E C A T I V E	I D E X	V O A M A R K S	I E
1	2	BRNS	1	129	20	15	00	1000.0569	1	17	410	1	1	1	0	0029	50	46	1	M0000	1132100
2	3	BRNS	1	129	20	15	00	1000.0517	1	17	409	1	1	1	0	0029	50	46	1	M0000	1133300
3	4	BRNS	1	129	21	05	00	1000.0506	1	17	410	1	1	1	0	0029	50	46	1	M0000	1133300
4	5	BRNS	1	129	21	05	00	1000.0519	1	17	410	1	1	1	0	0029	50	46	1	M0000	1133300
5	6	BRNS	1	129	21	05	00	1000.0522	1	17	410	1	1	1	0	0029	50	46	1	M0000	1133300
6	7	BRNS	1	129	21	05	00	1000.0525	1	17	410	1	1	1	0	0029	50	46	1	M0000	1133300
7	8	BRNS	1	129	21	05	00	1000.0528	1	17	410	1	1	1	0	0029	50	46	1	M0000	1133300
8	9	BRNS	1	129	21	05	00	1000.0531	1	17	410	1	1	1	0	0029	50	46	1	M0000	1133300
9	10	BRNS	1	129	21	05	00	1000.0534	1	17	410	1	1	1	0	0029	50	46	1	M0000	1133300
10	11	BRNS	1	129	21	05	00	1000.0537	1	17	410	1	1	1	0	0029	50	46	1	M0000	1133300
11	12	BRNS	1	129	21	05	00	1000.0540	1	17	410	1	1	1	0	0029	50	46	1	M0000	1133300
12	13	BRNS	1	129	21	05	00	1000.0543	1	17	410	1	1	1	0	0029	50	46	1	M0000	1133300
13	14	BRNS	1	129	21	05	00	1000.0546	1	17	410	1	1	1	0	0029	50	46	1	M0000	1133300
14	15	BRNS	1	129	21	05	00	1000.0549	1	17	410	1	1	1	0	0029	50	46	1	M0000	1133300
15	16	BRNS	1	129	21	05	00	1000.0552	1	17	410	1	1	1	0	0029	50	46	1	M0000	1133300
16	17	BRNS	1	129	21	05	00	1000.0555	1	17	410	1	1	1	0	0029	50	46	1	M0000	1133300
17	18	BRNS	1	129	21	05	00	1000.0558	1	17	410	1	1	1	0	0029	50	46	1	M0000	1133300
18	19	BRNS	1	129	21	05	00	1000.0561	1	17	410	1	1	1	0	0029	50	46	1	M0000	1133300
19	20	BRNS	1	129	21	05	00	1000.0564	1	17	410	1	1	1	0	0029	50	46	1	M0000	1133300
20	21	BRNS	1	129	21	05	00	1000.0567	1	17	410	1	1	1	0	0029	50	46	1	M0000	1133300
21	22	BRNS	1	129	21	05	00	1000.0570	1	17	410	1	1	1	0	0029	50	46	1	M0000	1133300
22	23	BRNS	1	129	21	05	00	1000.0573	1	17	410	1	1	1	0	0029	50	46	1	M0000	1133300
23	24	BRNS	1	129	21	05	00	1000.0576	1	17	410	1	1	1	0	0029	50	46	1	M0000	1133300
24	25	BRNS	1	129	21	05	00	1000.0579	1	17	410	1	1	1	0	0029	50	46	1	M0000	1133300
25	26	BRNS	1	129	21	05	00	1000.0582	1	17	410	1	1	1	0	0029	50	46	1	M0000	1133300
26	27	BRNS	1	129	21	05	00	1000.0585	1	17	410	1	1	1	0	0029	50	46	1	M0000	1133300
27	28	BRNS	1	129	21	05	00	1000.0588	1	17	410	1	1	1	0	0029	50	46	1	M0000	1133300
28	29	BRNS	1	129	21	05	00	1000.0591	1	17	410	1	1	1	0	0029	50	46	1	M0000	1133300
29	30	BRNS	1	129	21	05	00	1000.0594	1	17	410	1	1	1	0	0029	50	46	1	M0000	1133300
30	31	BRNS	1	129	21	05	00	1000.0597	1	17	410	1	1	1	0	0029	50	46	1	M0000	1133300
31	32	BRNS	1	129	21	05	00	1000.0600	1	17	410	1	1	1	0	0029	50	46	1	M0000	1133300
32	33	BRNS	1	129	21	05	00	1000.0603	1	17	410	1	1	1	0	0029	50	46	1	M0000	1133300
33	34	BRNS	1	129	21	05	00	1000.0606	1	17	410	1	1	1	0	0029	50	46	1	M0000	1133300
34	35	BRNS	1	129	21	05	00	1000.0609	1	17	410	1	1	1	0	0029	50	46	1	M0000	1133300
35	36	BRNS	1	129	21	05	00	1000.0612	1	17	410	1	1	1	0	0029	50	46	1	M0000	1133300
36	37	BRNS	1	129	21	05	00	1000.0615	1	17	410	1	1	1	0	0029	50	46	1	M0000	1133300
37	38	BRNS	1	129	21	05	00	1000.0618	1	17	410	1	1	1	0	0029	50	46	1	M0000	1133300
38	39	BRNS	1	129	21	05	00	1000.0621	1	17	410	1	1	1	0	0029	50	46	1	M0000	1133300
39	40	BRNS	1	129	21	05	00	1000.0624	1	17	410	1	1	1	0	0029	50	46	1	M0000	1133300
40	41	BRNS	1	129	21	05	00	1000.0627	1	17	410	1	1	1	0	0029	50	46	1	M0000	1133300
41	42	BRNS	1	129	21	05	00	1000.0630	1	17	410	1	1	1	0	0029	50	46	1	M0000	1133300
42	43	BRNS	1	129	21	05	00	1000.0633	1	17	410	1	1	1	0	0029	50	46	1	M0000	1133300
43	44	BRNS	1	129	21	05	00	1000.0636	1	17	410	1	1	1	0	0029	50	46	1	M0000	1133300
44	45	BRNS	1	129	21	05	00	1000.0639	1	17	410	1	1	1	0	0029	50	46	1	M0000	1133300
45	46	BRNS	1	129	21	05	00	1000.0642	1	17	410	1	1	1	0	0029	50	46	1	M0000	1133300
46	47	BRNS	1	129	21	05	00	1000.0645	1	17	410	1	1	1	0	0029	50	46	1	M0000	1133300
47	48	BRNS	1	129	21	05	00	1000.0648	1	17	410	1	1	1	0	0029	50	46	1	M0000	1133300

Figure C-3 Partial Listing of Magnavox AN/BRN-5 Master Data

OB S	S I T Y P E	R E C U M	D A Y	H R	M I N	S E C	Y D	O F C O R R	M O D E	G A	S M R	C V C L E	T O A	I D M A R K S	I I M E
1	8	AUST	1	2	3	3	0.00	0.005	AT	64	45	2.79	52129.22	M0000	1213205
2	8	AUST	1	2	3	3	1.5971	0.005	AT	64	45	2.79	52129.22	M0000	1213205
3	8	AUST	1	2	3	3	3.3000	0.005	AT	64	45	2.79	52129.22	M0000	1213205
4	8	AUST	1	2	3	3	0.00	0.005	AT	64	45	2.79	52129.22	M0000	1213205
5	8	AUST	1	2	3	3	0.00	0.005	AT	64	45	2.79	52129.22	M0000	1213205
6	8	AUST	1	2	3	3	0.00	0.005	AT	64	45	2.79	52129.22	M0000	1213205
7	8	AUST	1	2	3	3	0.00	0.005	AT	64	45	2.79	52129.22	M0000	1213205
8	8	AUST	1	2	3	3	0.00	0.005	AT	64	45	2.79	52129.22	M0000	1213205
9	8	AUST	1	2	3	3	0.00	0.005	AT	64	45	2.79	52129.22	M0000	1213205
10	8	AUST	1	2	3	3	0.00	0.005	AT	64	45	2.79	52129.22	M0000	1213205
11	8	AUST	1	2	3	3	0.00	0.005	AT	64	45	2.79	52129.22	M0000	1213205
12	8	AUST	1	2	3	3	0.00	0.005	AT	64	45	2.79	52129.22	M0000	1213205
13	8	AUST	1	2	3	3	0.00	0.005	AT	64	45	2.79	52129.22	M0000	1213205
14	8	AUST	1	2	3	3	0.00	0.005	AT	64	45	2.79	52129.22	M0000	1213205
15	8	AUST	1	2	3	3	0.00	0.005	AT	64	45	2.79	52129.22	M0000	1213205
16	8	AUST	1	2	3	3	0.00	0.005	AT	64	45	2.79	52129.22	M0000	1213205
17	8	AUST	1	2	3	3	0.00	0.005	AT	64	45	2.79	52129.22	M0000	1213205
18	8	AUST	1	2	3	3	0.00	0.005	AT	64	45	2.79	52129.22	M0000	1213205
19	8	AUST	1	2	3	3	0.00	0.005	AT	64	45	2.79	52129.22	M0000	1213205
20	8	AUST	1	2	3	3	0.00	0.005	AT	64	45	2.79	52129.22	M0000	1213205
21	8	AUST	1	2	3	3	0.00	0.005	AT	64	45	2.79	52129.22	M0000	1213205
22	8	AUST	1	2	3	3	0.00	0.005	AT	64	45	2.79	52129.22	M0000	1213205
23	8	AUST	1	2	3	3	0.00	0.005	AT	64	45	2.79	52129.22	M0000	1213205
24	8	AUST	1	2	3	3	0.00	0.005	AT	64	45	2.79	52129.22	M0000	1213205
25	8	AUST	1	2	3	3	0.00	0.005	AT	64	45	2.79	52129.22	M0000	1213205
26	8	AUST	1	2	3	3	0.00	0.005	AT	64	45	2.79	52129.22	M0000	1213205
27	8	AUST	1	2	3	3	0.00	0.005	AT	64	45	2.79	52129.22	M0000	1213205
28	8	AUST	1	2	3	3	0.00	0.005	AT	64	45	2.79	52129.22	M0000	1213205
29	8	AUST	1	2	3	3	0.00	0.005	AT	64	45	2.79	52129.22	M0000	1213205
30	8	AUST	1	2	3	3	0.00	0.005	AT	64	45	2.79	52129.22	M0000	1213205
31	8	AUST	1	2	3	3	0.00	0.005	AT	64	45	2.79	52129.22	M0000	1213205
32	8	AUST	1	2	3	3	0.00	0.005	AT	64	45	2.79	52129.22	M0000	1213205
33	8	AUST	1	2	3	3	0.00	0.005	AT	64	45	2.79	52129.22	M0000	1213205
34	8	AUST	1	2	3	3	0.00	0.005	AT	64	45	2.79	52129.22	M0000	1213205
35	8	AUST	1	2	3	3	0.00	0.005	AT	64	45	2.79	52129.22	M0000	1213205
36	8	AUST	1	2	3	3	0.00	0.005	AT	64	45	2.79	52129.22	M0000	1213205
37	8	AUST	1	2	3	3	0.00	0.005	AT	64	45	2.79	52129.22	M0000	1213205
38	8	AUST	1	2	3	3	0.00	0.005	AT	64	45	2.79	52129.22	M0000	1213205
39	8	AUST	1	2	3	3	0.00	0.005	AT	64	45	2.79	52129.22	M0000	1213205
40	8	AUST	1	2	3	3	0.00	0.005	AT	64	45	2.79	52129.22	M0000	1213205
41	8	AUST	1	2	3	3	0.00	0.005	AT	64	45	2.79	52129.22	M0000	1213205
42	8	AUST	1	2	3	3	0.00	0.005	AT	64	45	2.79	52129.22	M0000	1213205
43	8	AUST	1	2	3	3	0.00	0.005	AT	64	45	2.79	52129.22	M0000	1213205
44	8	AUST	1	2	3	3	0.00	0.005	AT	64	45	2.79	52129.22	M0000	1213205
45	8	AUST	1	2	3	3	0.00	0.005	AT	64	45	2.79	52129.22	M0000	1213205
46	8	AUST	1	2	3	3	0.00	0.005	AT	64	45	2.79	52129.22	M0000	1213205
47	8	AUST	1	2	3	3	0.00	0.005	AT	64	45	2.79	52129.22	M0000	1213205
48	8	AUST	1	2	3	3	0.00	0.005	AT	64	45	2.79	52129.22	M0000	1213205

Figure C-4 Partial Listing of Austron-5000 Data

O B S	D A Y	H R	M I N	S E C	L F A	S T A T I C N	M A S T E R	T I M E
1	130	0	7	1	10	X		11146021
2	130	0	28	38	10	X		11147318
3	130	1	20	50	10	X		11150450
4	130	11	47	25	-20	Z		11188045
5	130	11	47	38	-10	X		11188058
6	130	20	25	9	-10	X		11219109
7	130	20	27	7	-10	Z		11219227
8	130	21	25	2	10	X		11222702
9	130	22	55	52	10	X		11228152
10	131	1	22	37	-10	Z		11236957
11	131	3	18	12	-10	Y		11243892
12	131	3	22	34	-10	Y		11244154
13	131	13	6	39	-10	X		11279199
14	131	13	8	14	-10	Y		11279294
15	131	13	9	4	-10	Z		11279344
16	131	13	39	4	-10	X		11281146
17	131	14	9	27	-10	X		11282967
18	131	14	38	23	-10	X		11284703
19	131	15	8	42	-20	X		11286522
20	131	15	37	40	-10	X		11288260
21	131	17	7	55	-10	X		11293675
22	131	17	53	8	-10	Y		11296388
23	131	18	9	41	-10	Y		11297321
24	131	22	25	46	-10	Y		11312746
25	131	23	40	15	-10	Y		11317215
26	132	0	21	45	10	Z		11319705
27	132	0	52	1	20	Z		11321521
28	132	1	21	47	-10	Y		11323307
29	132	1	22	17	20	Z		11323337
30	132	2	45	10	-10	Y		11328310
31	132	12	24	31	10	X		11363071
32	132	12	24	56	-10	Y		11363096
33	132	12	24	56	-10	Z		11363096
34	132	13	19	20	10	X		11366360
35	132	13	19	20	10	Y		11366370
36	132	13	19	47	-10	Z		11366387
37	132	13	51	37	10	Y		11368297
38	132	15	46	58	-10	X		11375218
39	132	15	50	35	-10	Y		11385835
40	132	15	51	3	-10	Z		11385863
41	132	23	19	44	-10	X		11402384
42	132	23	21	52	-10	Y		11402512
43	132	23	22	11	-10	Z		11402531
44	132	23	51	31	-10	Y		11404291
45	133	0	22	50	-10	Z		11406170
46	133	0	53	24	-10	X		11406004
47	133	0	53	48	-10	Y		11406028
48	133	1	23	18	-10	Y		11405758

Figure C-5 Partial Listing of LPA Data

## REFERENCES

1. Warren, R.S., Gupta, R.R., and Healy, R.D., "Design and Calibration of a Grid Prediction Algorithm for the St. Marys River Loran-C Chain," The Analytic Sciences Corporation, Technical Information Memorandum TIM-1119-2, March 1978.
2. Warren, R.S., Gupta, R.R., and Shubbuck, T.J., "Design and Calibration of a Grid Prediction Algorithm for the St. Marys River Loran-C Chain," Proc. of Seventh Annual Technical Symposium of the Wild Goose Association (New Orleans, LA), October 1978.
3. DePalma, L.M., and Gupta, R.R., "Seasonal Sensitivity Analysis of St. Marys River Loran-C Time Difference Grid," The Analytic Sciences Corporation, Technical Information Memorandum TIM-1119-3, June 1978.
4. DePalma, L.M., "Observability and Control of Grid Instability in the St. Marys River Loran-C Chain," The Analytic Sciences Corporation, Technical Information Memorandum TIM-1119-4, October 1978.
5. DePalma, L.M., "Data-Base Management Software for the St. Marys River Loran-C Temporal Instability Experiment," The Analytic Sciences Corporation, Technical Information Memorandum TIM-1119-5, May 1979.
6. "St. Marys River Loran-C Mini-Chain Low-Density Analysis/Signal Characterization Report," U.S. Coast Guard Research and Development Center, Internal Memorandum, February 1980.
7. "St. Marys River Pre-Calibration Tests," U.S. Coast Guard, Memorandum from C. Isgett to A. Sedlock, October 1978.
8. Bean, B.R., and Dutton, E.J., Radio Meteorology, Dover Publications Inc., New York, 1968.
9. Campbell, L.W., Doherty, R.H., and Johler, J.R., "Loran-C System Dynamic Model: Temporal Propagation Variation Study," Analytical Systems Engineering Corporation and Colorado Research and Prediction Laboratory, Inc., Technical Report ASECR 79-107, July 1979.

#### REFERENCES (Continued)

10. "World Distribution and Characteristics of Atmospheric Radio Noise," Proc. of the Tenth Plenary Assembly of the International Radio Consultative Committee (Geneva, Switzerland), Report No. 322, 1963.
11. Gelb, A., (Editor), Applied Optimal Estimation, MIT Press, Cambridge, MA, 1974.
12. Jenkins, G.M., and Watts, D.G., Spectral Analysis and Its Applications, Holden-Day, 1968.
13. Rabiner, L.R., and Gold, B., Theory and Application of Digital Signal Processing, Prentice-Hall, 1975.
14. Harris, F.J., "On the Use of Windows for Harmonic Analysis With the Discrete Fourier Transform," Proc. IEEE, Vol. 66, No. 1, January 1978, pp. 51-83.
15. Johler, J.R., Keller, W.J., and Walters, L.C., "Phase of the Low Radio Frequency Groundwave," National Bureau of Standards Circular 573, June 1956.
16. St. Mary's River Loran-C Mini-Chain Low-Density Analysis/Signal Characterization Report," U.S. Coast Guard Research and Development Center, Internal Memorandum, December 1979.
17. Olsen, D.L., and Isgett, C.E., "Preliminary Stability Analysis of the St. Marys River Mini-Chain," Proc. of Eighth Annual Technical Symposium of the Wild Goose Association (Williamsburg, VA), October 1979.
18. Levy, L.J., and Schwab, V., "G Matrix Analysis for USCG Loran-C HHE Navigator Program," The Johns Hopkins University Applied Physics Laboratory, Memorandum S2R-79-008/ZT70S2R0, January 1979.
19. "Recommended Data Analyses to Support the Explanation of St. Marys River Loran-C Grid Instability," The Analytic Sciences Corporation, Slide Presentation SP-1119-9, April 1980.
20. Samaddar, S.N., "The Theory of Loran-C Ground Wave Propagation -- A Review," Journal of the Institute of Navigation, Vol. 26, No. 3, Fall 1979, pp. 173-187.
21. "St. Marys River Loran-C Mini-Chain," U.S. Coast Guard, Report No. CG-D-43-80 (Draft), July 1980.



ATE  
LME  
-8